“Identification and Characterization of electrical patterns underlying stereotyped behaviours in the semi-intact leech”

Thesis submitted for the degree of “Philosophiæ Doctor in Neurosciences”

CANDIDATE
León Jacobo Juárez Hernández

SUPERVISOR
Prof. Vincent Torre

With my mind to the knowledge of the leech

With my mouth to my Mexico & Italy friends

With my heart to my Family

Avalokita, the holy lord and Bodhisattva, was moving in the deep course of the wisdom which has gone beyond. He looked down from on high, he beheld but five heaps, and he saw that in their own-being they were empty.

Here, O Sariputra, form is emptiness and the very emptiness is form; emptiness does not differ from form, form does not differ from emptiness, whatever is emptiness, that is form, the same is true of feelings, perceptions, impulses, and consciousness.

Here, O Sariputra, all dharmas are marked with emptiness; they are not produced or stopped, not defiled or immaculate, not deficient or complete.

Therefore, O Sariputra, in emptiness there is no form nor feeling, nor perception, nor impulse, nor consciousness; no eye, ear, nose, tongue, body, mind; no forms, sounds, smells, tastes, touchables or objects of mind; no sight-organ element, and so forth, until we come to: no mind-consciousness element; there is no ignorance, no extinction of ignorance, and so forth, until we come to: there is no decay and death, no extinction of decay and death. There is no suffering, no origination, no stopping, no path. There is no cognition, no attainment and no non-attainment.

Therefore, O Sariputra, it is because of his non-attainmentness that a Bodhisattva, through having relied on the perfection of wisdom, dwells without thought-coverings. In the absence of thought-coverings he has not been made to tremble, he has overcome what can upset, and in the end he attains to Nirvana.

All those who appear as Buddhas in the three periods of time fully awake to the utmost, right and perfect enlightenment because they have relied on the perfection of wisdom. Therefore one should know the prajnaparamita as the great spell, the spell of great knowledge, the utmost spell, the unequalled spell, allayer of all suffering, in truth—for what could go wrong? By the prajnaparamita has this spell have been delivered:

gate gate paragate parasamgate bodhi swaha!!

This completes the Heart of Perfect Wisdom.

Heart Sutra

CONTENT

LIST OF FIGURES AND TABLES

AKNOWLEDGEMENTS

About this Ph.D. thesis, I want to express my gratitude to the next persons for the invaluable suggestions, discussions, help and the comments that contributed to the performance and conclusion of this work:

Prof. Vincent Torre, who permitted to me to perform this work in his laboratory, discussed and commanded-guided this work
Prof. Ph.D. Bill William Kristan Jr. & **Ph.D. Daniel Wagenaar**, for their suggestions and teachings in the neurobiology of the leech
Ph.D. Giacomo Bisson, an invaluable help in the realization of the complex analysis and likewise all the knowledge generously provided in the signals analysis and computational area
Ph.D. Ma. Elizabeth García Pérez & Ph.D. Alberto Mazzoni for the very beginning in the Computational Neurobiology of the Leech
To All the SISSA staff without exclusions
To the specimens of the taxonomic genre *Hirudo spp*

To all my laboratory mates (2006 - 2011): Majid Moshtag, Giulieta Pinato, Diana Bedolla, Walter Vanzella, Elisabetta Ruaro, Jelena Ban, Fredric Broccard, Paolo Codega, Madalena Pocceco, Silvia Pegoraro, Jummi Laishram, Daniela Avossa, Rajesh Shahapure, Anil Nair, Monica Mazzolin, Arin Marchesi, Monica Patti, Francesco Difato, "Pifa", Elisa Migliorini, Linh Thien Lien, Erika Ercolini, Ladan Amin, Shouvrav Maity, Wasim Sayyad, Giovani Iacono, Alejandro Valbuena, Shripad Kondra, Daniel Rueda, Giacomo Bisson, Alberto Mazzoni, Maria Elizabeth Garcia P. (Gracias a ti concí a muchos de ellos! ☺), Manuella S. Lough, Alessio Ansuini.

To my friends in Mexico & Italy: **H.L.M**., Laura Lagostena, Amanda Colombo, Alessia Franceschini, Alessandra Cifra, Ekaterina Kochegurova, Luca P. Mertens, Mayya Sundukova, Cinthya Samano, Melissa & Victor Roura, Federica Agostini, Alma Campos, Roberta Antonelli, Emanuele Costa, Sofia Alcaraz, Carlo Mercuri, Amanda Colombo, Mattia Visentini, Erika Melendez, Antonio Vasta, Natalia Rosso, Andrea Berenjeno, Celeste Roberts, Roberta Antonelli, Gabri & Guido Manfioletti (CXG), Stefano Benvegnu, The Leech, Carlos Barbosa, Luis Juarez, Carlos Zabetta, Ani Malvina Savio, Sonya Rahman, Saulo E. Juarez, Fam. Juarez, Rolando Hong, Claudio Anselmi, Liliana Rosas, Beatrice Pastore, Rita Abate, Natalia Rosso, Tullio Brigiani, Irais Rivera, Ana Carmen Delgadillo, Misael Gutierrez, Squinternautics, Rajesh&Jacob:Tabla&Guitar sessions, Broccard Reel camel drift, Lola Diaz, Ramon Pinzon, Paola Buendia, Ignacio Buendia, Abel Juarez V., Roxi Foti, Oscar Juarez, Mario Mena, M. Antonieta Montaño & Norberto Chavez, Ivan Marchioni, Octavio Reyes, Yolox Macias, Ceci Bañuelos, Karrucha & Irsael lopez, Elisa Azuara, Borbotones, Susu Diodato, Claudia Sagheddu, Marile' Griguoli, Marilena Raciti, Gabriele Giachin, Ila' poggiolini, Ila' Quadrelli, Nicola, Vavu ed Elia (Cesenat), Lujan Mazzone, Babel Letita, Wendy Fonseca, Dj. Carmen, Jorge Cruz, Ricardo Barrios, Fam Arce. All my thanks to Luciano & Adda Gasperini

Especially To Lisa Gasperini.

And also especially to my family who always supported me in near and far distance:
Arq. Daniel Juárez V. & Sra. Maria De la C. H. Montaño,
Ing. Angel R. Juárez H.; D.G. Perla C. Sutarova & Ph.D. Frantisek Sutara,
Sr. Guillermo Montaño P. & Sra. Josefina Montaño P.
Sr. Abel Juárez N. & Sra. Rosa Vilchis C.

NOTES

The work described in this dissertation was carried out at the Neurosciences-Neurobiology sector from the International School for Advanced Studies (SISSA-ISAS), in the city of Trieste, Italy. This work was performed between June 2006 and February 2011. All work reported has not been submitted, as in whole or in part, to any other University or Institute.

León Jacobo Juárez Hernández, Trieste, Italy.
Year 2011

ABBREVIATURES

5-HT	5-Hydroxytryptophan or Serotonine
$<AFR_j>$	Mean of the AFR
$<\rho_{ij}>$	Mean of the cross or auto covariance
ρ	Cross- and/or auto- covariance
σ	Standard deviation
AA	Anterior anterior branch of the anterior root
ADC	Analog to digital converter
AE	Annulus erector motor neuron
AFR	Average firing rate
AP	Action potential
AP	Anterior Pagoda Cell
CC	Caudal Connective
CNS	Central nervous system
CPG	Central pattern generator
CV	Ventrolateral circular excitatory motoneuron
DL-O	Dorsolateral-octopamine cells
DP	Dorsal posterior root
DPn	Numerated DP from a double ganglia experiment
ESV	Elongation – Shortening Vector
ESV_{head}	ESV from the head
ESV_{tail}	ESV from the tail
ESV_{total}	ESV total (head and tail added)
FCS	Fast Conducting System
FMRFamide	Peptide phe-met-arg-phe-amide
GABA	γ-Amino-Butiric Acid
G_n or g_n	Segmental ganglion number *n*
H1-H4	(Fusionated) head's ganglia (1 to 4)
HE	Heart excitatory motoneuron
Hz	Hertz units
IN_n	Interneuron number *n*

L	Large longitudinal excitatory motoneuron
LFP	Local field potential
MA	Medial Anterior Root
min	time in minute units
ms	time in milisecond units
N_l	Lateral nociceptive mechanosensory neuron
N_m	Medial nociceptive mechanosensory neuron
NMDA	*N-Methyl-D-aspartic* acid
N_n	Neuron number *n*
P_d	Dorsal pressure mechanosensory neuron
PP	Posterior Posterior root
P_v	Ventral pressure mechanosensory neuron
R3B1	Cell of crawling initiation and termination.
RAM	Random-Access Memory
RC	Rostral connective
ROC	Reciving operating characteristic
Rz	Reztius Cell
s	time in seconds units
S	Cell S (from the Fast conducting system)
SE1	Swim excitatory interneuron
SIN1	Swim inhibitory interneuron
SMR	Sensillar movement receptors
T1-T7	(Fusionated) Tail's ganglia (1 to 7)
T_d	Dorsal touch mechanosensory neuron
T_l	Lateral touch mechanosensory neuron
Tr1, Tr2, Tr3	Swim trigger interneurons)
T_v	Ventral touch mechanosensory neuron
UPGMA	Unweighted pair-groups method average
UPGMC	Unweighted pair-groups method centroid
V1 or V4	Cerebral cortex or Cortical regions in the brain.
V_{head}	Velocity from head
V_{tail}	Velocity from tail
WORMS	World register of marine species.

ABSTRACT

Neuroscience aims at understanding the mechanisms underlying perception, learning, memory, consciousness and acts. The present Ph.D. thesis aims to elucidate some principles controlling *actions*, which in a more scientific and technical language is referred to as *motor control*. This concept has been studied in a variety of preparations in vertebrate and invertebrate species. In this PhD thesis, the leech has been the subject of choice, because it is a well known preparation, highly suitable for relating functional and behavioural properties to the underlying neuronal networks. The ***semi-intact leech*** preparation (Kristan *et al.*, 1974) has been the main methodological strategy performed in the experiments. Its importance lies in the fact that it gives the possibility to access the information from the leech's central nervous system (CNS) and compare simultaneously some stereotyped behaviours. Thus, entering in this work it is necessary to make a brief summary of the steps followed before arriving to the conclusions written ahead.

The main objective followed in this work has been ***the analysis, identification and characterization of electrical patterns underlying different behaviours in Hirudo medicinalis***. This main objective has been reached focusing the project on three particular objectives, which have been pursued during the author's Philosophical Doctorate course.

The comprehension of the neural information related to behaviour has recently changed the strategies used to analyze large quantity of experimental data, especially in the case of techniques supported by the computational technology. Considering these advances, the first objective to achieve was ***to find an automated methodology to represent the information obtained from the preparations in a more compact and comprehensive manner***. This objective resulted in the obtaining and acquisition of primary information from the experiments with the simultaneously improvement of the electrophysiology experimental recordings and vision acquisition.

As in many works in neurosciences, once that consisting and convincing information is acquired from experiments, the next step is the analysis of the signals, which of course has two natural sources: nerves and behaviours. In this second particular objective, the analysis has been focused on ***the identification and characterization of neural and behavioural information obtained from experiments.*** This resulted in the use of computational algorithms to process, display and inspect the extracellular recordings up to the cell identification by the use of a spike's sorting algorithm obtaining two main kinds of descriptors: the Average Firing Rate (***AFR***) and the auto and cross-covariance from the combinations of *AFR* (**ρ**). For the behavioural

information, the automated operations by algorithms allowed to identify magnitudes (velocity) based on the primary signals processed, which facilitated the identification of patterns of behaviour.

With these two particular objectives achieved, the third one has been ***to relate the information between the automated, identified and characterized signals from the nervous system and behaviours elicited during the experiments performed***. This objective resulted in some stereotyped patterns of behaviour that have been recognized using the neural activity from the acquired recordings of roots and, therefore, identified neurons.

Having achieved these three particular objectives, it is necessary to point out four main results of this PhD thesis which contribute to the knowledge and understanding of *motor control* of the leech:

1 - The presence or absence of analyzed encoded *descriptors* - the average firing rate (***AFR***) and the *auto-* and *cross-covariance* (**ρ**) - has been associated to stereotyped behaviours defining, respectively, the ***stationary states*** and the motion behaviours, emphasizing that the information obtained from the covariance is a better classifier of the *stationary states*.

2 - Simple behaviours from the ***suckers*** situated in the head and tail of the animal have been associated to electrical patterns recorded from the connective fibres, giving the possibility to identify spikes form command-like systems.

3 - Neuronal information from ganglion's neural population and identified neurons have been associated to simple stereotyped behaviours from head (and/or tail), such as shortening (contraction), elongation and pseudo-swimming (ventilation) behaviours.

4 - The last and emphasizing result is the proposal of ***dendrograms,*** calculated from the correlation between the neuron's population sorted by an algorithm employed, as a new descriptor of the different simple and complex stereotyped behaviours.

General details, results, discussions and conclusions will be here presented. The author of this Ph.D. thesis (L.J.J.H) performed the biological preparations for the experiments, with all the

technical background required, analyzed the data and programmed some algorithms used in this work. Finally, it is worth mentioning that the author decided to use the passive form to avoid the most possible subjective language or personal merit. The real merit of this work is the biological subject of study: the leeches, because without them, this work could not be possible.

INTRODUCTION

The final aim of the life sciences is to understand the biological basis of consciousness and mental processes by which brain perceives, acts, learns, and remembers (Kandel, 2000). With the advances in technology and knowledge in biological sciences, the current view about single nerve cells, groups and layers, synergic ensembles, brain's structure and behaviour have been growing over the last century from a convergence of experimental disciplines like Psychology, Embryology, Physiology, Anatomy and Pharmacology (Kandel, 2000; Nicholls, 2001; Rolls & Treves, 1998). In an area of convergence of all these disciplines - as is the Neurobiology - the diversity of biological preparations in vertebrate and invertebrate systems had contributed to the creation of models which represent the physiology of nervous systems from different points of view. Some of the concluded models have provided important insights into the biophysics of cellular and molecular events like the action potential, mechanisms of signalling or neurotransmitter release. Beyond these cellular models, the simplicity and relatively easy access to invertebrate's nervous systems contributes, in others, to elucidate and encode the information required to compute and monitor a group of neurons (Networks) or the coordination of behaviours (Nicholls, 2001).

The nervous system of the invertebrate leech *Hirudo medicinalis* has became an important subject for neurosciences at the end of the nineteenth century and has provided an important quantity of answers to questions that cover cellular and molecular mechanisms and animal behaviour's coordination as well. The apparent simplicity of the leech's central nervous system (CNS) offers some advantages in the neurobiology: different types of cells can be recognized by visual inspection and electrophysiological properties; it presents high similarity between segmental nervous ganglia; a small number of cells in each ganglion makes easy the parallel extracellular recordings from motoneurons and mechanosensory neurons; neurons are highly accessible to intracellular recording and experimental semi-intact preparations allow long recordings; stereotyped behaviours such as swimming, pseudo-swimming, local bending, crawling, feeding, stretching, twisting and so on are characterized. To deeper understand this system, how it is organized and which are the recent information about the knowledge of this system, the next two chapters will be dedicated to the description of historic aspects, anatomy concepts, and updated information about what is know as the *motor control* of the leech.

CHAPTER 1

THE LEECH

History and Taxonomy

The practice of bloodletting by leeches (a practice used even by ancient Egyptians thousands years before) reached its peak during the last half of the 19th. In the years 1890-1921, Gustaf Retzius published his historic 19 volumes of the *"Biologische Untersuchungen. Neue Folge I–XIX"*, containing fundamental descriptions of anatomy form vertebrates and invertebrates including one detailed and schematic description of the nervous system of *Hirudo medicinalis* (Muller, 1981; Grant G, 2010), this led to consider leech's CNS as an important object of scientific research.

The common use of leeches to solve problems of war injuries during the Napoleonic wars almost depleted their population from Europe (Muller *et al.*, 1981). This practice was forgotten with the appearance of the concept of hygiene and the advances on medicine drugs. Nevertheless, the European medicinal leeches returned to the modern clinical toolbox in the context of flap and replanted surgery (Derganc & Zdravic 1960; Foucher *et al.*, 1981). Specifically, with artery-only replantation (e.g. of digits), free tissue transfer surgery (e.g. skin flaps) and cases of venous obstruction, the post-operative use of leeches to ameliorate congestion improves prognosis and tissue survival in a cost-effective and reliable manner that has yet to be supplanted by mechanical or pharmaceutical alternatives (Siddall *et al.*, 2007).

With regard to the Taxonomy, the vast majority of the world's 650 species of leeches are found in cool freshwater, shallow lakes, ponds and back waters of rivers and creeks. Some of them are marine species due to their proximity with the members of the Oligochaeta. The medicinal leeches are segmented worms belonging to the taxonomic branch of Hirudinea and they are related also to the earthworms. The systematic and taxonomy of leeches is still in need of review. The World Register of Marines Species considers the *Hirudo* genres as the next taxa (WORMS: http://www.marinespecies.org):

Animalia / Annelida / Clitellata / Hirudinea e / Arhynchobdellida / Rhynchobdellida / Oligochaeta / *Hirudo*

Recently, taxonomic discussions have risen up some controversies about the correct identification in ***Hirudo medicinalis*** and ***Hirudo verbana*** due the genetic variability observed on

the phenotype from commercial individuals (Siddall *et al.*, 2007): this is a cause by which in this work the leeches used for the experiments are named just by the gender: ***Hirudo spp.*** Although it is not official information, it is considered that leeches have the conservation status of *Near Threatened*, assigned to species (or lower taxa) that may be considered threatened with extinction in the near future.

ANATOMY OF THE LEECH

Anatomically, on of the major features of the leeches is the presence of the rostral and caudal suckers. Leeches do not add new segments to the body during their mature life and each species has the same number of body segments. This constancy allows a specialization of the different parts of the body and, as a consequence, of the nervous system; this specialization is remarkably identical from one individual to the other, making the leech a suitable organism for neurobiology.

The body of adult leeches from the genre *Hirudo* (without consider any difference between the species *verbana* and *medicinalis*) consists of 4 partially fused segments in the head region, 21 segments along the body and 7 segments in the posterior region forming the tail sucker (Payton, 1981b), 5 annuli correspond to each segment of the mid-body. Exceptions to this rule are the tail region and a fusion of segments on the head region called *Prostonium* (Kristan, 2005). Little organs sensible to light called sensilla are distributed around the central annulus of every segment. The front sucker contains three teeth used to bite the preys. Internally, the intestines containing the ingested blood run all along the body. The leech's own blood circulates in four main vessels: the dorsal sinus, the ventral sinus also containing the CNS and two lateral sinuses which form the beating heart system driven by a neuronal oscillating circuit (Calabrese, 1995). The sexual organs are located in segments 5 and 6, but there are 9 pairs of connected testes in segments 7 to 15. The excretory system is made up of 17 pairs of nephridia from segments 1 to 17 and it is open to the outside through two nephridiophores per ganglion.

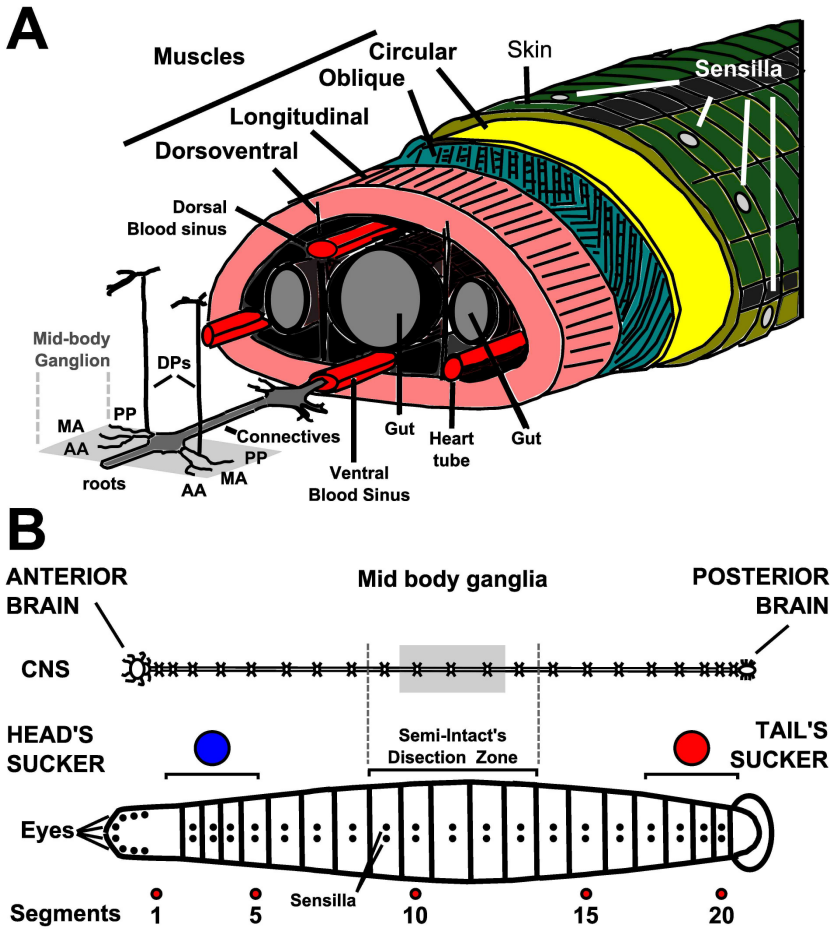

Figure 1.1 ***Leech's Body Structure.*** **A.** *Transversal section of the body.* Cartoon representing with different colours the arrangement and location of tissues and vital organs of the leech: sensilla, skin, gut, blood sinus and lateral heart tubes. The musculature is organized in 4 types: Circular, Oblique, Longitudinal and Dorsoventral. Every segment of the mid body (5 annuli) is innervated by the axonal processes contained in the roots of one ganglion: AA, MA, DP and PP (see text), indicated by gray square. The muscular activity depends on the innervations of the different motoneurons (excitors and inhibitors) that send their axonal processes from the ganglion to their respective segment and even beyond it. Together the musculature controlled by the CNS produces the different motivational behaviours. **B**. *Comparative description of the CNS and Whole Body*. Scheme of the CNS (upper) compared with the whole body (bottom scheme). CNS consists in 21 mid body ganglia connected to Anterior and Posterior Brains (which innervates head and tail respectively) by the connective fibres. One ganglion corresponds to one segment and can be located with visual inspection of the body by the presence of the sensilla in the respective annulus. Head is formed by the prostonium and 4 segments fused having the characteristic eyes-like structures. Tail is characterized by the presence of a sucker (with a different embryonic origin than head's sucker). On this works as will be discussed in posterior chapters, head and tail were tracked by beads glued at the dorsal side over the skin (in blue: segments 1 to 5 and in red: from 17 to 20). The Semi-intact consisted in access to CNS and record the neural activity from the segmental ganglia 9-13 (see methods). Panel **A** was modified from Muller *et al.* (1981).

The musculature is disposed in three layers (longitudinal, oblique, and circular) form the main part of the body wall and is, therefore, distributed uniformly around the perimeter of the body; another type of muscles (dorsoventral) connects internally the dorsal and ventral sides of

the animal. A further kind of muscles, the annulus erectors, is located immediately under the skin and is responsible for erecting annuli in ridges. The longitudinal muscles, the thickest and deepest layer, shorten the leech in the longitudinal direction when contracting; the oblique muscles, an outer thin layer, twist the body; the circular muscles lie just under the skin and are able to elongate the animal when they contract; finally, the dorsoventral muscles flatten the body.

CENTRAL NERVOUS SYSTEM OF THE LEECH

The CNS is a chain of ganglia all linked by the connectives fibres. The connectives are large bundles of axons crossing along the body and they are composed by a couple of thick nerves and a third named Faivre's nerve, running centrally between them. The 21 segmental ganglia (G1-G21) are numbered sequentially from the anterior to the posterior region and are almost identical, except for G5 and G6 which innervate the sexual organs. The first 4 ganglia in the head region (H1-H4) are fused and modified to form the head brain, which is composed by the specialized units: supraesophageal and subesophageal units, where the structure of 4 segmental ganglia is still recognizable. The last 7 ganglia (T1-T7) are fused in the specialized tail brain (Nicholls 2001; Kristan, 2005). The leech CNS presents high similarity between segmental nervous ganglia, a small number of cells in each ganglion of the nervous chain, easy access via extracellular recordings from motoneurons, high accessibility to intracellular recording both of neurons and glial cells, long duration of experimental preparations, and limited repertoire of stereotyped motor behaviours.

Several fundamental issues of neuroscience have been addressed in the last 35 years using the leech nervous system: physiology of glial cells (Kuffler & Potter, 1964; Kuffler & Nicholls, 1966; Deitmer & Kristan, 1999), action potential generation and conduction block (Gu, 1991; Mar & Drapeau, 1996; Melinek & Muller, 1996), motor system coordination (Kristan, 1982; Wittenberg & Kristan, 1992a & 1992b; Baader & Bächtold, 1997), oscillatory circuits (Calabrese, 1977; Stent, 1978; Pearce & Friesen, 1985a & 1985b; Brodfuehrer, 1995b; Calabrese, 1995), neurotransmitters (Willard, 1981; Gardner & Walker, 1982; Thorogood & Brodfuehrer, 1995; Szczupak & Kristan, 1995; O'Gara , 1999), neuromodulation (Hashemzadeh-Gargari, 1989, Gascoigne & McVean, 1991), sensory cells and signal transduction (Nicholls & Baylor, 1968; Blackshaw, 1981b, 1993; Friesen, 1981; Blackshaw, 1982, Peterson 1985a & 1985b), neural basis of learning (Boulis & Sahley, 1988; Sahley, 1994a & 1994b; Modney, 1997), development (Martindale & Shankland, 1990; Shain, 1998), axon growth and

regeneration (Jansen & Nicholls, 1972; Jellies, 1995), test for new experimental techniques (Wilson, 1994; Cacciatore, 1999; Canepari, 1996), models of complete real networks (Lewis and Kristan, 1998b). Each of the segmental ganglia innervates a well defined segment of the body wall by two pairs of nerves (roots) arising symmetrically from the left and right sides. The four roots are defined as anterior and posterior, left and right. The two posterior roots bifurcate near the ganglion, each one originating two branches called posterior-posterior nerves (PP) and dorsal posterior nerve (DP). Through these nerves the ganglion innervates the whole segment. The anterior and PP nerves innervate the territory corresponding to the lateral and ventral part of the animal, while the DP nerves innervate the dorsal part of the animal.

Ganglia and Neurons

Every segmental ganglion contains about 400 neurons, with the exception of ganglia 5 and 6, which innervate sexual organs and contain over 700 cells. The aspect and structure of the ganglion is conserved from segment to segment and from animal to animal; indeed, the same neurons are recurrent in each ganglion for their positions, dimensions and functions. All neurons in the leech ganglion are monopolar; the cell bodies are contained in six separated regions (packets), each enveloped by a glial cell, while their innervations take place in the central neuropil, a specialized region in which synapses are arranged, surrounded by two giant glial cells (Schmidt & Deitmer, 1996); two other glials form the nuclei of the connective nerves. Neurons (as in other biological systems) are divided into three categories over the base of their physiology: Sensory neurons, Interneurons and Motoneurons.

Sensory Neurons

This first type translate a physical input coming from the environment into membrane potentials, or more generally are specialized to transform a physical quantity like, pressure, heat, salt concentration into a change of their electrical properties. Motoneurons and sensory neurons project outside the ganglion to the periphery through the roots; sensory neurons also project in the connectives. Other excitable cells project their branches outside the CNS, for example Retzius cells whose firing is related to serotonin release (Willard, 1981; Mar & Drapeau, 1996; Fernandez De Miguel & Drapeau, 1995) and AP cells (Gu, 1991; Melinek & Muller, 1996) of still unknown function.

Classical studies on the leech cells were focused on sensory neurons, which are responsible for three different mechanosensory modalities (Nicholls and Baylor, 1968; Yau, 1976a; Yau, 1976b; Blackshaw, 1981a & 1981b; Blackshaw, 1982): T (touch) cells are three for each hemiganglion and respond to a light mechanical stimulus applied to the skin, P (pressure) cells are two for each hemiganglion and respond to stronger stimuli, N (noxious) cells are two for each hemiganglion and respond to a damaging stimulation of the skin, with a threshold more than three times higher than the P cells (Carlton & McVean, 1995). Recent studies have demonstrated that N cells exhibit also functional properties similar to those of polymodal nociceptive neurons in mammals (Pastor, 1996), i.e. they are not simple mechanosensitive cells but respond to different sensory modalities of noxious stimulus like temperature rise and irritant chemical substances.

The mechanosensory cells in each ganglion innervate a well defined territory of the skin in the corresponding segment (Nicholls and Baylor, 1968), for example the three T cells respond respectively to the stimulation of the ventral (T_v), lateral (T_l) and dorsal (T_d) region of the segment. Analogously, P cells respond one to ventral (P_v) and the other to dorsal (P_d) touch stimuli. For the two ipsilateral N cells (N_m, N_l) the receptive fields in the same ganglion are approximately coincident and span the entire hemi segment from dorsal to ventral midline (Blackshaw, 1982).

These neurons are characterized by a main process arising from the cell body that gives rise to several branches projecting through the ipsilateral roots and the connectives to innervate the roots of adjacent ganglia. The receptive fields span 12-13 annuli over the central and the two adjacent segments; they appear to be composed of several non overlapping sub-fields innervated by separate branches of the same cell (Nicholls and Baylor, 1968; Yau, 1976). T cells have the simplest branching pattern in the ganglion, while N cells have the most complex projecting also though contralateral neuropile. T cells branch extensively close to the surface in the epithelial layer of the skin, with a high density of terminals each one able to transduce independently a mechanical stimulus; the highest density of sensory terminals is in the central segment. The P cells branch less extensively and make far less terminals than the touch cells (Blackshaw, 1981a). The N neurons are different in that their branches end farther from the surface, below the epithelial layer, unlike the T cells, and also make distinct coil shaped terminals associated with large neurons (Hoovers cells) of the peripheral system: a feature that may be compatible with their polymodal function (Pastor, 1996), as previously explained.

Interneurons

The category of interneurons broadly contains all neurons whose entire arborisation does not exit from the CNS, but often exits the ganglion through the connectives: they are involved in a variety of functions such as heartbeat, motor control, reproduction, and learning. The best example of interneurons is the network of S cells, involved in the shortening reaction. There is one S cell per ganglion which projects a very large axon through the Faivre's nerve in the connectives; they are all strongly electrically coupled and represent probably the fastest electrical pathway connecting the two ends of the animal (Bagnoli, 1979; Baader & Bächtold, 1997). Other interneurons have been identified in head, tails and mid body ganglion, but for the case of this thesis, they are mentioned in subsequent chapters.

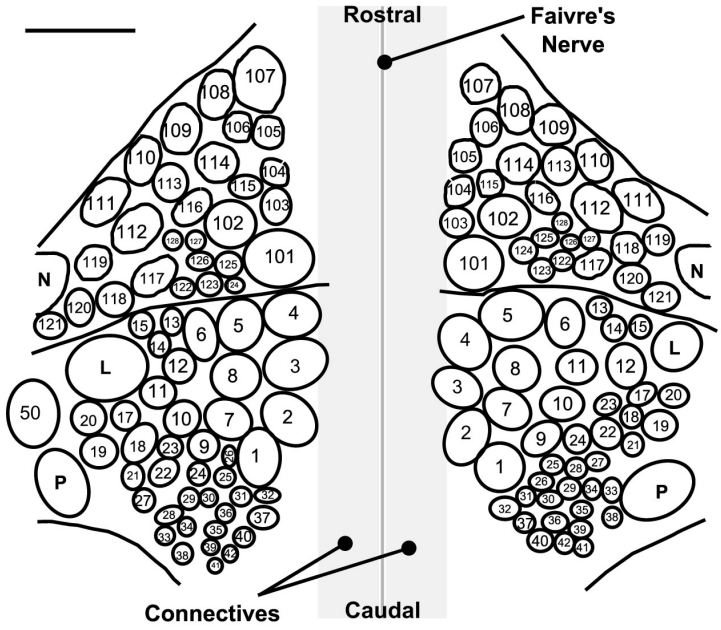

Figure 1.2, ***Structure and cell identification in the Dorsal side from a mid body ganglion***. This image shows the position from all identified sensorial neurons, interneurons and motoneurons. N and P cells correspond to mechanosensory neurons while L cell is one of the most important motoneurons. The gray zones in the centre correspond respectively to connectives fibres and the Faivre's Nerve, important structures for the axonal communication between neighbouring ganglia. Bar corresponds to 100 □m (figure modified from Ort *et al.*, 1974).

Motoneurons

For this work, this type of cells is the most relevant due to the relation between the patterns of motion or behaviour that can be associated to the different activators. In each hemiganglion

there are 21 excitatory and 7 inhibitory identified motoneurons (Stuart, 1970; Ort, 1974; Sawada, 1976; Stent, 1978; Muller, 1981; Norris & Calabrese, 1987; Baader, 1997). When the ganglion is observed in transmitted light, 25 of these can be observed on the dorsal side and a total of 3 on the ventral side (fig 1.2). All motoneurons have their contralateral homolog (and homonym) that lies almost in the same contralateral location. Motoneurons are responsible for the excitation or inhibition of muscles (Stuart, 1970; Ort, 1974; Sawada, 1976; Stent, 1978)

The Annulus Erector cell (AE) is an exception, due to the fact that it erects the skin at the centre of annuli and the heart excitor (HE) which supplies the lateral heart tubes, they are all responsible for the leech locomotion and movement. They can be divided into four groups, according to the muscle fibres they innervate: longitudinal, circular, oblique, dorsoventral. With the only exception of cell 4, a ventral longitudinal excitor, and cell 117, a dorsoventral excitor, all motoneurons exit the ganglion via the contralateral roots to innervate the corresponding body wall (Ort, 1974). Their fields of innervations extend longitudinally into adjacent body segments (Blackshaw, 1981a) and frequently overlap with those of neurons supplying the same muscles group. The motoneurons probably innervate muscle fibres by many terminals along their length, as it happens in crustacean (Stuart, 1970).

Excitatory motoneurons induce a smooth contraction of muscle fibres when increasing the firing frequency above a certain threshold level and over a functional range: each motoneuron in the ganglion shows a characteristic kinetics of the contraction. The rising of the firing frequency over the characteristic active range of the neuron increases the contraction rate and its peak amplitude (Mason and Kristan, 1982; Blackshaw & Nicholls, 1995).

Inhibitory motoneurons counteract the effect of excitors. Since inhibitor activity does not reduce basal tension, it is necessary for the excitors to be active in order for the inhibitors to exert a peripheral effect. The ability of inhibitors to oppose strongly the effects of excitors suggest they contact most of the fibres contacted by the excitors (Mason and Kristan, 1982). In addition to their direct action on body wall, they also inhibit centrally the excitatory cells which innervate the same muscle (Granzow, 1985). Unlike the contraction, the relaxation of muscles is much slower, but the leech provides a modulation system. Stimulation of Retzius cells evokes slow reduction of tone in the longitudinal muscle and increases the rate of the slow phase of relaxation following a contraction; these effects have a long latency and duration and are mimicked by direct application of serotonin. There are 7 to 9 serotonin-containing cells in the leech ganglion (Gascoigne and McVean, 1991) but among them only the Retzius cells send processes to the periphery. There is some evidence for serotonin as an inhibitory neuromuscular transmitter in the leech *Haementeria ghilianii*, and also as a central inhibitory transmitter, since

it is present in the blood and probably in the neuropil (Gardner and Walker, 1982; Mason and Kristan, 1982).

Intracellular recordings of motoneurons show traces in which the membrane potential apparently does not spike (Stuart, 1970). This is due to the lack of excitability of the soma; the action potentials arise at a site distant from the soma, near the primary bifurcation of the axon (Gu, 1991; Blackshaw & Nicholls, 1995). There is consistent evidence that the leech longitudinal nerve muscle junction is cholinergic (Gardner and Walker, 1982) and more generally that excitatory motoneurons synthesize, accumulate and release acetylcholine (Norris & Calabrese, 1987). FMRFamide (an amide peptide: Phe-Met-Arg-Phe-NH_2) appears to play a significant role in controlling the heartbeat: its immunoreactivity has been localized in heart excitors and heart interneurons (Norris & Calabrese, 1987). Leech inhibitory motoneurons are thought to be GABAergic (Blackshaw & Nicholls, 1995), since the longitudinal motoneurons take up and synthesise GABA from the precursor glutamate and, further, central and peripheral inhibitory synaptic effects are mimicked by GABA.

One of the best examples of identified motoneurons excitors of the leech system is the named cell 3. Concentrated results from many authors can be compared here. Cell 3 has been recorded using extracellular and/or intracellular electrodes (Stuart, 1970; Ort, 1974; Sawada, 1976; Stent, 1978; Muller, 1981; Norris & Calabrese, 1987; Baader, 1997; Kristan, 1974-1976-1998-2005; Shawn, 1997). Anatomically, it can be identified by its size; it is located in the dorsal face and in the central part of the ganglion; it is one of the biggest cells next to 1,2,4 and 5 cells (figure 1.2), but it is distinguished from the others by the important burst activity presented during different behavioural performance. The pair of cell 3 is coupled electrically and both cells present more or less the same burst activity contralateral to the other (as some other identified neurons). Cell 3 is easily identifiable in the extracellular recordings of the DP roots due to the big amplitude of the waveform and its axonal process is only present in this root, generating specific spikes (figure 1.3). It is associated to the whole-body shortening behaviour as it innervates the longitudinal dorsal muscles producing contractions. It produces oscillations in the membrane potential during intracellular recordings and it can be observed as intrinsically spiking on the extracellular traces during the swimming behaviour.

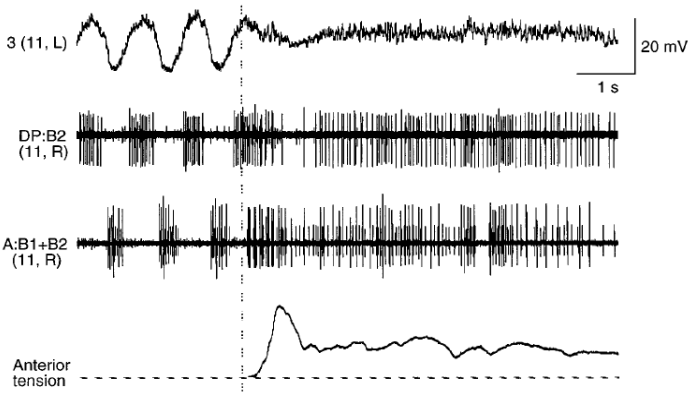

Figure 1.3 ***Motoneuron 3 activity properties*****.** Intra (upper trace) and extracellular (subsequent traces) recordings from cell 3 during two basic stereotyped behaviours: first instants of a swimming period (characteristic oscillations of the resting potential from cell 3 and intrinsic bursts in spike potentials of extracellular recordings) compared with a shortening behaviour (lack of oscillations on the resting potential that makes pass to a regular-fast burst activity) in a leech semi-intact preparation. Shortening behaviour (lower trace) is perceived from tracking the head position with a tensor (figure taken from Shawn, 1997).

CHAPTER 2

MOTOR CONTROL: BEHAVIOUR AND NEURONAL PROCESSING

The vast majority of animals have nervous systems able to construct internal representations of the world by integrating information from the different sensory systems. Some of these representations have been reconstructed from results obtained in experiments made with invertebrates, so it is a fact that in evolutive low levels of the *Animalia* kingdom these representations occur and gradually grow up in with the evolutive chain from the integral response and sensorial information to the point of cognition in higher evoluted vertebrates. Whatever the case, the mechanism is more or less the same: sensory representations help the motor systems to plan, coordinate and execute motor programs responsible for generating movements. Motor systems are essential to balance and regulate the posture, to move and to communicate through speech or gestures. From the free energy point of view, sensory systems transform physical energy into neural signals (inputs) which are, in turn, processed and translated into contractile muscular forces which generate movements. These processes are the origin of the motion and the combination of motions lead to the complexity of the behaviours (Nicholls, 2001; Enquist & Ghirlanda, 2005).

What is animal behaviour? And, what does it mean to understand animal behaviour? Different theories of behaviour have the same scope: they deal with how the animal as a whole interacts with its physical, ecological and social environment, in particular through reception of sensory stimulation and actions produced by motor patterns, pheromone release or change in body's coloration. These theories want to explain, predict or control what animals do and they also consider situations in which internal factors such as memory and physiological states are not easily accessible (Enquist & Ghirlanda, 2005).

Ethology and comparative psychology are two major research traditions dealing with behaviours. Within these disciplines, it is still important to explore behaviour as a function of external stimuli and observable factors. Nevertheless, internal factors such as physiological states and memory are studied indirectly from observations of behaviour and event's history along the time. It is relatively easy to monitor and control external situations, but the access to internal factors is usually limited. However, it is not possible to ignore internal factors because external factors are not alone in causing behaviour. So integration of different mechanisms facilitates the development of behaviour models (Enquist & Ghirlanda, 2005).

In Biology, there are two causal explanations of the behaviour, named as *proximate* and

ultimate explanations (Baker, 1938; Mayr, 1961). *Proximate explanations* appeal to motivational variables, experiences and genotype as the cause of behaviour. *Ultimate explanations* refer to selection pressures and other factors that cause the evolution of behaviour. These two kinds of causal explanations are independent and complementary, but one cannot replace the other. Nevertheless recent studies propose three new explanations and consider that these exist in three levels: *Motivation*, *Ontogeny* and *Evolution* (Enquist & Ghirlanda, 2005; Tinbergen, 1951).

A *motivational explanation* refers to individual behaviour, and the goal is to predict behaviour from variables such as external stimulation and internal physiological states understanding behaviour mechanisms (Hogan, 1994). The term *motivation* refers to generally reversible and often short term changes in behaviour. The causes are the external stimuli and internal states that change and produce an effect: a behavioural response. In this explanation there is strong consideration in the *Internal States* of the body and the Nervous System. A simple example is how animals use behaviour to regulate food and water intake, this of course follows to know mechanisms of perception, decision making, motor control, etc. For the *Ontogeny* explanation, it refers to the development of the behaviour mechanism during an individual's lifetime. As causes of this explanation, the genotype and all the experiences from an individual are essential. The effects of this explanation are considered as behaviour maps, and the states to study are in the level of changes in the structure of the nervous system and memory (Hogan, 1994). Particular phenomena include learning, maturation, genetic predispositions and the development of the nervous system. The *Evolutionary* explanation considers the behaviours in population of individuals and is manifested by changes in the population's gene pool (Futuyama, 1998). The causes include mutations, recombination, natural selection and chance.

In animals, there are two motivational variables: the external and internal states (McFarland, 1999). Both variables can be considered as stimuli and will have a response considering the internal motivational states. Internal variables can be classified in state variables of the body and states from the nervous system. The nervous system is divided into memory and regulatory states. *States of memory* are considered as all the long-term storage, encoded in structural properties such as the pattern of connections between neurons. In the meanwhile, *regulatory states* are those which are not memory but contribute to structuring the behaviour in time. Instances are the activity state of neurons, concentration of neurotransmitters and neuromodulators. External stimuli and body states influence behaviours via specialized receptors which transform various physical realities into neural activity. The *memory* and *regulatory states* differ from body states in the crucial aspect of the regulation of behaviour. These two first

mentioned storage information and structure the behaviour in the time, in such a way that their lack could be translated into a behaviour controlled totally by current input from senses (McFarland, 1999; Enquist & Ghirlanda, 2005). Considering that the behaviour mechanism is produced by this internal and external variables, animals follow 3 steps to produce any behaviour: the *Sensory* information is the first part, followed by the process of *decision* to select any position or convenient behaviour and, finally, the *motor control* acting as regulator of the behaviour, producing a feed back to accurate or discriminate behaviours on a new decision process.

Motor control means how the nervous system and skeleton-muscular apparatus contribute to behaviour (Enquist & Ghirlanda, 2005). It is implemented by circuits within the central nervous system and importantly with the contribution of central pattern generators that produce autonomous motor patterns related to control and sensory information (Hinde, 1970; Lorenz, 1970; Cohen & Boothe, 2003; Enquist & Ghirlanda, 2005). Historically, central pattern generators were conceived in 1918 by Graham Brown, who showed that cats, deprived of their sensory inputs, could still produce coordinated stepping and he even suggested a possible mechanism (Hill *et al.*, 2003). The idea of the central pattern generators was accepted considering that before animals were seen as reactive, reflexes-machines. Eric Von Holst (1937) was among the first to propose the evidence of the central pattern generators (and also this idea had been mentioned in works by Lord Adrian in 1931) analyzing the rhythmic activity of the locomotion in the earthworm, cutting the afferent nerves and isolating the nerve cord in a physiological solution.

The origin of the behaviours in leeches can be explained from the point of view of the *motivational* definition (McFarland, 1999). However, to achieve this goal, it is not sufficient to have a complete scheme of how a leech behaves (that is actually what a researcher measures, e.g. on intact animals in any artificial or natural environment), but it is also necessary a list of characterizations of the internal states when the animal produces certain behaviours at the most possible. The list started the first years of the visual inspection of ganglia (as shown in previous chapter), and it is growing up with the contributions from many authors in more than one century of Neurobiology of leeches. Obviously, this is strictly related to the technological advances in electrophysiology, which have permitted to standardize many techniques beneficially (e.g. the semi intact preparation) up to know the state of a neural network (or central pattern generators) during some behaviours (Briggman & Kristan, 2006; Briggman & Kristan, 2008). However, even if the electrophysiological technique has been selected to study behaviour in leeches, one

should consider integrating electrophysiological information with observation of behaviour in intact animals. Furthermore, it may be highly relevant the comparison with animal's groups (Bisson G. & Torre V; personal communication): this integration would finally allow covering an entire panorama of the *motivational* definition. Talking about the technique used as strategy in this work to monitor behaviours and internal states, the analysis of spontaneous behaviours in leech semi-intact preparations (Kristan *et al.,* 1974B) is the tool that permits to search explanations of behaviours from the point of view of the *motor control*. As result, a collection of stimulated or spontaneous events could help to understand behaviours and even to predict some of them. Precisely, next lines are focused on what is known about the *motor control* in leech behaviours.

LEECH BEHAVIOURS

The leech exhibits a limited repertoire of basic adult motor behaviours that are already present in the embryonic phase (Sawyer, 1981; Baader & Kristan, 1992; Reynolds *et al.*, 1998): local bending and the associated local shortening, whole-body shortening, crawling, swimming. Bending and shortening are essentially escape reactions, crawling is a locomotory movement and swimming can be both (Arisi *et al.*, 2001; Zoccolan *et al.*, 2002). Instead, other kinds of behaviour still do not have a clear comprehension on their origin; examples are the pseudo-swimming (ventilation or local swimming) and the stationary states (Mazzoni *et al.*, 2005). It is not clear yet if pseudo-swimming is either a behavioural signal of comfort, communication, alert (wakefulness) in groups of animals or even a temperature stress in single animals (Bisson, G., personal communication). The stationary state is present with high occurrence in many of the observational experiments with intact leeches (Mazzoni *et al.*, 2005; Garcia-Pérez *et al.*, 2005), but it is not know yet if it can be originated by the lack of water motion on the observational tanks or by the lack of environmental stimulus as the animals are isolated. Moreover, it is unknown whether the leech sleeps during these moments of rest since there is not neural information reported during these behaviours.

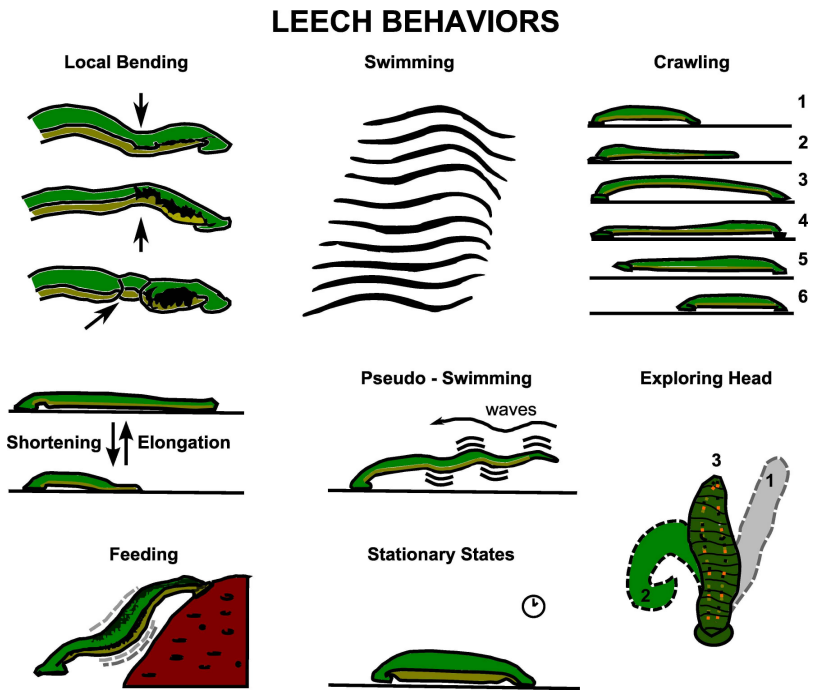

Figure 2.1 ***Leech behaviours***. Cartoons representing the different behaviours in leeches that have been object of research nowadays. The ***local bending*** is an escape reaction, touching any segment from animal's body; the response is a mechanical retraction of the segment. The retraction is opposite to the side from which the stimulus is coming (represented as the arrows here), and can be dorsal, ventral or lateral. ***Swimming***: sequential video frames of a freely swimming leech. A full sinusoid-like swim wave is developed along the leech body, with a crest and a through passing backward while the leech is swimming forward. ***Crawling***: the front sucker release and the commencement of a front-to-back wave of segmental elongations ***(1&2)***; afterwards, the front sucker attaches and a front-to-back wave of contraction ensue ***(3)***; there is an overlap between contraction of anterior segments and elongation of posterior segments ***(4)***. During the contraction wave the rear sucker releases ***(5)*** and later it attaches after the animal has fully shortened, completing the step ***(6)***. The ***Shortening*** is presented when the animal strongly contracts the whole body or mid body (local shortening) while the ***Elongation*** is presented when the leech is extending itself sending on the longitudinal plain one or both extremes of the body (been head or tail). In the ***Feeding***, leeches loose the capacity to enter in any of the shown behaviours once they achieve the prey and start to feed. In this behaviour, the head's sucker attach to the prey producing damage and vacuum in the selected region eliciting rhythmic contractions from the first segments to the mid body (ingesting blood to the gut).The rear part stay immobile and the rear sucker looses motion as soon as the gut is filled. Animals can fold their body's volume and obviously their weight around three times. This behaviour cancels many important patterns of sensibility, and even the animal can be damaged completely without detaching the head. ***Pseudo-Swimming*** is produced when rear sucker is attached and head elicits oscillations similar to those observed in swimming. The period of the oscillations is less than those elicited in swimming episodes and there are still doubts about the origin of this behaviour. ***Exploring s***cheme represents an exploring event resumed in 3 steps and viewed from a dorsal side. Exploring is a behaviour that can be combined with episodes of swimming or crawling and is related to the searching for any prey, although it could be part of the process of accustoming to any environment. The head can move without any periodic frequency and it touches the environment with the front sucker, in the meanwhile the rear sucker stays firmly attached. Numbers are just a representation of a temporal change of position that starts on the right side of the body ***(1)***, passes to the left ***(2)***, and finishes in a "present" position ***(3)***. ***Stationary states*** it is considered the behaviour more frequent during the leech's life. Animals can enter in this state being immobile for long times (With exception of the Pseudo-Swimming, Stationary States and Exploring head, this figure was modified from Kristan, 2005).

Local Bending

Local bending consists of a contraction of longitudinal muscles on the stimulated side of the segment and of a relaxation on the opposite side, leading the segment away from the stimulus in the opposite direction (Kristan, 1982). Main mechanosensory neurons are the P and the T cells (Kristan, 2005). The stimulus direction is encoded almost completely by the P cells, with the T cells playing an accessory role (Lewis & Kristan, 1998a, 1998b and 1998c). The amplitude of the response depends on P cells more than N or T. Thus, P cells are more important for this behaviour. The receptive field of each P cell is the top of a cosine function, cut off at ±90°, considering the circumference of the body as 360° (Kristan, 1982; Lewis & Kristan, 1998a, 1998b and 1998c). Seventeen interneurons are involved in the local bending, 6 bilateral and 1 unpaired (Lewis & Kristan, 1998b). The centre of the receptive field for each identified interneuron is characteristic of that cell, and the locations of the centres are distributed fairly evenly around the dorsal and lateral body wall, but they do not have ventral receptive fields. The connections from interneurons to motoneurons have been inferred from the responses of motoneurons to stimulating P cells, both individually and in adjacent pairs. Motoneurons are characterized by a cosine function also, and they are considered to be inhibited from P cells at the opposite side, which allow the retraction on the opposite side to the stimulus zone. The receptive fields of the motoneurons, like those of the P cells and interneurons, are distributed uniformly over the body wall. In fact, the tactile receptive fields of the motoneurons are very similar to their motor units. For instance, excitatory dorsal longitudinal motoneurons have receptive fields centred on the dorsal surface and excitatory ventral motoneurons have receptive fields centred on the ventral surface (Kristan, 2005). Local shortening is strictly associated with local bending; around the stimulus site a number of segments increasing with the stimulus intensity are involved, but the stimulated segment only bends and does not shorten (Wittenberg & Kristan, 1992b).

Swimming

This is the most studied behaviour in the leech, extending the knowledge from the simple contraction on longitudinal muscles to the conceived idea of the oscillatory cells as central patterns generators. During swimming, the leech body is flattened to form an elongated ribbon by tonic contractions of dorsoventral muscles, the alternating contraction and relaxation of dorsal

and ventral longitudinal muscles act against internal pressures, with a period of about 0.3–1.0 s, to generate rhythmic bending in body segments (Uexküll, 1905; Gray *et al.*, 1938; Kristan *et al.*, 1974a; Wilson *et al.*, 1996b). The neural activity characteristic of this behaviour occurs in the isolated nerve cord (fictive swimming: period of 0.5–2 s) and also in isolated ganglia if serotonin is provided to the preparation. A complete study on this behaviour is roughly described over the central oscillator which generates the swimming rhythm and includes studies on the central and sensory mechanisms which control initiation and termination of swim episodes, as well as on the mechanisms for chemical modulation of swim expression and, most recently, on the role of sensory feedback in intersegmental coordination (Kristan, 2005).

The swimming model consists of an antiphasic contraction and relaxation of the dorsal and ventral longitudinal muscles modulated by a cascade of stimulated and inhibited interconnected neurons (Stuart, 1970; Ort *et al.*, 1974; Kristan *et al.*, 1974B; Norris & Calabrese, 1987; Brodfuehrer *et al.*, 1995a; Pearce & Friesen, 1985a and 1985b; Poon *et al.*, 1978; Weeks, 1982; Friesen & Hocker, 2001; Briggman & Kristan, 2005; Briggman & Kristan, 2006). Four types of sensory neurons can initiate the swimming (T, P, N and SMR). Apart from these, four types of trigger and control neurons influence the sustaining, finishing or initiating the behaviour: Tr2, Tr1, SE1, and SIN1. Five pairs of gating-control neurons: 256, 21/61, 204/205, 208. Finally, the oscillatory neurons have been described with voltage sensitive dyes in both faces of the ganglion using a prediction map that combines information obtained from the dyes and previous works; these neurons are divided as follows: nine pairs of active neurons during dorsal contraction phase (most of them exciter motoneurons): 107, 115, 123, 119, 5, 3, 2, 7 and 17; four pairs of neurons active on ventral contraction (most of them inhibitory motoneurons): 108, 102, 4 and 8; two types of target neurons in the dorsal-ventral contraction phase: 27 and 33; two types of target neurons in the ventral-dorsal contraction phase: 28 and 1 (Briggman & Kristan, 2006).

The research on the identification of the participating interneurons has been focused on finding three main properties of those interneurons: (a) membrane potential phase-locked to the swimming rhythms, (b) current injection into the interneuron soma: either depolarization or hyperpolarisation shifting the phase of swimming activity, and (c) synaptic interactions with other candidate oscillator interneurons. Obtained results showed that these interneurons are small-sized, inhibitory and bilaterally paired cells: 27, 28, 33, 60, 115, 123 and cell 208, considering the last one as unpaired medium-sized excitatory (Poon *et al.*, 1978; Weeks, 1982; Friesen & Hocker, 2001). However, definitive information about maximal projections for individual oscillator interneurons remains elusive. The current understanding is that interneurons

project about six segments, but no more than seven segments (Pearce & Friesen, 1985b; Friesen & Hocker, 2001), except for cell 208, which may project as far as 10 segments (Kristan, 2005).

Multiple and unknown factors determine whether swimming will occur in response to any stimulus (Cellucci *et al.*, 2000). With respect of the control of the swimming by initiators and terminating neurons, it is known that in the head there are some key interneurons, not present in the segmental ganglia, which are considered the best candidates to control this behaviour: cells Tr1, Tr2, Tr3 (swim trigger interneurons), SIN1 (swim inhibitory interneuron), SE1 (swim excitatory interneuron). These neurons are at the highest level in the hierarchy of the circuit, indeed above the CPG, and project caudally probably along the entire nerve chord, exciting swim oscillatory cells in every ganglion. Tr1, Tr2, Tr3 can trigger swimming when stimulated, SIN1 is part of the swim inactivating system, while SE1, together with Tr1 and Tr3, is part of the swim activating system. Body wall stimulation, followed by Tr1 activation, elicits concurrent depolarization of all cell 204 gating neurons. Tr2 is particularly interesting since it acts like a toggle switch: brief stimulation can elicit swimming activity, while a second stimulus, once swimming has commenced, brings that activity to an abrupt halt (O'Gara & Friesen, 1995). Cells 204/205, in turn, drive both inter- and motoneurons (Weeks, 1982; Nussbaum *et al.*, 1987). Interestingly, only three identified members of the central swim oscillator receive direct input from cells 204/205: cells 115, 28, and 208. At present, the only identified target for Tr2 is cell 256, a neuron that terminates swimming activity (Taylor *et al.*, 2003).

Control of leech swimming is obviously more complex than this suggested linear cascade of triggers, interneuron and motoneurons. Head's brain has a marked inhibitory effect on swimming, while the tail's brain facilitates swim initiation and duration, by reversing the inhibitory action of the head's brain and prolonging swim episodes (Brodfuehrer *et al.*, 1993). These effects of the head and tail brains reverse within seconds when the impulse traffic to the brains is interrupted and reinstated. Hence synaptic (rather than hormonal) mechanisms appear to play a role, although those that mediate the excitatory actions of the tail ganglion are unknown. The study of the agonistic or antagonistic effects of different hormones in the swimming activity revealed that Serotonin (5-HT) is a modulator of animal locomotion and, indeed, it is present in the leech blood. The addition of serotonin to preparations like nerve cord and single isolated ganglion proves that the coordination is maintained by a CPG present in all ganglia. Moreover, intracellular stimulation of the serotonergic system (including the giant Retzius cells) facilitates swimming (Willard, 1981).

Serotonin is recognized as the major CPGs modulator due to the synapses induced by serotonergic interneurons over oscillators, and peripherally, acting on the muscle. Leeches with a

high blood concentration of 5-HT swim more frequently, and isolated nerve cord preparations engage in swimming activity spontaneously when 5-HT levels are elevated (Willard, 1981; Brodfuehrer *et al.,* 1995). On the contrary, bath application of dopamine to isolated nerve cords inhibits all ongoing and nerve-evoked swimming; this is correlated with the discovery that dopaminergic neurons are directly coupled to Tr2 (Crisp & Mesce, 2004). Thus, dopamine can coordinate biting with the termination of swimming.

Octopamine can induce swimming when bath applied to isolated nerve cords with the brain removed (Hashemzadeh-Gargari & Friesen, 1989) or attached (Crisp & Mesce, 2003). The dorsolateral-octopamine cells (DL-O) have been identified as the set of segmental neurons containing and synthesizing octopamine (Gilchrist *et al.*, 1995; Crisp *et al.*, 2002). The segmental Leydig cells, which closely neighbour the DLOS, were at first thought to contain octopamine (Belanger & Orchard, 1988). Leydig cells are not octopaminergic (Crisp *et al.*, 2002), but their study helped to establish that octopamine is a natural neuromodulator in the leech. These cells may act in parallel with the Retzius neurons and other serotonergic cells (61 and 21). Subsequent studies documented bath application of a mixture of serotonin-octopamine in isolated nerve cords with brains, resulting in a novel non-additive suppression of swimming, followed by a robust activation of swimming after the mixture is removed during a 30 min saline wash (Mesce *et al.*, 2001).

Another CPGs modulator is the glutamate, which is involved, as excitatory neurotransmitter, in the activation of oscillating circuits by the leading trigger interneuron, cell 204 (Thorogood & Brodfuehrer, 1995). Recently it has been reported that it acts through non-NMDA receptors at synapses between P cells and Tr1, between Tr1 and cell 204, and between cell 204 and cells 28, 115, and 208 (Brodfuehrer & Cohen, 1990 and 1992; Thorogood & Brodfuehrer, 1995; Brodfuehrer & Thorogood, 2001).

Crawling

Crawling is the normal locomotory behaviour of the leech in the terrestrial environment. A vermiform crawling locomotion cycle in the medicinal leech consists of elongation and contraction phases: The leech is initially attached to the substrate both by the front and the rear suckers, then it releases the front sucker and a head-to-tail wave of elongation leads the leech to attach farther the front sucker. This last event triggers the release of the rear sucker, and then the leech shortens completely while the front sucker remains attached, finally rear sucker attaches again. In intact leeches, a step takes 3–10 s (Stern-Tomlinson *et al.*, 1986), although it can take

up to 20s in dissected leeches. Two different modes of crawling have been reported: the common crawling and the so called ‘‘inch-worm crawl’’ (or ‘‘looping’’), that is faster (1–3 s) and brings the suckers adjacent to one another at the end of contraction. Inch-worm crawling can be observed only when the leech is under the water and it is strongly stimulated when the animal is pinched or very hungry. Inch-worming is more efficient than a vermiform step because it allows the leech to progress by nearly a fully-extended body length with every inch-worm step (Kristan, 2005). Most of the work has been focused on vermiform steps since it is difficult to provide a leech with the appropriate conditions for inch-worming while recording from its nervous system (Kristan, 2005). Crawling is a highly variable behaviour and leeches, sometimes, make this transition from elongation to swimming spontaneously with no obvious stimulation of any sort (Kristan, 2005). Stimuli delivered to a contracting leech will speed up the contraction, but will never evoke swimming. In fact it seems impossible to elicit swimming in a leech with its front sucker attached (Kristan, 2005).

The crawling is a central pattern generator and differs from the swimming because precise intersegmental coordination is not essential and much more flexibility is needed to make variable exploratory movements on the solid substrate before deciding where to attach and continuing the cycle. On the contrary, the swimming takes place in an aqueous uniform environment (Cacciatore *et al.*, 2000). Therefore, a crucial role is played by sensory feedback to modulate the central pattern generator’s activity. The circuit is certainly located part in the head and tail brains and part in the mid body ganglia, since leeches with either or even both brains removed are still able to crawl, though slowly. However, a prominent role seems to be played by the head brain (Cacciatore *et al.*, 2000).During the initiating part of the crawling step the elongation of a segment is produced by a contraction of the circular muscles and the subsequent contraction is produced by all the longitudinal muscles in that segment. For both elongation and contraction, the behaviour begins at the front end and moves smoothly to the posterior as a wave. Hence, in a single segment, crawling appears as an alternation of bursting in the circular and longitudinal motoneurons. This pattern repeats itself with a delay in successively more posterior segments, thereby producing the intersegmental progression of the elongation and contraction waves. This pattern has been recorded in semi-intact and isolated nervous systems (Baader & Kristan, 1992; Baader, 1997).

Recordings from motoneurons activated in the crawling have been achieved in preparations of semi-intact and isolated nerve cord preparations, fully consonant with kinematics (Baader & Kristan, 1995; Baader, 1997). Circular muscle motoneurons produce impulse bursts in each segment which alternate with bursts in motoneurons which innervate longitudinal muscle

These bursts appear progressively later in more posterior segments in both semi-intact preparations and isolated nerve cords (Baader & Kristan, 1995). Firing rate form L cell is high up to ~10 Hz in the initial phase of the crawling step (Baader, 1997). Afterwards, motoneurons cell 3 and cell 5 exhibit depolarization in the resting membrane potential which can be reflexed in high burst activity during half of the contraction step on the crawling (Baader, 1997). Some other interneurons and inhibitors have been recorded and present preference for contraction (S, AP, and 159) and elongation (1, 2, CV, 4, 151 and 152; interneurons 204 and 208, 258, 213) steps (Baader, 1997; Baader & Bächtold, 1997). In the tail brain the interneurons IN902, IN904 and IN401 and motoneurons N31-33 and N41 are different neurons that can be activated with the initiation of the crawling, pointing that they are activated with the sucker detach (Baader & Bächtold, 1997). A possible candidate of decision is the interneuron 204 (Baader, 1997; Baader & Bächtold, 1997), as it has been previously recorded and presented in the initiating of swimming firing rates of 10–30 Hz (Weeks & Kristan, 1978). Concerning its architecture, it is known that it connects with the 208, which receives monosynaptic input from cell 204 and makes excitatory connections with several excitatory and inhibitory longitudinal and dorsoventral motor neurons (Weeks, 1982*b*). In the initiation, one of the most important cells is the R3b1, located in the third neuromere of the subesophageal ganglion, which can initiate the crawling motor pattern in both semi-intact and isolated nerve cord preparations (Esch *et al.*, 2002). R3b1 oscillates above its resting potential during the continuation of the behaviour and, surprisingly, R3b1 depolarization can also produce swimming, or a combination of swimming and crawling.

The comparison of the cycle periods of intact leeches with preparations (semi-intact and isolated nerve cord) revealed that crawling lasts longer in preparations than in intact animals, although the coordination is more or less the same (Cacciatore *et al.*, 2000). Nevertheless, several differences have been identified: (a) the period is much longer than in intact animals (30 s), (b) there is much more variability in the full period from intact or in the semi-intact preparations, and (c) the duration of the bursts is greater than in semi-intact preparations. In the recordings, the bursts are so long that the circular motor bursts (elongation) overlap with the longitudinal motor bursts (contraction), particularly in the rear end of the nerve cord since the contractions occur relatively close to the elongations in this part of the animal.

Two kinds of models have been proposed to explain leech crawling. The first is a neuronal model that simulates the motoneurons patterns along the nerve cord. The second is a biomechanical model that explains how the motor patterns produce movements. The neuronal model (Cacciatore *et al.*, 2000) suggests a simple explanation for intersegmental coordination,

but it is agnostic about the location and nature of the underlying neuronal circuits (Kristan, 2005). Instead, in the biomechanical model (applied first to crawling with success), motoneurons' bursts from isolated nerve cords (Eisenhart *et al.*, 2000) and from semi-intact preparations (Baader & Kristan, 1992) are used to make estimations of the motor bursts from the kinematic studies. Comparing the model and the data, movements look very similar to a crawling leech, and this is not surprising since the model was tuned to produce these movements. However, it is interesting that, although the pressures generated by the model are in no way constrained, they produce amplitudes that are very close to those measured in a crawling animal (Baader & Kristan, 1992; Kristan, 2005; Baader & Bächtold, 1997).

In recent works, with the advantageous technique of the voltage sensitive dyes, it has been possible to monitor the activity of the ganglion's network during the crawling phases of contraction and elongation. The results concluded canonical models which predict neuronal activity in dorsal and ventral face of the ganglion (Briggman & Kristan, 2005; Briggman & Kristan, 2006). Moreover, results indicate the activation of eleven pairs of neurons during the contraction phase: 108, 107, 106, 101, 16, 17, 4, 3, 5, 8, and 7 (most of them excitors) and AE, 166 S and 166 from the dorsal side. In addition, during the elongation phase another nine pairs of neurons have been detected on the dorsal face: 109, 102, 119, 117, 112, 11, 12, 1 and 2 (most of them inhibitors), and 255, 257, CV and 213 in the ventral side. Cells 152 and 151 have been found to be involved in the contraction to elongation phase of the behaviour.

Shortening

The leech's shortening is due to a contraction of all longitudinal muscles in body segments. Contractions can occur in all segments (whole-body shortening) or in only a few segments (local shortening). *Whole-body shortening* is a very overpowering behaviour and it appears to override all behaviours but feeding (Shaw & Kristan, 1997). The stimulus in P cells reliably produces whole-body shortening through the activation of two parallel interneuronal pathways: a fast, weak one and a slower, more prolonged one. The S cells are essentials for the fast pathway. Unpaired in each ganglion, the S cells send axons to rostral and caudal sides into the Faivre's nerve (Frank *et al.*, 1975). The Faivre's nerve consists is known also as the fast conduction system(FCS): Unpaired ganglion's S cells are interconnected in the whole body of the animal (Bagnoli *et al.*, 1975) and carry action potentials from the site of spike initiation to every ganglion in the nerve cord (Frank *et al.*, 1975). In a ganglion, the S cell connects with the L cells that cause contraction of all longitudinal muscles. The FCS is strongly activated during whole-

body shortening (Magni & Pellegrino, 1978). Nevertheless, the S-to-L connection is weak, and the stimulation of the S cell at high rates produces only a very weak motor response (Shaw & Kristan, 1999). The strongest pathway, instead, comes mainly from unidentified interneurons, which have much slower conduction velocities but which produce a strong and prolonged activation of the motoneurons. This system produces full-blown shortening. The interneuronal pathways activate all the excitatory motoneurons to the longitudinal muscles in all segments of the body with short latencies. In addition, the motor-inhibitors are strongly inhibited during whole-body shortening (Shaw & Kristan, 1995). There is significant variability in the response of individual motoneurons during whole body shortening, but the ensemble average of their response is much less variable since the responses of each motoneuron is statistically independent from all the others (Pinato *et al.*, 2000; Arisi *et al.*, 2001).

As mentioned before, in the *local shortening,* a mechanical stimulation of the skin in mid-body segments elicits a local shortening response (Wittenberg & Kristan, 1992). P cells are the most effective in producing local shortening; longitudinal muscle excitors are excited and all the inhibitors are inhibited. The two types of shortening can be distinguished since the local one is restricted to the segments that are added to the stimulus and the other can be culminated in a whole shortening. The segments involved locally increase with increasing stimulus intensity. Furthermore, the local shortening differs from the whole body in that the segment being stimulated produces a bend rather than a shortening (Kristan, 2005).

Feeding

All the leech species feed by ingesting prey or blood through their anterior sucker (Sawyer, 1986). Feeding behaviour dominates all the mechanically elicited behaviours in intact animals (Misell *et al.*, 1998). The anterior sucker is attached to the host or prey while a muscular pharynx, just posterior to the esophagus, produces suction by contraction of extrinsic muscles which pull open the lumen of the pharynx. A major distinction among leech families is based upon their propensity to ingest their prey whole or to suck its blood or other internal fluids.

The medicinal leech attaches its front only to hosts much larger than itself, rasps through the host's skin with eversible jaws, and sucks the blood that oozes from the tripartite wound. After biting through the skin, which starts the consummatory phase, the pharynx begins to contract rhythmically at about 2 Hz, pumping the blood into the crop (Wilson *et al.*, 1996). Peristalsis body waves usually accompany ingestion, but they have a lower frequency than the pharyngeal pumping (Lent *et al.* 1988). Very occasionally, dorso-ventral flexions occur which

resemble swimming. The frequency of both pharyngeal pumping and body peristalsis decreases as the consummatory phase continues. During ingestion, the front of a leech will continue to feed, even during lesions to the back of the animal, showing that their response to noxious stimuli is greatly reduced. The consummatory phase of feeding can last for 30–45 min, during which the leech can ingest up to nine times its mass in blood, a meal that can sustain it for up to a year. It has been suggested that serotonin is central to the production of this behavioural pattern (Lent, 1985; Lent *et al.* 1988; Wilson *et al.*, 1996). Leeches increase their body mass by near to 10-fold during a single blood meal (Lent & Dickinson, 1984; Lent *et al.*, 1988). Anticoagulants and anti-platelet substances are exuded into the wound to keep blood oozing from the cut during the 10–30 min that it takes a leech to complete feeding. In fact, blood continues to ooze from the leech bite for several hours after the leech completes its meal. This ability to remove quantities of blood was the initial appeal of leeches medicinally (Payton, 1981).

Mimicking the feeding-induced distension by injecting saline (or even air) into a leech terminates feeding (Lent & Dickinson, 1987) and makes swimming less likely to occur (Groome *et al.*, 1993), presumably because of the activation of stretch receptors. To help the coordination of swimming movements, stretch receptors in the dorsal longitudinal muscles are activated during the ventral contraction phase of each swim cycle and ventral stretch receptors are activated during the dorsal contraction (Yu & Friesen, 2004). The circuitry related to the feeding behaviour is still not deeply understood, but, interestingly, it is known that the activity exhibited by the Leydig cells suppresses the local bending response and are active during feeding (Gaudry & Kristan, 2010A; Gaudry & Kristan, 2010B).Moreover, it is known that feeding in leeches appears to inhibit the swim circuit in a distributed and modularized manner. The decision to stop swimming is distributed in that it most likely arises from two distinct sources: one that generates ingestion, and the other that is activated by distension (Gaudry & Kristan, 2010B). Ingestion activates a descending pathway that targets the pressure mechanosensory neurons (P-cells) of the leech (Gaudry & Kristan, 2009). This descending inhibition decreases the probability of release measured at presynaptic release sites of the P-cells. Severing the nerve cord is sufficient to relieve posterior segments of this inhibition and allows swimming to occur simultaneously with feeding (Gaudry & Kristan, 2010B). Hence, the inhibition of the leech swim circuit by distension must originate from a different source, most likely from the stretch receptors located within the body wall musculature of the animal. Unlike ingestion, distension targets components of the swim circuit downstream of the sensory neurons (Gaudry & Kristan, 2010B). Concerning ingestion and distension, it seems that there are two distinct sources and targets for swimming inhibition as unique decision-making modules. These two are better described as

complementary, for instance, ingestion prevents the initiation of swimming and distension inhibits the maintenance of swimming. More importantly, the effects of ingestion broadly inhibit all mechanically elicited behaviours, whereas distension leaves some behaviour intact while suppress another (Gaudry & Kristan, 2010B).

Pseudo-swimming

The pseudo-swimming behaviour has been reported statistically in intact animals with beads glued to their head and tail and tracked with an algorithm. Results have indicated two forms of swimming (Mazzoni *et al.*, 2005; Garcia-Perez *et al.*, 2005). One is the common swimming, and the other one is characterized by the tail sucker fixed to the bottom of the dish and the head oscillating with a frequency of 1.5 Hz. This second behaviour has been referred to as pseudo-swimming, characterized by an oscillation of the elongation with a frequency identical to that observed during swimming, although with smaller amplitude and with the rear sucker attached to the bottom of the dish. The amplitude of the swimming movements of a free leech corresponds to approximately the 15–20% of the length of the full-extended leech, matching with previous evaluations (Stent *et al.* 1978). During pseudo-swimming, the average amplitude value is only the 10% of the length (Mazzoni *et al.*, 2005). Swimming and pseudo-swimming can be easily distinguished by analyzing velocity of the trajectories since in the pseudo-swimming state the tail can not move quickly enough to allow real swimming. The pseudo-swimming can be associated with previously reported behaviour of ventilation (Magni & Pellegrino 1978). In the case of restrained leeches, swimming and pseudo-swimming can not be dissociated because the rear sucker of the animal is kept stationary by the pinning (Mazzoni *et al.*, 2005; Garcia-Perez *et al.*, 2005). In this case, the amplitude of the swimming movements is again the 10% of the full length of the leech, and the frequency of oscillation in pinned leeches during such swimming or swimming-like motion is slightly lower than in free leeches since it is approximately 1 Hz. The responsible circuit in the pseudo swimming behaviour is still not elucidated but it can be hypothesized that the cells participating in it can be those involved in swimming episodes.

Stationary states

Stationary states are defined visually as moments of rest (motionless) in free intact leeches. Automated tracking algorithms helped to define this behaviour calculating the velocity of motion

of tracked beads (Mazzoni *et al.*, 2005; Garcia-Perez *et al.*, 2005). As a result, convolving the position of the beads in a *x, y* coordinates with a Gaussian filter over the time spend in the experiments, these moments have been identified and defined as those in which the velocity of the beads (glued to head and tail) compute values near to cero (~1 pixel/s) and a standard deviation around 1 pixels, concluding a mathematical definition of the behaviour of the rest state. The identification of these points represented the first step of the automatic classification of the leech's behaviours and, using pinned and free animals (all intact), the stationary states were subdivided into *still*, *peristalsis-like*, and *head attached*, with a minimal variation of the standard deviation from 0.7 to 2.2 pixels. This small variability in the peak location and its width indicated that the proposed state identification captured fundamental properties of leech motion consistently identified across individuals (Mazzoni *et al.*, 2005).Up to now, there is no evidenced report about any circuit activated during this moment of rest in the animal.

Exploratory head

Beside the stationary states, the analysis of trajectories of beads glued to leeches allowed the identification of another series of events. These events have been clusterized into a low-frequency category using a three-dimensional histogram in which occurrence, maximal velocity and dominant frequency, calculated from a smoothed power spectra (V_{max} (n) = 50 pixels/s, $f_{50\,d}$ (n) around 0.2 Hz), have been plotted. The resulted method led to the discrimination of the crawling events from exploratory behaviour as they resulted to be very near in the plot (Mazzoni *et al.*, 2005; Garcia-Perez *et al.*, 2005). Observations were confirmed with videos, in which the behaviours matching perfectly correlated with the exploratory motion. These were irregular oscillations of the head and the anterior part of the body, while the rear sucker, which was stuck on the bottom of the recording chamber, kept the tail motionless (Mazzoni *et al.*, 2005; Garcia-Perez *et al.*, 2005). Up to now, there is not a rough characterization of the neural activity during the stationary states.

Networks and Choice for motor behaviours

As a final comment in this introduction, the recent ideas of functional neural networks (named segmental multifunctional circuits) related to behaviours are the next step in the understanding of the leech behaviour mainly due to two factors: the large quantity of information

about cellular circuitry and the new methodologies and techniques that permit to record complete networks (i.e. the use of voltage sensitive dyes or magnetic resonance). These methods can be accepted because it is known that in the leeches' motor behaviours there is an undoubted control by distributed processes. The swimming, crawling and shortening circuits are partially superimposed, since some interneurons and motoneurons are active during different motor behaviours. Different models of reorganization in the neural architecture are accepted, where different motor responses can be produced by altering the same circuit. It is an example the existence of "command systems" (decision or command neurons) whose stimulation produces behaviours through the activation of neuronal populations (Kupfermann & Weiss, 1976; Kristan, 2008). Moreover, it seems that the command entities are decision makers but this hypothesis has not been tested. This concept produces the idea that the decision to behave in one manner rather than in another is a winner-take-all among command neurons, with a possible winner inhibiting all the losers. Early evidence has been reported after intracellular recordings from 'looser' command neurons receiving inhibition from a winning behaviour (Kristan, 2008).

Specifically in the choice between swimming and crawling of the leech, it is known that, previous to the behaviour, there is a period of elongation and this decision is mediated by descending interneurons (Esch, 2002). Descending interneurons make a decision based on the level of bath saltiness of the semi-intact preparation, which suggests a hierarchy of sensory stimulus that prompts the leech to move in an appropriate behaviour. In other study, at the level of the multifunctional circuits in one segment, the decision between swimming and crawling is determined by the activity of a neuron population (Briggman & Kristan, 2005). The decision provoked by a sensory pathway can be produced manipulating the membrane potential of a neuron from the population. Putting together all the pieces, sensory pathways, descending commands, and multifunctional circuit pattern selection, is necessary to elucidate further the mechanisms of behavioural choice (Briggman & Kristan, 2008).

CHAPTER 3

SIGNAL ANALYSIS

Analogue or digital Signals

In this chapter, the basic methodologies performed to analyze the acquired signals will be briefly described. In particular, five concepts will be developed: signal's definitions, the average firing rate, the cross-covariance, the dendrogram and the receiver-operating characteristic (*ROC*) curves as types of classifiers used.

An **analogue** signal ***s*** is a finite real-valued function ***s (t)*** of a continuous variable ***t*** (called time), defined for all times in the interval **$-\infty < t < +\infty$.** Instead, a **digital signal s** is a bounded discrete-valued sequence **s*n*** with a single index ***n*** (called discrete time), defined for all times ***n* = $-\infty \ldots +\infty$** (Stein, 2000). The discrete digital signals permit the simplification and condensation of large quantities of experimental information as well as a faster analysis. Digital signals are acute and reproducible with precision in contrast to analogue ones. This precision is naturally due to the number of bits used in computation, and the inaccuracy is avoided thanks to error-correcting codes (Oppenheim, 1997). A digital recording copy is always identical to the original, with no added noise and no 'drift' caused by temperature or ageing (Stein, 2000).

The first step in signal processing consists in the conversion of an analogical into a digital discrete one. This is done by a circuit called analogue-to-digital converter (*ADC*). The result is a series of numbers, kept in a computer memory (*RAM*) and eventually written on a disk or on any suitable storage medium. A "sample" is thus defined as a single numerical measurement from a continuous discrete signal (Stein, 2000). To find the essential properties of sampled signals, a theory called sampling theory was developed in the period 1930–1950 by Shannon and Nyquist. A first, basic rule is that *one cannot make inference on processes that did not sample* (Stein, 2000). A sampled signal has two important quantities: the sampling interval and the total sampling time. Electrophysiological signals are in their origin analogue and are sampled in the experimental set up with the necessary equipment; then they are converted into discrete signals. To process and analyze them, the mathematical concepts used in general are focused in the field of the random processes. Neural signals can be subdivided into the following broad categories*: intracellular voltages, extracellular voltages and transmembrane currents* (Stein, 2000). In this work extracellular signal have been the motive of interest; two main concepts are the bases for the analysis of extracellular signals: the firing rate and the cross-covariance.

DESCRIPTORS: ACTION POTENTIALS AND FIRING RATES

In Computational Neuroscience's field the most important signal is the action potential (AP), referred also as spike action potential and defined as a ***regenerative electrical signal whose amplitude does not attenuate as it moves down the axon*** (Kandel, 2000). The APs are generated and carried over long distances by neurons and arise from sequential changes in the membrane's selective permeability to Na^+ and K^+ ions, which influence their speed and conduction depending on the passive properties of the membrane. Hodking and Huxley postulated the equations which explain the behaviour of Na^+ and K^+ ions (Kandel, 2000; Hodking & Huxley, 1952). With the advances in technology and knowledge on membrane's structure and physicochemical properties, it has been possible since the late 80's to record membrane pore-proteins from neurons obtaining stochastic steps of currents from single membrane proteins called *ion channels* that are critical for generating and propagating AP. Thanks to the open-close state of these ionic channels, the excitability property of the nervous and muscular units is possible (Sigworth, 1994; Hille, 2000).

The AP signal can be recorded extracellularly. However, acquiring extracellular signals from a cell differs from acquiring signals in roots, as it has been preformed in this work. The proposed technique is the use of glass electro pipettes of hundred microns diameter which, combined with suction applied to an extreme of leech's ganglion roots, produces fluctuations in the voltage (in a range of microvolt: μV), that can be observed as spikes on the time (fig M.2). These fluctuations are called *train of impulse*, *burst activity* or *spike's trains* and represent the coded information between excitable cells. Since spike trains are sent messages, once they are extracted from a recording session, their interpretation and analysis require their conversion into *descriptors* (Kumar, 2010; Quiroga, 2009; Buonomano & Maass, 2009). Furthermore, there are some models that explain the form of the spikes, but these will not be described since not included in the purpose of this work.

Firing rate

Usually, the neuronal regular spiking is not interesting, its occurrence is not covering any information, only the deviation from the regular spiking conveys information (Trappenberg, 2002). The presence of irregular spikes justifies the extracellular signals recording in experiments and gives sense to the information, especially when the objective is to know the firing pattern of neurons. The spike's information could be related to the *Morse* code, but the

spiking neurons have many differences in comparison to this code. Neuronal spiking is approximately constant due to the stereotyped waveform, so there are not analogues for the short and long single of the Morse code. It is possible to divide alternative codes when only one length of a signal, for example a dot, and the time between the occurrences of that dot is used. However, it is not possible to think that a neural code represents an alphabet like the Morse code. Usually, neuroscientists have the common aim of deciphering the neural code that means just the relevance of particular node activities for representation, transmission and processing of the information from nervous system (Trappenberg, 2002).

Neuroscientists try to decipher the neural code by searching for reliable correlations between firing patterns and behavioural consequences or correlations between sensory stimuli and neural activity patterns (Trappenberg, 2002). One of the first scientists who was interested in measuring this code was Lord Douglas Adrian (1926-1931), who explained in a series of papers the way to amplify the spiking signals form nervous and muscular tissues. He recognized that the number of spikes from a neuron increases when receive any stimulus. This corresponds to an increase of the instantaneous firing rate. So, this detectable increase on the firing rate is necessary to know the stimuli necessary to drive a neuron. The information obtained counting these spikes can be adjusted into a tuning curve for example, and this is a reflex of what is called the *Firing rate hypothesis* (Trappenberg, 2002).

The most common procedure to obtain the instantaneous firing rate consists in taking a spike train in response to the stimulus and to convolve it with a smoothing filter such as a Gaussian profile, $\varphi(t) = \exp(-t^2/2\tau^2) / \sqrt{2\pi\tau^2}$ (Gabbiani & Cox, 2010). In this equation, τ represents the time window over which spike times are averaged. There is no fixed rule to choose τ and usually its value is set in relation to the typical inter spike interval observed during stimulus presentation so as to average over a few spikes. For inter spike intervals of 10–20 ms, τ would be chosen to be around 20–50 ms. It has be kept in mind that longer time windows will average over more spikes at the expense of temporal resolution. Letting $j = 1, 2, \ldots$ the index for the trial number and also $\delta(t - tji)$, $i=1, \ldots, Nj$ the i**th** spike of trial j so that the j**th** response to the stimulus is given by:

$$r_j(t) = \sum_{i=1}^{N_j} \delta(t - t_i^j).$$

Then, the definition of an estimate of the instantaneous firing rate during trial j via the convolution is:

$$f_j(t) = r_j(t) \star \phi(t) = \int_{-\infty}^{\infty} r_j(s)\phi(t-s)\,\mathrm{d}s = \sum_{i=1}^{N_j} \phi(t-t_i^j).$$

This simply corresponds to place a filter function φ(*s*) around each spike. The convolution can be computed efficiently using the fast Fourier transform algorithm; so finally, the estimated instantaneous firing rate is then obtained by averaging across trials:

$$f(t) = \frac{1}{N}\sum_{j=1}^{N} f_j(t).$$

Correlations & Cross-covariance

In the study of signal processing systems, there are two concepts which must be clarified and which are sometimes related the concept of 'convolution' and the concept of 'correlation'. In fact, convolution by a symmetric FIR filter can be considered a correlation as well, but the two should be considered as different. Convolution is usually between a signal and a filter; thought as a system with a single input and stored coefficients. *Cross-correlation* is usually between two signals input and no stored coefficients (Stein, 2000; Trappenberg 2002; Rieke *et al.*, 1997; Gabbiani & Cox, 2010).

At the level of whole animals, behaviour under identical conditions exhibits random components, thus it can be studied as in signal processing. To describe this "randomness", it is necessary to know tools of probability theory. An interpretation of the relation between two *random vectors* is known as *correlation: in this work* the firing rates tare the random vectors. The correlations are used measurement studies, including studies conducted to obtain validity and reliability evidences. Correlations can be displayed in scattergrams or scatter plots inferring tests for its significance and giving interpretation to results (Goodwing& Leech, 2006). The basic principles of a correlation are elucidated in statistics concepts, like variance and covariance (Stein, 2000; Trappenberg 2002; Rieke *et al.*, 1997; Gabbiani & Cox, 2010). Considering this, the probability density of two random vectors X_1 and X_2 is:

$$p(x_1, x_2) = \frac{1}{2\pi\,(\det \mathbf{C})^{1/2}} \exp(-(\mathbf{x}-\mathbf{m})^T \mathbf{C}^{-1}(\mathbf{x}-\mathbf{m})/2),$$

$$\mathbf{x} = \begin{pmatrix} x_1 \\ x_2 \end{pmatrix}, \quad \mathbf{m} = \begin{pmatrix} m_1 \\ m_2 \end{pmatrix}, \quad \text{and} \quad \mathbf{C} = \begin{pmatrix} \sigma_1^2 & \sigma_{12} \\ \sigma_{12} & \sigma_2^2 \end{pmatrix}.$$

C is defined as a matrix of covariance, where E [(**v**X **–m**) (**v**X **–m**) T] is called the *covariance* of $\mathbf{v}_X$

$$\mathbf{C} = \begin{pmatrix} \sigma_1^2 & 0 \\ 0 & \sigma_2^2 \end{pmatrix} = \begin{pmatrix} E[(X_1 - m_1)^2] & 0 \\ 0 & E[(X_2 - m_2)^2] \end{pmatrix} = E[(\mathbf{v}_X - \mathbf{m})(\mathbf{v}_X - \mathbf{m})^T].$$

The estimation of the ***correlation coefficient*** (**ρ**) considers that when the variance from both variables is $\sigma_1\,\sigma_2 \neq 0$, then the correlation coefficient of both variables X_1 and X_2 is:

$$\rho \equiv \frac{\sigma_{12}}{\sigma_1 \sigma_2}.$$

An important property of ρ is that it lies between −1 and 1 irrespective of the values of σ_1, σ_2. To see this, note that

$$\mathbf{C} = \begin{pmatrix} \sigma_1^2 & \sigma_1\sigma_2\rho \\ \sigma_1\sigma_2\rho & \sigma_2^2 \end{pmatrix}, \quad \det\mathbf{C} = \sigma_1^2\sigma_2^2(1-\rho^2).$$

Thus, det**C**>0 ($\sigma_1 \neq 0$, $\sigma_2 \neq 0$) implies that $-1 < \rho < 1$. If σ_1 (or σ_2) is equal to zero, the random vector $\mathbf{v_X}$ is *degenerate*, as explained above. In this case X_1 (or X_2) is essentially equal to its mean value and the vector $\mathbf{v}_X = (X_1, X_2)^T$ does not have a proper density since **C** is not invertible. If σ_1, $\sigma_2 \neq 0$, and $\rho = \pm 1$ then det**C** = 0 and $\mathbf{v}_X$ is *degenerate* as well. In this case, a rotation matrix **A** that diagonalizes **C** will yield an eigenvalue λ_1 (or λ_2) equal to zero. Summarizing, let **ρ** be the correlation coefficient between two jointly Gaussian random variables X_1 and X_2, so the correlation have the values $-1 \leq \rho \leq 1$. If **ρ** = 1, then $X_1 - m_1$ is proportional to $X_2 - m_2$ and if $\rho = -1$ then $X_1 - m_1$ is proportional to $m_2 - X_2$. Thus, the correlation coefficient is a measure of *linearity* between the two Gaussian random variables.

CLASSIFIERS

ROC analysis

The *signal detection theory* is defined as the mathematical theory used to optimally detect signals embedded in noise. It tries to answer the question: is the signal present or absent in the noisy background? If the noise is a random variable with a known probability distribution, then it is possible to exploit this knowledge to determine an optimal method of detecting the signal. ***ROC*** curves are often plotted as the psychophysical threshold (Gabbiani & Cox, 2010). To understand this types of curves, the first aspect to be considered is to know that the information encoded in spike trains have two types of noise models, a Poisson one and a Gaussian one, so there must be a way to discriminate if it is or it is not present any signal. This choice of a particular value for any threshold entails a trade-off between two types of error that may arise in a detection task. The two possible types of error are: 1) defining the stimulus as present when it was not, i.e., a ***false-alarm***, and 2) defining the stimulus as absent when it was present, i.e., a ***miss***. So, there are two probabilities to define, one for a false-alarm ($\boldsymbol{P_{FA}}$) and the other for the miss one ($\boldsymbol{P_M}$), considering that P_M is equal to $1-P_D$, where $\boldsymbol{P_D}$ is the probability of correct detection. Both probabilities are represented in the next equations:

$$P_D = \sum_{k \geq k_{th}} \frac{m_1^k}{k!} e^{-m_1}, \quad \text{and} \quad P_{FA} = \sum_{k \geq k_{th}} \frac{m_0^k}{k!} e^{-m_0}.$$

A plot of the P_D as a function of the P_{FA} is the so called *Receiver-Operating Characteristic* (*ROC*) curve (fig 3.1), an arcane term that originated in the initial application of signal detection theory to radar signals during World War II. The *ROC* curve fully characterizes the performance of the *decision rule* based on a threshold number of spikes. If one would like to obtain a probability of correct detection between two probabilities P_D, then the decision rule is defined as $(P_{D1} + P_{D0}) / 2$. Considering this, the *ROC* curves are based on *optimal (ideal) decision rule*s which are always based on the likelihood ratios, one of the more powerful decision rules is the *Neyman–Pearson lemma* (Gabbiani & Cox, 2010).

A *Neyman–Pearson* ideal observer is one that maximizes the probability of detection P_D for a false fixed value, termed α, of the P_{FA}. Such a decision rule is called the most *powerful* test of size α. The achieved probability of correct detection, β, is called the power of the test. A minimum error ideal observer is one that minimizes the probability of error **ε** or equivalently maximizes the probability of correct decisions, P_C (Gabbiani & Cox, 2010).

Characteristics: ROC curves are plots of the P_D as function of P_{FA} for fixed signal strength. These curves fully characterize the performance of the observer for a fixed set of physical stimulus conditions and have some important properties. The diagonal $P_D = P_{FA}$ corresponds to chance performance while perfect performance essentially means P_D =1 independent of P_{FA}. *ROC* curves are concave and their slope determines the threshold value of the corresponding optimal test (Gabbiani & Cox, 2010).

Concavity: the fact that *ROC* curves are concave follows the next argument: if we have two points (tests) (P_{FA1}, P_{D1}) and (P_{FA2}, P_{D2}) on a *ROC* curve, the randomized tests built as linear combinations of these two tests yield a straight line connecting the two points. The most powerful tests of the *Neyman-Pearson-lemma* have to beat at least as compellingly as the randomized tests, i.e., they have to lie above the straight line connecting (P_{FA1}, P_{D1}) and (P_{FA2}, P_{D2}). By definition, this means that a *ROC* curve is concave.

Slope: the slope of a *ROC* curve is the threshold value of the corresponding *Neyman–Pearson* test. This means that:

$$\left.\frac{\mathrm{d}P_D}{\mathrm{d}P_{FA}}\right|_{\alpha} = k,$$

This equation can be written in integral notation, and, after determining *k,* it implies that the *ROC* curve cannot decrease, so, when this equation is derived, the final result is:

$$\frac{\mathrm{d}P_D}{\mathrm{d}P_{FA}} = \frac{\mathrm{d}P_D}{\mathrm{d}k}\frac{\mathrm{d}k}{\mathrm{d}P_{FA}} = \frac{q(k|s_1)}{q(k|s_0)} = k.$$

In practical terms, applying this curves to two random processes like the behaviour of the leech and the descriptors acquired from the roots represented as < AFRj > and < ρ ij >, one can determine which of both descriptors is better in classifying any behaviours.

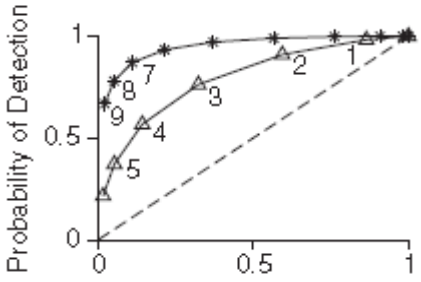

Figure 3.1 ***Example of a ROC curve***: corresponding probabilities of detection as a function of the probability of false-alarm (triangles). The number next to each symbol indicates the corresponding threshold in the number of spikes. As the threshold increases, the false-alarm rate decreases but so does the detection rate. The asterisks correspond to an example in which the case m_0 =4 and m_1=10 (taken from Gabbiani & Cox, 2010).

HIERARCHICAL CLUSTERING

Cluster analysis is an approach that finds structure in information by identifying natural groupings (clusters) in the data. There is no definitive cluster analysis technique, instead the term relates to a rather loose collection of algorithms that group similar objects into categories: clusters (Fielding, 2007). In the hierarchical clustering there are some representations of tree structures called dendrograms. In a dendrogram, the root of the tree consists of a single cluster containing all observations, and the leaves correspond to individual observations. Dendrograms are often used in computational biology to illustrate the clustering of genes or samples.

The creation of a dendrogram depends on the type of data that must be clustered and although some clustering algorithms have been present in 'standard' statistical software packages for many years, they are rarely used for formal significance testing. Algorithms for hierarchical clustering are generally either *agglomerative*, in which one starts at the leaves and successively merges clusters together; or *divisive*, in which one starts at the root and recursively splits the clusters. Any valid metric may be used as a measure of similarity between pairs of observations. The choice of which clusters to merge or split is determined by a linkage criterion, which is a function of the pair wise distances between observations (Fielding, 2007).

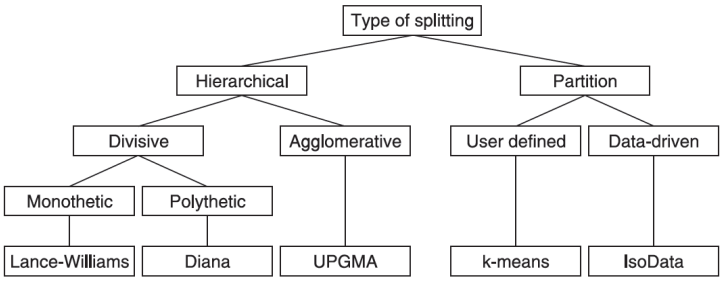

Distances

All clustering algorithms begin by measuring the similarity between the cases to be clustered. Cases that are similar will be placed into the same cluster. It is also possible to view similarity by its inverse, the distance between cases, with distance declining as similarity increases. This leads to a general conclusion that objects in the same cluster will be closer to each other (more similar) than they are to objects in other clusters. It also means that there must some means of measuring distance. Each group has a final box listing one representative algorithm. There are a surprisingly large number of methods (metrics) by which distance can be measured. Some are restricted to particular data types but all share the property that distance

declines with increasing similarity. However, they do not share a common distance between the same two cases, i.e. distance changes with the similarity measure (Fielding, 2007).

Selecting the appropriate distance metric is important because different metrics will result in different cluster memberships and a consequential change to the biological interpretation. The most obvious distances are Euclidean (straight lines that can be measured with a 'ruler') while others, often based on similarity, are non-Euclidean. For example, 'as the crow flies' (a Euclidean distance) the city of York is closer to Manchester than it is to Canterbury. However, if distance (similarity) is measured in terms of city characteristics, York is closer to Canterbury.

There are three general classes of distance measures: ***Euclidean*** metrics measure true straight-line distances in Euclidean space. In a univariate example the Euclidean distance between two values is the arithmetic difference, i.e. $x - x_i$. In a *bivariate* case the minimum distance between two points is the hypotenuse of a triangle formed from the points (as in the Pythagoras theorem). For *three variables* the hypotenuse extends through three-dimensional space. Although difficult to visualize, an extension of Pythagoras theorem gives the distance between two points in *n*-dimensional space: distance $(a, b) = (P (a_i - b_i) 2)^{½}$.

Non-Euclidean metrics are distances that are not straight lines, and obey in general four rules: three simple plus one more complex. Let d_{ij} be the distance between two cases, *i* and *j*:

d_{ij} must be 0 or positive (objects are identical, $d_{ij} = 0$, or they are different, $d_{ij} > 0$).

$d_{ij} = d_{ji}$ (the distance from A to B is the same as that from B to A).

$d_{jj} = 0$ (an object is identical to itself).

$d_{ik} + d_{ij} \leq d_{jk}$ (when considering three objects the distance between any two of them cannot exceed the sum of the distances between the other two pairs). In other words the distances can be constructed as a triangle. For example, if $djk = 10$ and $d_{ij} = 3$ and d = 4, it is impossible to construct a triangle, hence the distance measure would not be a non-Euclidean metric (Fielding, 2007).

Agglomerative hierarchical methods

Partitioning methods produce a flat allocation of cases to clusters which provides no additional information on the relatedness of cases. Although some of them have advantages relating to computational efficiency and an ability to classify new cases, they suffer from problems. The solution is very dependent on the choice of algorithm and distance measure and there is no easy way to identify the number of 'major' groups that would equate to the value of k. Nonetheless, it is a very efficient tool for organising data into groups. For example, Kaplan *et al.*

(2005) used hierarchical clustering to produce a taxonomical tree for over one million protein sequences. As should be expected with such a large dataset some of the clusters are biologically irrelevant. However, using a cluster stability index, and relevance to existing database functional annotations, 78% of the clusters could be assigned names with confidence. They also use a reordered matrix to provide evidence for sub-groups within a cluster.

Clustering algorithms

Hierarchical cluster analysis involves two important decisions. The first decision is the selection of an appropriate distance measure. Once this has been selected a distance matrix, containing all pairwise distances between cases, can be calculated as the starting point for the second phase which begins with each case in a cluster by itself. The second stage to the clustering process is choosing the clustering or linkage algorithm, i.e. the rules which govern how distances are measured between clusters and then used to fuse clusters. As with the distance measures, there are many methods available. The criteria used to fuse clusters differ between the algorithms and hence different classifications may be obtained for the same data, even using the same distance measure. This is important because it highlights the fact that, although a cluster analysis may provide an objective method for the clustering of cases, there may be subjectivity in the choice of the analysis details. It appears that most combinations of distance measure and algorithm are compatible. It has been probed that only the C*entroid* and *Ward's algorithm* had a distance measure constraint; for both cases, Euclidean distance metrics are recommended. Although there is a large number of linkage algorithms most can be illustrated using five algorithms.

Average linkage clustering: The distance between clusters is calculated using average values. However, there are many ways of calculating an average. The most common is *UPGMA* (*unweighted pair-groups method average*). The average distance is calculated from the distance between each point in a cluster and all other points in another cluster. The two clusters with the lowest average distance are joined together to form the new cluster.

There are other methods based on centroid and median averages. *Centroid*, or *UPGMC* (*unweighted pair-groups method centroid*), clustering uses the cluster centroid as the average. The centroid is defined as the centre of a cloud of points and is calculated as the weighted average point in the multidimensional space. A problem with the centroid method is that some switching and reversal may take place, for example as the agglomeration proceeds some cases may need to be switched from their original clusters. This makes interpretation of the

dendrogram quite difficult. There are weighted variations to these algorithms that use cluster size (number of cases) as a weight and they are recommended when cluster sizes are very heterogeneous.

Complete linkage clustering: also known as the *maximum* or *furthest neighbour method*, the distance between clusters *i* and *j* is the greatest distance between a member of the cluster *i* and a member of the cluster *j*. This method tends to produce very tight clusters of similar cases and performs well when cases form distinct clusters. If the cases are more loosely spread the next algorithm may be better.

Single linkage clustering: also known as the *minimum* or *nearest neighbour method*, the distance between clusters *i* and *j* is the minimum distance between members of the two clusters. This method produces long chains which form loose, straggly clusters. This method has been widely used in numerical taxonomy.

Within-groups clustering: This is similar to UPGMA except that clusters are fused so that the within-cluster variance is minimised. This tends to produce tighter clusters than the UPGMA method. This approach means that distances between clusters are not calculated.

Ward's method: Cluster membership is assessed by calculating the total sum of squared deviations from the mean of a cluster. The criterion for fusion is that it should produce the smallest possible increase in the error sum of squares. This approach means that distances between clusters are not calculated.

Dendrograms

The results of a hierarchical cluster analysis are best viewed in a graphical form known as a dendrogram. A dendrogram is a tree that shows, via its bifurcations, how clusters are related to each other across a series of scales. Understanding how a dendrogram is constructed, and how it should be interpreted, is one of the most important aspects of cluster analysis. The calculations, and the resultant dendrogram, depend on the distance measure and/or clustering algorithm. The process is demonstrated by a simple example that ignores a lot of details. The data set has five cases and two variables (v1 and v2):

case	v1	v2
1	1	1
2	2	1
3	4	5
4	7	7
5	5	7

A simple Euclidean distance matrix is calculated as the starting point. For example, the distance between cases three and four is the square root of $((4 - 7)^2 + (5 - 7)^2)$, which is 3.6. Only the lower triangle of the distance matrix is shown below because the distance between cases *i* and *j* is the same as that between cases *j* and *i*. Distances are presented with two significant figures. Using these distances the most similar pair of cases are one and two.

	1	2	3	4	5
1	0.0				
2	1.0	0.0			
3	5.0	4.5	0.0		
4	8.5	7.8	3.6	0.0	
5	7.2	6.7	2.2	2.0	0.0

These two cases are fused to form the first cluster. Distances must now be calculated between this cluster and the other cases. There is no need to recalculate other distances because they will not have changed. For the purpose of this exercise assume that distances are calculated from the means of v1 and v2, *i*.e. mean $v1_A = 1.5$, mean $v2_A = 1.0$. This produces a revised distance matrix in which cases one and two are replaced by A, the first cluster.

	A	3	4	5
A	0.0			
3	4.7	0.0		
4	8.1	3.6	0.0	
5	6.9	2.2	2.0	0.0

The smallest distance in this matrix is between cases four and five (distance = 2.0). These cases are fused to form cluster B (means: $v1_B = 6$, $v2_B = 7$) and the distances are recalculated.

	A	B	3
A	0.0		
B	7.5	0.0	
3	4.7	2.8	0.0

The new smallest distance (2.8) is between cluster B and case three. Case three is fused with cluster B and cluster B now has three members. The mean values are: $v1_C = (4 + 5 + 7)/ 3 = 5.3$, $v2_C = (5 + 7 + 7) / 3 = 6.3$. Obviously, there are now only two clusters and they must be the next to be fused at a distance of 6.4.

The entire process of fusions is summarized by the next dendrogram. The vertical axis is the distance at which clusters were fused and the horizontal lines link fused clusters. The vertical lines, joining the links, illustrate the hierarchical nature of the fusions.

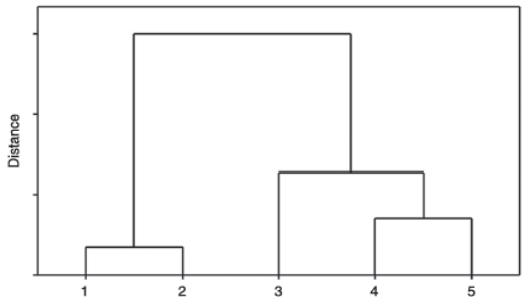

PROBLEMS UNDER INVESTIGATION & HYPOTESIS

The theoretical background cited on the previous chapters originated some general questions to solve about the *motor control* of the leech: How to describe computationally the encoding information from a neural population on the leech system? Which is the state of the multiple signals recorded from the nervous system during the performing of spontaneous behaviours on a semi-intact experiment? Is the population of neurons in a ganglion synchronic during the absence of motion? It is possible to associate patterns of ensembles of neurons to stereotyped behaviours? Is the population of neurons in a leech ganglion correlated, anti-correlated or uncorrelated during the behaviours elicited? Knowing that the motor control of the leech is modulated by the presence or absence of synchrony in its central nervous system resulting in different stereotyped behaviours -grouped mainly in stationary and motioned behaviours-, these questions conducted to apply the next hypothesis of the work:

-When the neural population activity in charge of the motor control in mid body ganglia produces uncorrelated activity between its members, the semi-intact leech enters in a stationary state.

-Otherwise, when the motoneuron's population activity from mid body ganglia originates bursting changes reflected in the presence of correlations and/or Anti-correlations between the members present, the semi-intact leech enters in a motion state.

AIM OF THE WORK & SPECIFIC OBJECTIVES

The aim of the work was **to analyze, identify and characterize electrical signals underlying stereotyped behaviours during the performance of spontaneous recordings from semi-intact preparations of *Hirudo medicinalis*.** To conclude satisfactorily this aim, were originated the next particular objectives:

- *To find an automated computational methodology to represent the experimental information in a simplified and comprehensive way for its subsequent analysis.*
- *To identify and characterize the encoded information (patterns) form a neural population and behavioural elicited from experiments*
- *To relate the information between the automated, identified and characterized signals from the encoded population and behaviours elicited during the experiments performed*

METHODS

Animals and Semi-Intact Preparations

Adult leeches (*Hirudo medicinalis or Hirudo verbana*) obtained from Ricarimpex (Eysines, France) were kept at 5°C in tap water dechlorinated by previous aeration for 24 h. Before each experiment, animals were anesthetized with an 8% ethanol (ethanol: water) solution at room-temperature for 15-20 minutes. Leeches were extended and the skin was dried carefully. Colour beads of 5 mm diameter were glued on the dorsal side of the leech with Nexaband S/C tissue adhesive (Abott Labs, Chicago, USA) near their head and tail. Once beads were correctly glued, leeches were moved to a Petri dish covered with sylgard elastomere (Corning corp., U.S.A.). The leech was immersed in 150-200 ml chilled normal ringer solution (in mM: 115 NaCl, 1.8 Ca Cl_2, 4 KCl, enriched with 10 glucose and buffered with 10 Tris-maleate pH 7.4 with NaOH). Leeches still under anaesthesia were pinned with fine needles in their mid-body. Animals were dissected exposing two central ganglia (fig M.1A, right image). During the dissection, the temperature was maintained at 6-8°C using a cold chamber. Roots and connectives were cleaned carefully, as suggested by W. B. Kristan Jr. (personal communication). In some experiments, a complete segment, corresponding to the skin from the mid dorsal to the mid ventral, was left innerved by roots form one side. This allowed to record contralateral electrical signals and to analyze the changes of the skin area. At the end of the dissection, animals were left to recover from anaesthesia and left to adapt to room temperature for 30 minutes. Experiments were performed at room temperature (19-22° Celsius) and the semi-intact leech was illuminated using a white light lamp without abrupt spatial and/or temporal gradients (Olympus Highlight 3100, Europe).

Imaging

A colour CCD camera (640×480 pixels; model WAT-231S; Watec, Tsuruoka, Japan) was used to obtain images of semi-intact preparations (fig M.1A). Acquired images were sent by a frame grabber (PCI-1394; Texas Instruments) to a personal computer, able to process images in real time. Colour beads were tracked at 25 Hz using an appropriate algorithm employed in a previous work to detect the beads and transform the image into coordinates (Mazzoni, *et al.,* 2005). Images were directly acquired in the hue/saturation/lightness colour space. The algorithm was modified to facilitate the performance and the detection. The identification of stereotyped behaviours and activity elicited by suckers over the time (attach/detach) was obtained by visual

inspection of acquired video records using a standard software (VirtualDub v. 1.6.14; General Public License, 2006).

Glass suction electrodes

Suction pipettes were obtained from borosilicate glass capillaries (World precision instruments, Germany) pulled by a conventional puller (P-97, Sutter Instruments Co., U.S.A.). The electrode tip was cut using a diamond sharpen tip mounted on a manipulator under a stereoscopic microscope (Olympus SZ40, Europe). Suction electrodes with a final diameter 150-200 μm were polished using an incandescent filament under a 20x objective mounted on an upright microscope (Zeiss, Germany).

Recording electrical activity

Suction electrodes filled with normal ringer leech solution were connected to an extracellular recording amplifier with a gain of 1 x 10^4 and a bandwidth of 200–3000 Hz (Pinato & Torre, 2000; Pinato *et al.*, 2000; Mazzoni *et al.*, 2007). Extracellular signals were digitized at 10 kHz using an A/D converter (model Digidata-1322, 16 bit converter; Axon, molecular Devices, U.S.) and data were transferred, stored and analyzed on a PC computer. Signals were recorded and reviewed for analysis using respectively Clampex v.8.1 and Clampfit v.9.2 software (Molecular Devices, USA). Electrical recordings were obtained from cleaned roots or connectives (in *en passant* configuration) from one or two ganglia. Recordings from single ganglia were obtained with 8 electrodes sucking at left and right sides of Anterior (AA), Medial Anterior (MA), Dorsal Posterior (DP) and Posterior (PP) roots, as in a previous work (Pinato *et al.*, 2000; Arisi *et al.*, 2001). Recordings from two ganglia were obtained with a total of 8 electrodes sucking the left and right MA and DP roots of the identified rostral and caudal ganglia. Ganglia were dissected from the mid body between the 9^{th} and the 13^{th} segments.

OFF-LINE ANALYSIS

Automated quantification of behaviours

In order to quantify automatically the leech behaviour, the following computed data were processed off-line using MATLAB v.R2009b (MathWorks, U.S.A.):

Suckers attach/detach: the time occurrences of sucker's events, like attach and/or detach, were determined inspecting video recordings with common software. Attach and detach behavioural occurrences were represented as steps, respectively up and down. An example of the results form one experiment is visualized as two step traces corresponding to the head (in blue) and tail (in red) sucker (fig M.1B: *suckers*).

Head / tail position and velocity: head and tail bead's coordinates were tracked with the CCD detection algorithm and were represented as the coordinates $H_{(x,\ y)}$ and $T_{(x,\ y)}$ on pixel units (fig M.1B: *Head & Tail Position*). The time series obtained from beads were convolved and smoothed using a Gaussian filter as in a previous work (Mazzoni *et al.*, 2005) resulting in the $H_{velocity}$, $T_{velocity}$. The quantified elongation-contraction ($ESV_{velocity}$, see below) was calculated expressing quantities in pixels/sec. The contribution of head and tail velocities to primary behaviour's information was poor (traces not shown), instead $ESV_{velocity}$ from head and tail traces were useful to compare motion detection to electrical patterns (fig R.2C: *ESV-velocity*).

Head and tail shortening-elongation vector: ESV. Shortening/Elongation quantity was obtained off-line, calculated as the distance between two reference points (see *eq. 1*): a point representing the centre of the semi-intact preparation denoted as $M_{(x,\ y)}$, and the coordinates of the bead (head or tail) denoted as $C_{(x,\ y)}$; *ESV* was calculated for head and tail. The shortening (contraction from mid body) was denoted as a fall in the time varying signal which corresponded to the diminished distance from *M* to *C*. Instead, the elongation was denoted as the rising of the signal (see: figs M.1B, R.2C, R.6A&D and R.7A&B). The total elongation of the leech indicated as ESV_{tot} (*eq. 2*) was equal to the sum of the head and tail's *ESV*s (see figs R.1A and R.5A).

$$ESV_{head\,/\,tail} = \sqrt{(C_{x\,(head/tail)} - M_x)^2 + (C_{y\,(head/tail)} - M_y)^2} \qquad (1)$$

$$ESV_{tot} = ESV_{head} + ESVtail \qquad (2)$$

Partial or total *ESV* quantity was normalized in some trace inspections; in those cases the data was divided by the maximum number found in the time-varying series.

Angle theta (θ) of the ESV: As the coordinates values from head and tail were not useful, the angle of the vector quantity *ESV* was calculated to know the position of the beads at the left

or right side of the animal. The angle in radians (or degrees) units was calculated using the MATLAB command `angle.m` applied to the absolute value `abs.m` of *ESV* vector recalculated again which have a real part and an imaginary one (see script above). This quantity as the case of the *ESV* was interpolated and normalized to inspect traces dividing by the maximal number present in the time series.

MATLAB Script:

```
                                                MX=input('X coord: centre?');
                                                MY=input('Y coord: centre?');

                                        HMY= input('Y point of Head for theta?.. ');
                                        TMY= input('Y point of Tail for theta?.. ');

                                VH =sqrt ((MX-HX).^2+(MY-HY).^2);     %ESV FROM HEAD
                                VT =sqrt ((MX-TX).^2+(MY-TY).^2);     %ESV FROM TAIL


                        %---------------------theta calculated from ESV--------------
disH= abs(HX-MX)+(sqrt(-1)*(HY-HMY)); %ESV (Real & complex part) of the Head
disT= abs(TX-MX)+(sqrt(-1)*(TY-TMY)); %ESV (Real & complex part) of the Tail

      thetaH = angle(disH;    % Angular Value of the ESV vector head(radians)
      thetaT = angle(disT);   % Angular Value of the ESV vector tail(radians)
```

Identification of stereotyped semi-intact leech behaviours

During the experimental sessions, the CCD camera was connected to a frame grabber to acquire the beads and in parallel to an image recording unit (Pinnacle Studio, Avid Technology, Inc., USA, 2006) to record and store the videos from the preparations (fig M.4). The visual inspection of the videos helped to analyze and identify the stereotyped behaviours. The videos recorded were used to find times of occurrence of the sucker events (fig M.1B: *suckers*), and also to inspect and corroborate the stereotyped identified behaviours.

Spike detection & spike sorting

Spike detection was carried out by a set of programs able to extract information from the whole extracellular recordings. Detected spikes were stored as two file destinations, indexing the indiscriminate times of maximum peak's occurrence and 64-points-divided waveforms. Computing the amplitudes and event duration of the extracellular spikes (as in Pinato *et al.,*

2000), the detection algorithm fitted automatically the maximum peak (indexed) in correspondence with the 20th point of the waveform (fig M.2).

After spikes detection, the information pursued to be sorted, clustering the spikes with an appropriate algorithm resulting in units attributed to different motoneurons. Discriminate identification consisted in a convergence of three simultaneous methodologies:

- A thoroughly inspection of short extracellular recording traces (from milliseconds to a pair of minutes) around the event(s) of interest detecting the presence or lack of twin spikes on parallel recordings (see fig M.1C: *inset*).
- A comparison between the temporal evolution of *AFR* from the spike sorted units, identified then as motoneurons (fig M.1C, *Firing Rates*), and
- Identification was supported with bibliographic information from other author's contributions (Stuart, 1970; Muller & Nicholls, 1974; Kristan *et al.*, 1974B; Magni & Pellegrino, 1978; Stent *et al.*, 1978; Muller *et al.*, 1981; Bagnoli *et al.*, 1975; Baader & Kristan, 1995; Baader, 1997; Shaw & Kristan, 1999; Pinato *et al.*, 2000; Arisi *et al.*, 2001; Zoccolan *et al.*, 2002; Kristan, 2005; Briggman & Kristan, 2006; Mazzoni *et al.*, 2007; Briggman & Kristan, 2008; Puhl & Mesce, 2008; Puhl & Mesce, 2010). The programs for detection, spike sorting and Firing Rate's presentations were written and modified on MATLAB.

Average firing rate (AFR)

Following the common methodology to obtain the firing rate from spikes, time series of detected spikes from recordings were divided into bins of constant width. The number of spikes occurring in each bin was counted and the result was represented as discrete time series: Average Firing Rate (*AFR*). Different bin widths (50-500 ms; information supported with Mazzoni *et al.*, 2007) were applied to inspect the *AFR* from roots or connectives in different time scales (fig M.3). The same methodology was applied to obtain the *AFR* of identified motoneurons (fig M1.C & R.1A). In some occasions, to inspect the data, the AFR was normalized using the maximal value on the times-varying series.

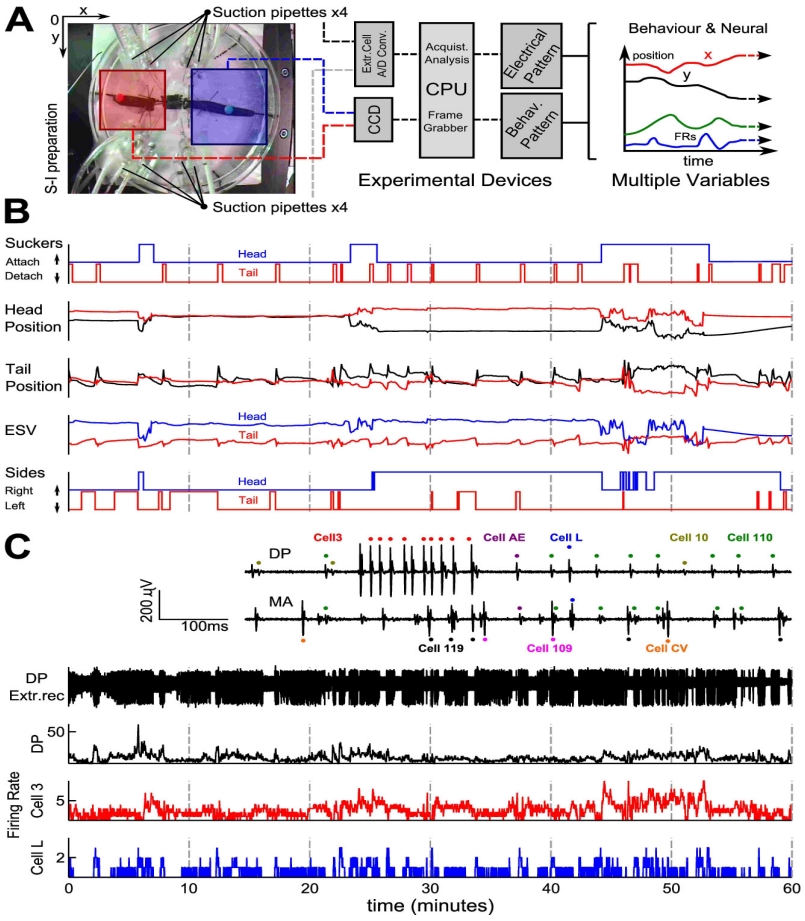

Figure M.1 ***Recording set-up and signals processing of behavioural and electrical information***. **A**. *Experimental Set up used to track the preparation*. The image on the left shows a freeze frame of a semi-intact preparation taken with the CCD camera. Over- imposed squares represent computed selected region where the head (in blue) or the tail (in red) were usually located. The algorithm was able to detect and track the regions of interest (ROI: beads) for long time during the experiment. Four suction pipettes were positioned at left and right sides of the leech (in total: 8) in such a way that no beads were occluded. Centre diagram represents in a simplified way the devices required to obtain image and electrical signals. Right diagram represents the resulted processed information plotted against the time. The beads position and the firing rate from roots were the primary signals to acquire. **B**. *Behaviour characterization*. Temporal evolution of behaviours was obtained via off-line analysis showing multiple variables, some of them were detected with visual inspection (sucker attachment and detachment) and others with automatic algorithm processing. *Suckers*: head and tail suckers correspond respectively to blue and red step traces. Step up indicates that sucker was free (detached) while step down indicates attached sucker. *Head and tail positions*: the *x* and *y* coordinates (red and black respectively) represent the head and tail beads position. Initial *y* bar at 0_{time} = 450 pixels for the head and 60 pixels for the tail. *ESV*: Elongation-Shortening-Vector was obtained computing the position of the detected head and tail beads using an automated process based on a trigonometric function, in which the blue trace corresponds to head performance while the red one to tail. Initial *y* bar at 0_{time} = 280 pixels. *Right-Left*: the position of the head and tail at the animal body's side are represented in blue and red respectively. A step-up indicates that the bead was located on the right side; step-down indicates the bead positioned on the left side. **C**. *Electrical recording analysis*. *Inset DP & MA*: amplified trace (800 ms) from simultaneous extracellular recordings showing activity from DP and MA root. Burst spikes from Cell L (blue dots), Cell 110 (green dots) and Cell AE (purple dots) are present on MA and DP roots as axonal innervations and are sent on both structures. Instead, Cell 3 (red dots) and Cell 10 (yellow dots) are waveforms exclusively present on DP recordings. In MA roots it was possible to identify Cell CV (orange dots), Cell 109 (magenta dots) and Cell 119 (black dots). *DP root*: extracellular recording from a DP root obtained with a suction pipette electrode. Initial *y* bar at 0_{time} = 420 µVolts. *Firing Rate*: spike-per-bin's counts (histogram) were obtained processing the detected spikes from DP root (upper trace), bin size = 500 ms. *Cell 3 & Cell L FRs*: firing rates from motoneurons Cell 3 (red) and Cell L (blue) were identified by spike sorting algorithm. B and C correspond to acquired data from an experiment performed.

Auto- and cross- covariance on time's windows

To compare the synchronic activity between roots or neurons *AFRs*, a moving-window cross- or auto-covariance analysis (**ρ**) was applied to determine the temporal co-modulation of signals. The MATLAB algorithm followed the next steps:

- Two temporal sequences of *AFR* were fixed at the same bin width (commonly 500 ms bin width; see Mazzoni *et al.*, 2007) throughout their time duration.
- A set time-width window was moved in steps of 1 s across each pair of *AFR*. The window's width to compute **ρ** was set to 50 seconds (n = 100 samples) although it could be variable considering that each sample corresponded one bin of the *AFR*. The choice of the moving-window width relied on the time-scale of interest and ensures a good estimation.
- The cross- and/or auto-correlation between both signals were calculated using an *unbiased* covariance method: `xcov.mat, 'unbiased'` (MATLAB); then, was averaged over the first ±5 time lags (for the common bin width: ±2.5 lags).
- The result: a correlation number (**ρ**) level was placed at the centre of the sliding time window; so, the algorithm slid the window to next point (fig M.3).
- In the initial and final n samples from the *AFR* traces, **ρ** was not calculated as the resulted window had n- *1* samples, computing an error; so, the algorithm was programmed to calculate the **ρ** with only the n number of samples assigned.
-

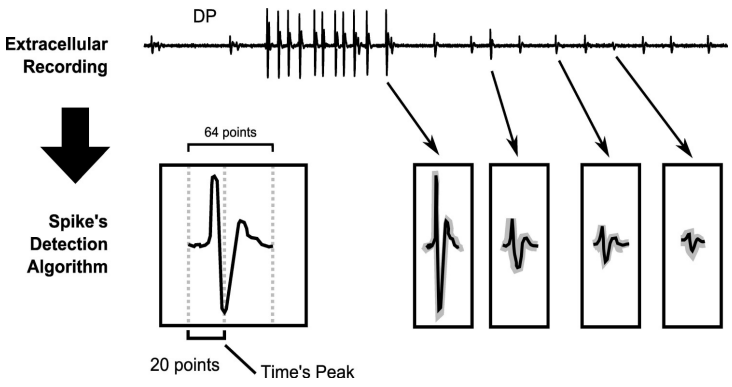

Figure M.2 ***Spike's detection*****.** The algorithm used was written modifying other previous programs and consisted on extracting times of spikes form the extracellular recordings, detecting the time at the peak of every spike and setting it on a window of 64 points (interpolation from the digitized original recordings). The time of the peak was aligned and adjusted situating it on the point number 20. In this way, to manipulate information, two kinds of archives were generated: a time's peak index archive and a waveform archive. The primary information achieved from extracellular recordings were all the peaks without discriminate.

Details about `xcov.m` ***command***

This brief description was based on the MATLAB definition for the cross- and auto-covariance calculated. `The command function xcov` estimated the cross-covariance sequence of random processes. The true cross-covariance sequence was the cross-correlation of mean-removed sequences:

$$\phi_{xy}(m) = E[(x_{n+m} - \mu_x)(y_n - \mu_y)^*)]$$

where μ_x and μ_y were the mean values of the two stationary random processes, the asterisk (*) denoted the complex conjugate, and $E\{\cdot\}$ was the expected value operator. `xcov` estimated the sequence because, in practice, access is available to only a finite segment of the infinite-length random process. By default, `xcov` computed raw covariances with no normalization. For a length *N* vector, the output vector `c` had elements given by:

$$c\ (m) = c_{xy}(m\text{-}N), \quad \text{where: } m = 1, ..., 2N\text{-}1.$$

$$c_{xy}(m) = \begin{cases} \sum_{n=0}^{N-|m|-1} \left(x(n+m) - \frac{1}{N}\sum_{i=0}^{N-1} x_i \right)\left(y_n^* - \frac{1}{N}\sum_{i=0}^{N-1} y_i^* \right) & m \geq 0 \\ c_{yx}^*(-m) & m < 0 \end{cases}$$

The covariance function required normalization to estimate the function properly. In all cases, `xcov` gave an output in such a way that the *zeroth* lag of the covariance vector was in the middle of the sequence, which was defined as element `maxlag`. The program had different modalities to select a method, the one chosen here was the `'unbiased'`. In some cases covariance was estimated with `'coeff'` method (which normalized and got values between -1 and +1. In most of the cases of inspection of the traces, the auto-covariance correlations were not calculated (fig M.3).

Discriminant analysis

Another approach to decode the behavioural state of the leech from the spike sorted activities was to run a *discriminant* analysis on some time-varying features that were believed to vary accordingly to the particular behavioural state of the animal. A set of features were chosen: the *n (n- 1) / 2* coefficients of the covariance matrix were estimated (using the `xcov.m` function in unbiased mode) from the spike sorted activities in a sliding time-window (100 s wide, 2 s step), or the raw activities alone. This was achieved by using the function `classify`.m

implemented in MATLAB, passing as input argument the matrix of all the time-varying covariance coefficients (or the matrix of the raw activities) and a short training episode; half containing 0-class events (i.e. not during the behaviour under consideration) and half containing 1-class events (i.e. during the behaviour under consideration). Different types of classifier options were tested: *linear*, which fits a multivariate normal density to each group, with a pooled estimate of covariance, *diaglinear,* i.e. naive Bayes classifier with a pooled estimate of covariance, *quadratic*, which fits multivariate normal densities with covariance estimates stratified by group and *diagquadratic*, i.e. naive Bayes classifier with covariance estimates stratified by group (Krzanowski, 1998 for a thorough review). The function output assumes unity values when the behaviour under consideration is supposed to be performed and 0 values on the contrary. When classifiers on all the 276 covariance matrix coefficients were tested, the dimensionality was forced to be reduced; thus, also the number of available coefficients in order to obtain a training set covariance matrix that was definitely positive. This was achieved with a principal component analysis on the original covariance matrix `pcacov`.m, and selecting the first 100 principal components, reducing thus, the feature space dimensionality.

ROC analysis

To assess the performance of a classifier, being it the simple threshold classifier, the *discriminant* analysis or the dendrogram matcher, *Receiver operating characteristics* (*ROC*) graphs were used. Given a classifier and an instance, there were four possible outcomes to consider. If the instance was positive and it was classified as positive, then it was counted as a true positive; if it was classified as negative, then it was counted as a false negative. If the instance was negative and was classified as negative, then was counted as a true negative; if it was classified as positive, then it was counted as a false positive. Given a classifier and a set of instances (the test set), a two-by-two confusion matrix (also called a contingency table) was constructed representing the dispositions of the set of instances; this matrix formed the basis for many common metrics. The true positive rate (*TPR*) of a classifier was estimated as the ratio of the true positives counts to the sum of the true positives and false negatives counts. Contrary, the false positive rate (*FPR*) of a classifier was estimated as the ratio of the false positives counts to the sum of the false positives and true negatives counts. In the *ROC* graphs *TPR* was plotted on the Y axis and *FPR* was plotted on the X axis (fig R.1). The perfect classifier was represented by the point (0, 1: upper-left corner). By varying the classifier type (as in the discriminant analysis case) or the threshold parameter (fig R.1B) it was possible to get different performances.

Informally, one classifier in the ROC space was better than another if it was to the northwest (*TPR* is higher, *FPR* is lower, or both) of the first. Analyzing the *ROC* space, it was determined which classifier performed better by looking at the closest point to the upper-left corner.

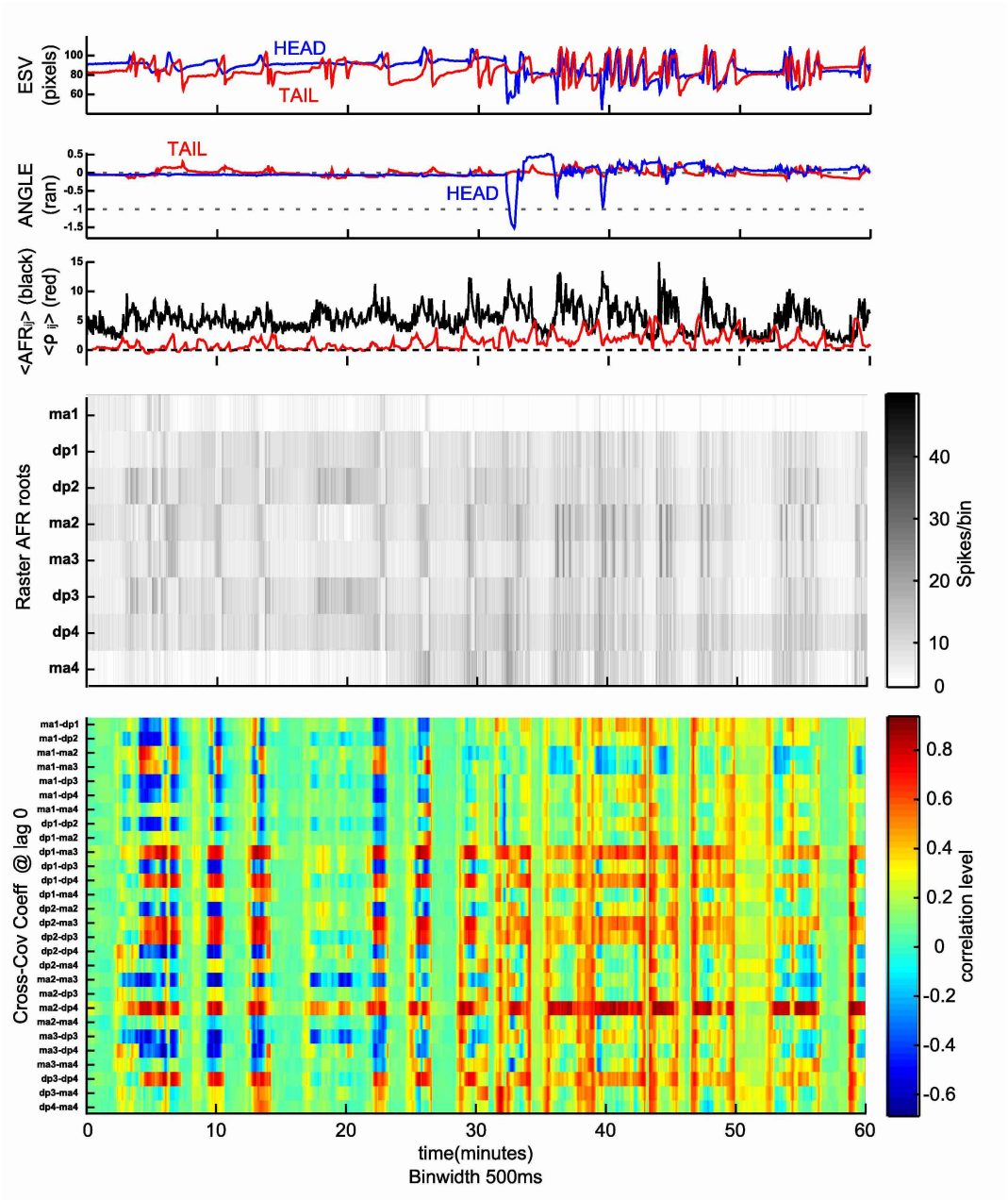

Figure M.3 ***Inspection of trace from roots recording***. Sixty minutes of an experiment showing some processed variables; from top to bottom: ***ESV*** Elongation calculated from coordinates. ***ANGLE:*** angular variable theta (**θ**). Negative values are the position of the bead at left side while positive values the right. Third panel shows **<AFR$_i$>** calculated with the roots firing rates and **< ρ$_{ij}$ >** calculated with all correlations from roots and amplified x 10 times to compare with the firing rate. Units are spikes/bin. ***RASTER***: is the firing rate from 8 roots along the experiment. ***Cross-covariance*** (coefficient) calculated from the combination between every root firing rate. Correlation is denoted by red, non-correlation by green and anti-correlation by blue colour.

Inspection of the traces

In many occasions the large quantity of information displayed using traces from behaviour, *AFR* and ρ produced computationally heavy images to work on. This happened by the differences in the sampling frequency acquisition originated by the equipment (fig M.4) in the set up (*AFR* at 2 Hz while behaviours 25 Hz). To resolve this problem, all the traces where interpolated (`interp1.m`) to the same sampling number of the *AFR* (fig M.3). This gave the possibility to speed up the inspection and advantageously the calculation of scatters with the corresponding slope fit line (fig R.2D & E),

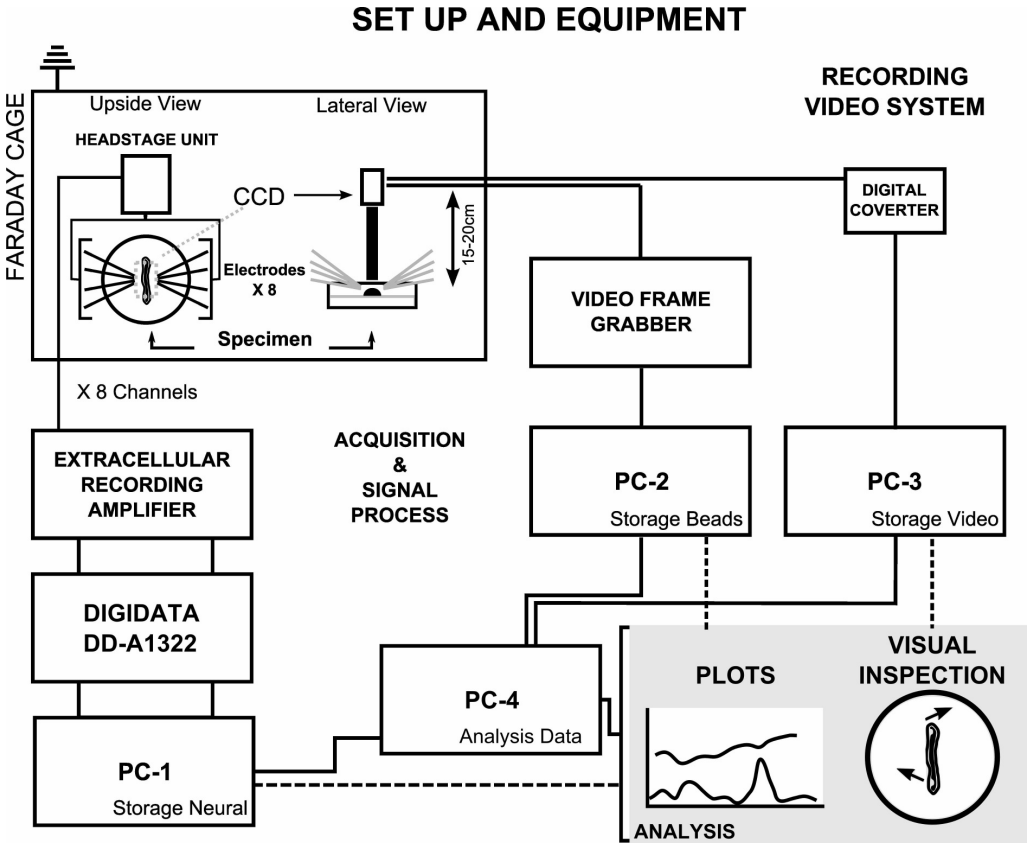

Figure M.4. ***Set up and equipment:*** diagram of the set up necessary to record the experiments in the laboratory. A Faraday cage containing the preparation, CCD camera and the headstage from the extracellular amplifier where connected to three acquisition computers (PC 1 to 3) using the diagrammed interfaces. The extraction of the information resulted in low-noise extracellular recordings, acquisition of beads at 40 Hz of sampling frequency and videos in Mpeg format. The information obtained was analyzed with the help of a fourth computer (PC-4), applying algorithms to visualize plots and inspecting videos. The information was interchanged between all PCs.

Dendrograms

The firing rates of up to 26 spike sorted motoneurons can be classified into clusters that contain similar activities. One of the most intuitive measures of similarity between two firing rates is the Pearson's correlation coefficient. The work continued to investigate how single neuron activities are related to one another and if a particular hierarchy may encode a stereotyped behaviour, such as swimming or crawling: this leads to an interest in hierarchically-nested sets of partitions, commonly represented in rooted tree diagram, or a *dendrogram*. The uncentred correlation coefficient was used as a metric (i.e. one minus the sample Pearson's correlation between single cell activities), and a dissimilarity matrix was constructed using the functions `pdist.m` and `squareform.m` implemented in MATLAB. The dissimilarity matrix $[d_{ij}]$ contained the n x n pairwise dissimilarities between the ith and jth objects (where n is the number of objects to be classified). Once the dissimilarity matrix was obtained, the hierarchical cluster tree was obtained by means of the *linkage* function (using the complete linkage method) and visually represented with the *dendrogram* function. We used the *complete linkage method* because it is used extensively in the social sciences where the interest is more in forming compact clusters that are as internally homogeneous as possible (Baker, 1974), it is less sensitive to noise (Baker, 1974) and may be used with non-Euclidean dissimilarity matrices, such as the uncentred correlation. The hierarchical clustering procedure explained above was run on time intervals during which the leech was either swimming, pseudo-swimming, crawling, elongating or shortening. Separated episodes were clumped together.

Comparisons between dendrograms

By considering time intervals during which the animal was crawling, swimming, or pseudo-swimming, as well as shortening or elongating, a dendrogram was estimated for each of these behaviours by running the aforementioned hierarchical clustering algorithm on the spike sorted activities up to 30 motoneurons. Once these dendrograms were estimated, were used as templates to be compared with a generic dendrogram calculated on a sliding time-window of 100 s width and 2 s sliding step. To compare two dendrograms, one needs a measure of similarity between them. Usually, similarity indexes were normalized and ranged 0- 1, where 0 represented complete dissimilarity while 1 equality. The best comparisons were obtained with *Fowlkes-Mallows Index* (B_k) and *Normalized Mutual Information* by Fred & Jain (2003). The former index was interpreted as the geometric mean of precision (ratio of the number of retrieved

relevant documents to the total number of retrieved documents) and recall (ratio of the number of retrieved relevant documents to the total number of relevant documents), while the latter had its origin in information theory and was based on the notion of entropy. Values near to zero were usually observed when comparing a dendrogram resulted from time intervals during which the animal was stationary (fig R.1) and the correlations were known to be low, resulting in flat dendrograms. Values near to one could be expected when comparing a dendrogram estimated over an episode of motion behaviour (e.g. crawling) and the reference dendrogram was estimated apart.

RESULTS

Leeches gently dissected were able to move their head and tail, surviving for several hours on the recording dish (fig M.1A left). Animals could be studied for several hours while their electrical activity and beads attached to skin were tracked by the electronic equipment (figs M.1A and M.4). Visual inspection of traces and videos permitted to display patterns of electrical activity and relate them to specific behaviours, once the variables were plotted against the time (fig M.3). The CNS of anesthetized leeches was exposed in 3 to 5 segments of the mid-body (fig 1.1B) removing skin, muscles, gut and excessive fibres attached to ventral blood sinus, in which the CNS was contained (fig 1.1A). Leeches demonstrated strong resistance against the damage provoked to the skin and tissue removal (cleaning). In many cases, adding culture medium *L-15* - ringer (1:1) during the dissection helped to preserve the nervous system and maintain it with the necessary nutrients.

Roots were cleaned from tissue debris and 1- 4 ganglia were exposed depending on the type of preparation. Common nomenclature for root's identification was used. The connectives were recorded positioning suction electrodes on the anterior (rostral) and posterior (caudal) sides of the selected ganglia. Before starting the recordings, the solution, in which the preparation was immersed, was changed using normal ringer. Solutions were changed constantly every hour during dissections and during recording sessions.

The set up to acquire both type of signals consisted on a classic electrophysiology anti-vibration table surrounded by a faraday cage situating a CCD camera, a stereoscopic microscope, and eight electrode holders connected to the main headstage from an extracellular amplifier (fig M.4). Neural signals were acquired connecting roots to an extracellular amplifier by suction electrodes inserted into suction electrode holders (fig M.1A). Following basic concepts of electrophysiology, all the electronic systems and the preparations were grounded to obtain extracellular recordings with the minimum quantity of noise (around 10 μV, fig M.1C). Simultaneously, behavioural signals were acquired with a computer using a software that tracked glued beads to the extremes (head and tail) of the animal's body (figs 1.1A and M.1B). The algorithm (used as in Mazzoni *et al.*, 2005) was modified to obtain more stable tracked signals. The glass electrodes were situated over the preparation in such a way that beads were visible by the camera situated over during the recording. In this way, five primary behavioural variables (signals) of continuing tracking over the time were displayed in addition to the simultaneous extracellular recordings from 4-8 electrodes (fig M.1B & C).

The resulting primary variables of behaviour to be analyzed were the head and tail position (*x* and *y*), and the variation of the area from a segment innervated by one ganglion (information not shown). Experiments with at least 4 extracellular roots were analyzed and experiments with extracellular recordings ≤3 roots were excluded for the analysis. Experiments which exhibited poor behaviours or deficiency in the acquisition of the signals were also discriminated. Patterns of behaviour and electric patterns were observed, identified and analyzed off-line (figs R.1 to R.7).

Stereotyped semi-intact leech behaviours

Six different stereotyped behaviours were previously detected in intact leeches (Mazzoni *et al.*, 2005, García-Perez *et al.*, 2005). These behaviours were: *Swimming, Exploring Head, Pseudo-swimming, Crawling, Peristalsis and Stationary States*. Similar behaviours could be detected also in semi-intact preparations and were characterized by visual inspection describing the activity performed by the body and suckers:

Swimming leeches detached front and rear suckers from the bottom of the plate and the head and tail beads oscillated with a relatively stable frequency around 1.5 Hz.

*Pseudo-Swimming (*or *Ventilation)* leeches kept their tail sucker attached and the head sucker detached; the head bead swayed as during swimming episodes but with a lower frequency: ~1 Hz.

Exploring (Head) leeches detached the front sucker keeping rear in attach position to rubber substratum. Head bead presented variable and irregular elongations or contractions (forward- backward) without any side preference (right-left). Periodic signals were not elicited.

Crawling leeches (both pinned and semi-intact) alternated front and rear suckers (attaching and detaching) in coordination with their body's elongation-contraction. The pattern was relatively similar to that observed in crawling intact animals. The frequency in crawling episodes was lower than in intact leeches (fig R.5A).

Peristalsis was detected on leeches maintaining front and rear suckers in attached position; animal body's elongation elicited slightly periodic cycles of stretching with a frequency of about 0.03 Hz.

Stationary states were detected when front and rear suckers were maintained in attach position and bodies did not exhibited motion pattern or any slightly change in the elongation. This behaviour was deeply analyzed with classifiers of electrical patterns analysis (fig R.1A).

Signal processing

To achieve the relation between behaviour and nervous system signals, both types of primary signals obtained were processed off-line. Three *behavioural signals* were processed to obtaining new automated variables: *ESV* or *Elongation-Shortening Vector* which represents the magnitude of contraction (local or whole body) in pixels calculated by the distance from a selected point ($M_{x, y}$ as centre of the preparation) and the position of the bead from head or tail ($C_{x, y}$) plotted over the time (*ESV*; fig M.1B). The second was the *Right-Left* position, calculated manually as an imaginary line parallel to x with the same y magnitude of M and plotted in time as steps (fig M.1B). However, considering the redundancy of these steps, this signal was computed again calculating the angle position (θ) of the vector *ESV* (head and tail) with respect to point M in radians units (fig. M.3); the angle (θ) variable was used to identify moments in which some neurons or roots *AFR* entered in anti-correlation phases (see this discussion ahead). The third type of behaviour's signal employed was the *Sucker Attach-Detach* (fig M1.B), identified off line reviewing the videos of the experiments recorded. The times of occurrence of events were plotted as steps (fig M1.B) and were useful to analyze the statistics of the sucker that are discussed ahead (fig R.4).

Electrical signals. To analyze in a reliable way the neural activity, extracellular recordings were visualized using two kinds of descriptors: the *AFR* over time (fig. M.1C and R.1A) and the correlation between signals defined as the *Auto-* and/or *Cross-Covariance* index over the time ($\boldsymbol{\rho}$) calculated from the *AFR* (fig R.1A). The recordings were processed detecting spikes with an algorithm (fig M.2), which reorganized the original signal interpolating it and producing time series of the peaks and the waveforms. The time series of detected spikes from recordings resulted in the *AFR* when the spikes were counted in every bin producing discrete time series. Different bin widths were applied to inspect the *AFR* from roots or connectives, especially in the case of neurons identified, which demanded small bin widths to identify patterns along the experiments. The correlation descriptor or $\boldsymbol{\rho}$ was calculated displaying the relation between roots or neurons on the time, resulting in 3 possible cases: correlation (positive values), anti-correlation (negative values) and non-correlation (absence).

Cell identification

The spike's detection from extracellular recordings allowed to manage easily the information and to discriminate noise from recordings with the subsequent cell's identification

by spike sorting. The visual inspection of extracellular recordings simultaneously to unit's *AFR* permitted to determine the identity of the *bursters* (Kristan *et al.*, 1974B) and to associate them to some stereotyped behaviours. The so named bursters Cell 3 (which send its axonal process just to DP) and Cell L were identified easily as they produced the largest extracellular AP's on the DP (Stuart, 1970; Kristan *et al.*, 1974B; Baader & Kristan, 1995; Baader, 1997). The next spikes identified according to the spike's shape on DP traces were: AE > Cell 110 > Cell 10 with the support of previous contributions (Stuart, 1970; Arisi *et al.*, 2001; Zoccolan *et al*, 2002). The counterparts of largest spikes in the MA roots were the Cell CV and Cell 109 respectively (Kristan *et al.*, 1974B; Zoccolan *et al.*, 2002). An important property of identified cells L, AE and 110 was the presence of their twin spikes in parallel recordings as they send their axonal processes to another roots like MA root (figs M.1C: *inset* and R.2B). Some inhibitors (like the shown Cell 102 and Cell 119) were identified preferably with their *AFR* activity associated to motion behaviours like swimming, pseudo-swimming or crawling episodes (figs R.5A and R.7A & B). Other cells were identified easily by their long spike's shape on recordings from AA and PP roots: respectively Cell 107 and Cell 5 (results not shown in this work).

ELECTRICAL PATTERNS UNDERLYING BEHAVIOURS: STATIONARY STATES AND MOVEMENT

Stationary states

Semi-intact leeches spent a considerable time in stationary states (Mazzoni *et al.*, 2005), during which they do not move and the head and tail velocity is negligible. A leech was assumed to be in a stationary state when its head and tail velocities ($H_{velocity}$ and $T_{velocity}$) were near zero and no longer than 1 pixels/sec and had a time's duration at least of 1 minute. Considering that in the preparations it was possible to record the signals from four MA and four DP roots, in a typical experiment the firing rates from 8 roots were plotted and inspected to compare them with behaviours in multiple variable plots in searching of any specific pattern (Figs R.1A mid traces: *DP* and *MA*). Changes in the *AFR* from roots were noticed when traces were plotted over the time (fig R.1A), and as a consequence this influenced the change in their **ρ**. Inspecting the traces in detail, it was possible to distinguish that during motion changes were presented in accordance with the total elongation (ESV_{total}). Thereafter, arithmetic operations between traces were applied to search patterns. The total firing rate $\langle AFR_i \rangle$ was obtained averaging all the electrical signals

recorded form the roots (fig R.1A: *average firing rate*, upper trace) and the average covariance $<\rho_{ij}>$ was calculated from the mean of 8 traces of auto-correlations summed to 28 cross-correlations obtained as all the possible combinations between the root's *AFR* (fig R.1A bottom trace). During the stationary states, both the electrical signals, the $<AFR_i>$ and $<\rho_{ij}>$, elicited low values (fig R.1A: horizontal bars over bottom and upper traces). These observations helped to discriminate between motion and stationary states in the CNS of the leech.

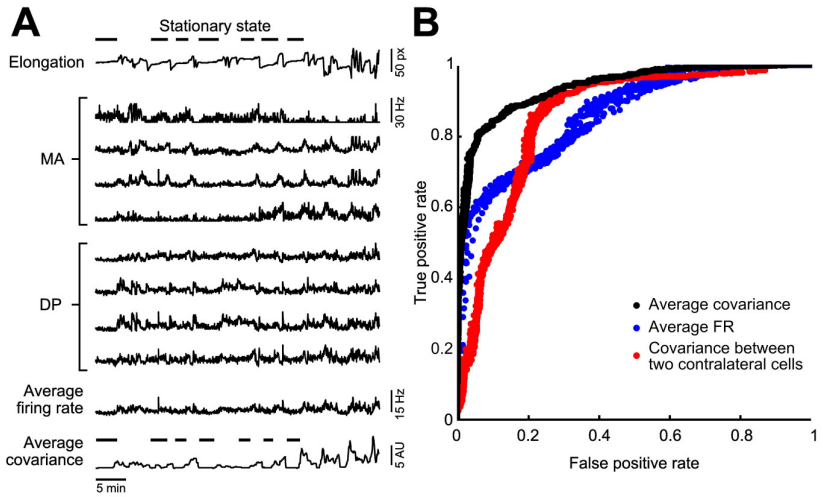

Figure R.1 ***Stationary states classification***. **A**. A representative experiment in which the total leech elongation was measured (upper trace) and compared to the *AFR* recorded from four DP and four MA roots located in 11th and 12th segmental ganglia (mid traces). The 8 signals were averaged and they can be shown as the time-varying $<AFR_i>$ (*Average firing rate*). Bottom trace represents the average of 8 auto-covariances and 28 cross-covariances that correspond to all the possible combinations to correlate or $<\rho_{ij}>$ (*Average covariance*). **B**. To compare the performance of different classifiers a *ROC* analysis was performed considering as a reference the velocity of each classifier to test. Varying the binarization parameters (i.e. the threshold level, the minimum time interval between two subsequent events and the minimum duration) results in a ROC curve. The perfect classifier is represented by the point (0, 1). Three classifiers were compared: the binarized average cross-covariance calculated with roots *AFR* (black dots), the binarized roots *AFR* (blue dots) and the binarized cross-covariance calculated with two contralateral motoneurons 3 identified with a custom spike sorting algorithm (red dots). The former of the three represents the best choice as it is closer to the perfect classifier in the upper-left corner.

So, whit this information we assumed that during motionless the total firing rate $<AFR_i>$ of the roots was maintained in low frequencies with a strong tendency to be uncorrelated in its average covariance $<\rho_{ij}>$. Instead, when the animal was moving the $<AFR_i>$ from roots rose with subsequent variations and $<\rho_{ij}>$ elicited positive and negative values. During the stationary states, the leech elongation does not change and both or at least one sucker was attached to the bottom of the observation disc.

Thereafter, with these observations the work demanded a receiver operating characteristic analysis (*ROC)* to discriminate which of the descriptors could be better classifier. A *ROC* curve

is a graphical plot of the sensitivity, or true positive rate vs. false positive rate, for a binary classifier system as its discrimination threshold is varied (Fawcett, 2004). It proceeded as follows: a level of threshold (T) was set identifying all the times $T_{<AFRi>}$ in which the $<AFR_i>$ was less than T; in the same way, a threshold was calculated for all times $T_{<\rho ij>}$ in which $<\rho_{ij}>$ was less than T. The rate of true positive identifications was computed for each value of T identifying the stationary state. Instead, the rate of false positive identifications was computed as all the times erroneously identified as a stationary state. These true and false positive identifications were computed for both $T_{<AFRi>}$ and $T_{<\rho ij>}$ as a function of T providing a pair of numbers corresponding to the true and false positive rates. The value of T for $<AFR_i>$ varied from 0 to 10 pixels and for $<\rho_{ij}>$ varied from 0 to 1 Hz^2 for the case of unbiased covariance.

These pairs were plotted, displaying the $<AFR_i>$ classifier and the $<\rho_{ij}>$ classifier (fig R.1B, blue and black dots respectively). When the T value decreased, the rate of both true and false positive decreased and the ideal classifier had a true positive rate approaching 1 and a false positive rate approaching 0. As shown in fig R.1B, the identification of stationary state based on the average cross-covariance $<\rho_{ij}>$ approaches the ideal classifier better than the identification based on $<AFR_i>$. It was noticed that the identification of stationary states based on the cross-covariance ρ_{ij} of a single pair of identified contralateral motoneurons (cell 3) is less efficient that the identification based on properties averaged over a population of neurons (fig R.1B, red dots). Together, these results shown that during stationary states both $<AFR_i>$ and $<\rho_{ij}>$ have small values and that the absence of correlation among the electrical activity of neurons firing is a good marker of them.

Patterns of electrical activity during head and tail motion

As it was previously shown, during a stationary state the electrical activity of roots and neurons is poorly correlated (fig R.1). The following hypothesis was that, when the leech moves, the electrical activity from roots rises giving a higher correlated activity, so this rising could be better seen at the level of identified single motoneurons. In order to measure the cross-correlation of the electrical activity elicited by motoneurons at the left and right side of a ganglion (contralateral) and in the neighbouring ganglia, experiments with 8 roots (four MA and four DP) were analyzed (fig R.2A). From the extracellular recordings the Cell 110 and Cell 3 motoneurons were identified and their *AFR* traces were inspected (fig R.2B green and red traces respectively). Both motoneurons presented a low firing rate during stationary states (less than 3

AP/sec), but they fired vigorously when their *AFR* was compared with rising values of the $ESV_{velocity}$ from head and tail (blue and red traces on top of fig R.2C). The electrical activity of the same contralateral motoneurons (3 and 110) and neighbouring ganglia appeared to be similarly modulated during the leech motion, so the cross-covariance between the four cells was calculated (fig R.2C). The cross-covariance computed on a bin width of 500 ms was consistently higher for pairs of motoneurons 3 than for pairs of motoneurons 110. When the leech moved its head or its tail, all pairs of motoneurons 3 contralateral or ipsilateral computed values of cross-covariance close to 0.7; similarly for a slow or a fast motion, as if the cross-covariance had binary values, being close to 0 during stationary states and close to 0.7 when the leech moved. An almost similar behaviour was observed for motoneuron 110, but for these motoneurons the cross-covariance reached values close to 0.5 when the leech moved.

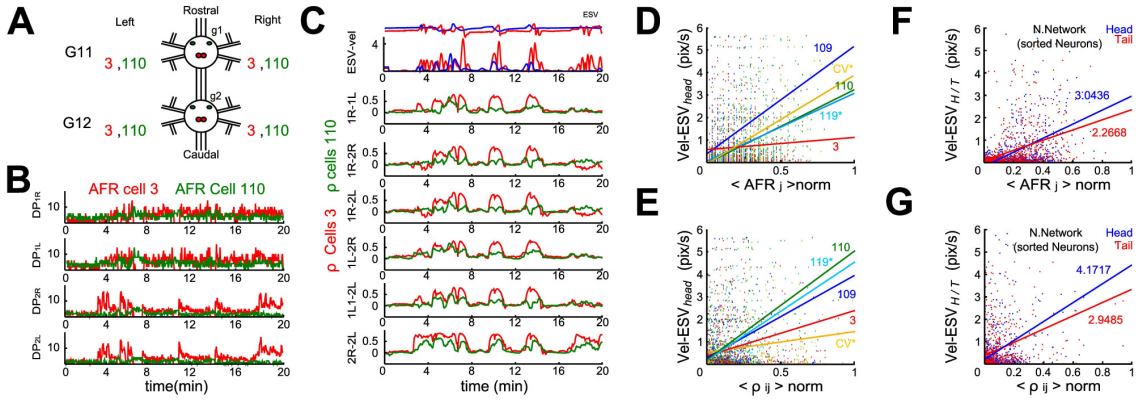

Figure R.2 ***Relationship between motion and values of neuronal AFR & covariance***. A. Schema representing the double ganglia recorded from semi intact preparation. G11 (g1) and G12 (g2) are the respective rostral and caudal ganglia. Each ganglion contains pairs of motoneurons cell 3 and cell 110; cells' positions are represented by the small circles in red and green respectively. The signals from both kinds of cells can be acquired in the DP root. **B**. twenty minutes of recorded *AFR* from 8 cells isolated by spike sorting algorithm and arbitrarily identified as cell 3 and cell 110 (red and green respectively). Bin width 500 ms. **C**. Comparison between the velocity of the elongation (*Vel-ESV*) and the cross-covariance coefficient calculated in time windows (6 traces correspond to combination of 4 cells) applied between cells from the same type. Motoneurons cell 3 correlations (red) presented higher **ρ** levels than cells 110 (green). **D**. Scatter plot of the $<AFR_j>$ calculated with 4 cells of the same type *vs. Vel-ESV*$_{head}$; identified motoneurons: 109 (blue), CV (yellow), 110 (green), 119 (cyan) and 3 (red) elicited respective slope values: 4.78, 3.97, 3.29, 3.05 and 0.54. Cells marked with (*) correspond to scatters and slope values calculated with $<AFR_j>$ or $<\boldsymbol{\rho}_{ij}>$ from 2 cells instead of 4. **E**. Scatter plot of $<\boldsymbol{\rho}_{ij}>$ *vs. Vel-ESV* with the same identified motoneurons from panel D; elicited slope values were: 3.63, 0.95, 4.85, 4.39 and 2.05 respectively. **F**. Scatter plot of neural network population's $<AFR_j>$ vs. *Vel-ESV* from head (blue) and tail (red); the neural network contained the *AFR* from 40 units sorted; slopes indicated. **G**. Scatter of the neural network $<\boldsymbol{\rho}_{ij}>$ vs. the *Vel-ESV* from head and tail (as in F); slope values are indicated. For all the scatters shown the $<AFR_j>$ and $<\boldsymbol{\rho}_{ij}>$ were normalized dividing by the maximal value obtained.

The next step consisted in understanding how the velocity of the behaviours from head and tail is coded in the electrical activity, i.e. which features of the electrical activity are associated to a low or high velocity, as the velocity was considered a good detector of motion. Initially, the

slope calculated with the data from roots and ESV_{head} was higher for $\langle AFR_i \rangle$ than for $\langle \rho_{ij} \rangle$ (not shown), indicating that velocity was better coded or represented by the average firing rate over an extended population of motoneurons. Nevertheless, using the $\langle AFR_i \rangle$ calculated with the *AFR* from 40 units sorted with the program, the values of slope were favourable to $\langle \rho_{ij} \rangle$ (fig R2.F & G). Data from identified motoneurons was collected measuring their $\langle AFR_i \rangle$ (bin width 500 ms) and unbiased $\langle \rho_{ij} \rangle$; the relation between $\langle AFR_i \rangle$ and ESV_{head} and between $\langle \rho_{ij} \rangle$ and ESV_{head} could be fitted by a straight line with different slopes (fig R.2D & E).

Electrical patterns underlying the sucker attachment and detachment

Head and tail suckers are formed by layers of circular, radial and longitudinal muscles (Muller *et al.*, 1981; Baader & Kristan, 1995; Reynolds *et al.*, 1998; Kristan *et al*, 2005) and have a complex network of neurons and sensory units connected to their respective brains. The head sucker is essential during feeding and its sensory units are used also during exploration (Payton, 1981). The tail sucker is formed by the fusion of seven modified segments in the posterior region and is usually attached to substrate when the leech is at rest (Kristan *et al*, 2005). A controlled attachment and detachment of the head and tail suckers is essential during crawling (Schlüter, 1933; Gray *et al* 1938; Baader & Kristan, 1995) and it is not known whether sucker attachment/detachment is controlled by command neurons such the pair of neurons R3b-1, controlling swimming and/or crawling (Esch *et al.*, 2002) and the trigger neurons Tr1 and Tr2 initiating and terminating swimming (Brodfuehrer and Friesen, 1986). For this reason, the properties of sucker attachment and detachment were investigated with the aim to identify associated patterns of electrical activity.

The statistics of sucker attachment and detachment in preparations with intact-pinned leeches and semi-intact leeches were first analyzed and compared (fig R.3). Inspection of videos recorded simultaneously during the experiments was achieved determining whether the head sucker was attached (H') or detached (H) and similarly whether the tail sucker was attached (T') or detached (T). In this way, the leech could enter into four different states: H'T', H'T, HT' and HT (fig R.3A), according whether its suckers were attached and/or detached. Comparing the performed behaviours from semi-intact and pinned leeches, an important question emerged: whether the removal of part of the animal body had effects on the suckers attachment and detachment. Four semi-intact and four intact-pinned preparations, leeches were analyzed for hours quantifying the occurrence and statistics of the four sucker's states. Both preparations

exhibited similar occurrences in attach/detach from head and tail suckers (fig R.3B). Making statistics about this behaviours, for semi-intact leeches the fraction of time spent in states H'T', H'T, HT' and HT was respectively 0.48±0.20, 0.33±0.15, 0.16 ±0.11 and 0.03±0.03 (fig R.3C, obscure bars). For intact-pinned leeches the fraction of time spent in each state was respectively 0.58±0.29, 0.18±0.20, 0.23 ±0.12 and 0.01±0.02 (fig R.3C clear bars). These observations indicated that semi-intact and pinned leeches produced the same occurrences in the time spent for attach/detach behaviours, and importantly that the events of the sucker were not influenced by the tissue removal.

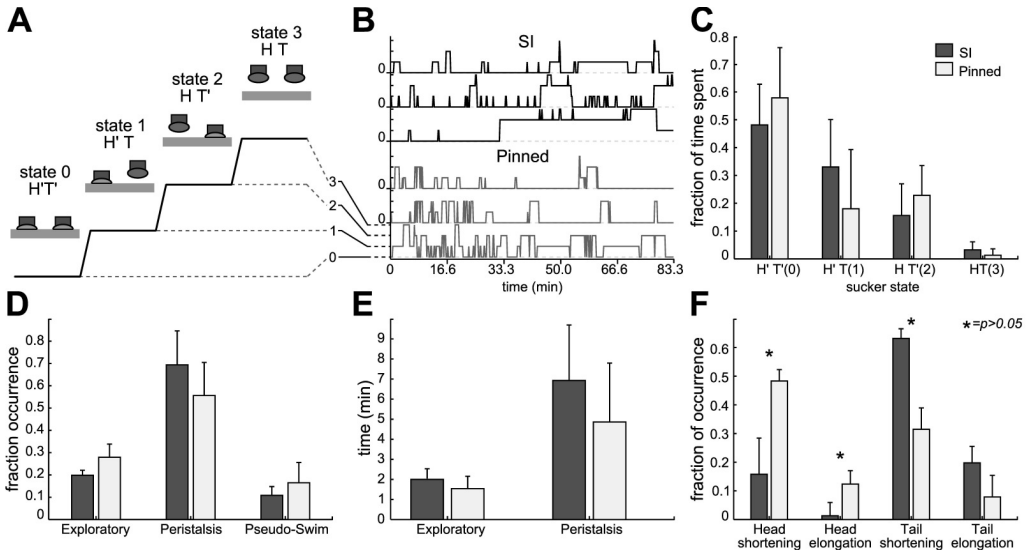

Figure R.3 ***Behaviours from head and tail sucker.*** **A**. Diagram representing the four behavioural states of the suckers: State 0, both suckers are attached (H'T'). State 1, head's sucker is attached while tail's sucker is detached (H'T), State 2, head sucker is detached while tail's sucker is attached (HT'). State 3: head and tail's suckers are detached (HT). **B.** Sucker states evolution from three semi-intact experiments (top traces in black) and three pinned experiments (bottom traces in gray). **C**. Frequency distribution of the four sucker states averaged from experiments. Semi-intact is represented with dark bars while pinned-intact with gray bars. **D**. Fraction of occurrence of exploratory, peristalsis and ventilation when the tail sucker was attached but not the head sucker (state HT'). Comparison between pinned but intact (dark bars) and semi intact (clear bars) leeches. **E**. Mean duration (minutes) of exploratory and peristalsis episodes averaged from experiments of pinned-intact (clear bars) and semi-intact (dark bars) leeches. **F**. Fraction of occurrence of body contraction and elongation following head and tail detachment of pinned but intact (dark bars) and semi intact (clear bars) leeches.

From the inspection in both types of preparations, it was also possible to identify periodic and no-periodic behaviours elicited during the suckers' behaviour types in a 0-type (stationary) or type 2 (head free). Three of the behaviours were similar according to the head's motion: leeches produce *exploring* (moving the head), *peristalsis* motion when head's sucker was attached (with high occurrence) and in rare occasions they produced periodic behaviours like *pseudo-swimming* (fig R.3D). Comparing these three behaviours between pinned-intact and

semi-intact, there was no statistical difference in the occurrence of them (fig R.3D). Therefore, the mean's duration of complete episodes of exploratory and peristalsis behaviours were counted resulting the sucker state type-0 a good indicator to measure stationary states. The mean's time duration of the pseudo-swimming computed values lasted less than 10 seconds, but it was not shown because of an excessive variation in the experiments (data not shown). Semi-intact and pinned preparations computed an averaged duration in the elicited exploring episodes of 2.01±0.49 and 1.77±0.55 minutes respectively; in the same way, for the peristalsis the preparations computed 7.06±2.80 and 4.68±2.73 minutes respectively (fig R.3E).

Following detachment of the head sucker in intact but pinned preparation, leech shortened its whole body, more often than a semi-intact leech (fig R.3F). A different behaviour was observed following detachment of the tail sucker: in this case the semi-intact leech shortened its body more often than an intact but pinned leech (fig R.3F). The results shown in Fig R.3 suggest that semi-intact leeches are able to attach and detach their head and tail suckers very similar to what observed in intact-pinned leeches. So, the next question was if it is possible to identify patterns of electrical activity underlying sucker attachment and detachment.

Having identified transitions between different states, the electrical activity recorded during these transitions was aligned and events were investigated in a time window of 30 sec before and after sucker attachment and detachment. In these experiments, suction electrodes were used in an *en passant* configuration (Pinato *et al.*, 2000; Arisi *et al.*, 2001; Zoccolan *et al.*, 2002) to record the electrical activity from the connectives also. In order to identify APs from possible command neurons associated to sucker attachment and detachment, one electrode was positioned in such a way to record from the rostral connective (RC) and another electrode was positioned in such a way to record from the caudal connective (CC) relative to the dissected and exposed ganglion. Other suction electrodes were used to record APs from the DP and MA roots.

When the head sucker detached and the leech shortened its whole body, a significant increase of the *AFR* in the RC, CC, DP and MA roots was observed (fig R.4A). When the head sucker attached, a small decrease of *AFR* in the RC and in the DP roots, but not in the CC and in the MA roots, was observed (Fig R.4B). Significant changes of the *AFR* from the RC, CC, DP and MA roots either when the tail sucker detached (Fig R.4C) or attached were not detected (Fig R.4D).

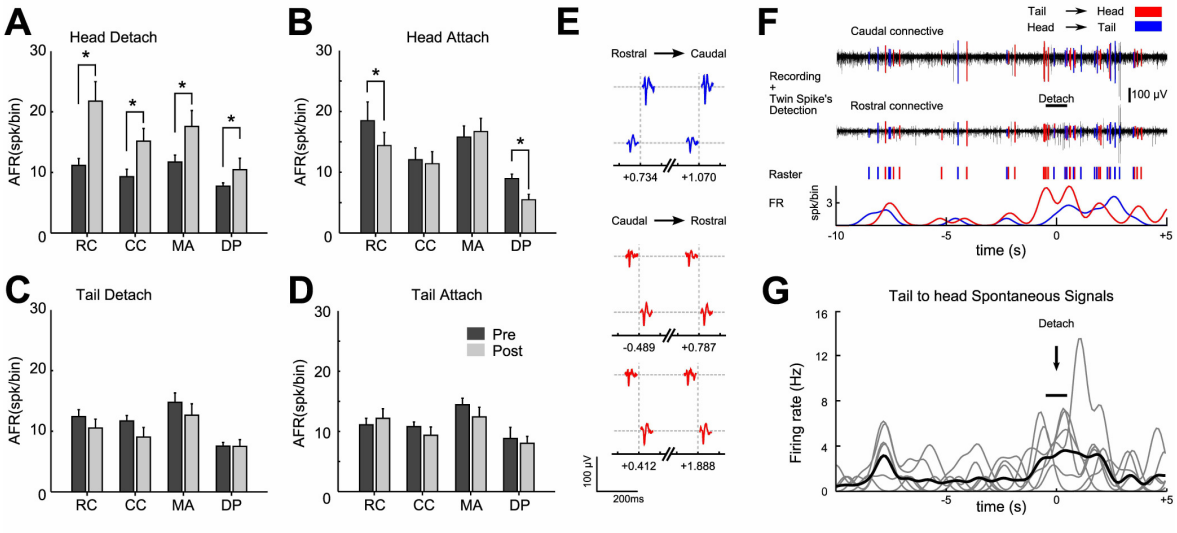

Figure R.4. ***Identification of electrical patterns underlying head sucker detach***. **A.** Averaged <AFR_j> 60 seconds before (dark bars) and after (clear bars) an event of head's sucker detach. The *AFR* was obtained from a single ganglion preparation in which where acquired the rostral connective (RC), caudal connective (CC), medial anterior root (MA) and dorsal posterior root (DP). **B**, **C** and **D**. Bars shows as in A, the same averaged <AFR_j> but for the head attach, tail detach and tail attach respectively. **E**. Twin spikes identified from connective recordings during the head's detach event shown in F. Three different spikes were identified computing the same latency (~6 ms). Twin spikes in blue correspond to the same signal that travelled from head to tail (as in F). Red spikes corresponded to signals travelling from tail to head (as in F; delay time ~6 ms). Fro the three cases shown, the spike amplitude of the waveform was essential for their identification. **F**. Electrical recording window of 15 seconds in which occurred a head's sucker detach (at time = 0). Top: electrical activity recorded from two connectives (black traces). Selected spikes with fixed latency of ~6 ms between the rostral and the caudal connectives superimposed to the analogical traces and highlighted in blue (from head to tail) and red (tail to head). Middle: raster plot from the highlighted spikes in blue and red respectively. Bottom: smoothed <AFR_j> of the blue and the red selected spikes shown in the middle and upper plots. Notice the rise in the AFR near the detach event marked by Detach and the Black bar. Bar = 1 s. **G**: Firing rate of 7 units (gray traces) identified as described in panel F: Top, and mean firing rate (black trace). A common activation pattern can be observed for the identified cell: a burst of 3-4 Hz precedes (by about 8 seconds) the head detach, during which another burst of the same average frequency occurs. The detach events marked with the arrow and the bars (as in F) occurred with an imprecision of about 1 second.

As it was possible to detect a significant increase of the *AFR* of signals measured from the connective fibres during the head sucker detachment, the analysis focused in the APs travelling along the connectives with the aim to identify possible command neurons for head attachment. Several APs in electrical recordings obtained from the RC and CC were identified (fig R.4E) travelling from the head to the tail (indicated in blue) and from the tail to the head (indicated in red). These APs appeared always as twin APs with a stereotyped shape and amplitude in the CC and RC separated by a delay of 4-6 msec. APs travelling from the head to the tail and vice-versa appeared approximately 8 seconds before the detachment of the head sucker (Fig R.4F). This burst of 3-8 APs was followed by a larger burst of APs during sucker detachment. APs

preceding the detachment of the head sucker could be part of the electrical commands underlying this behaviour. This pattern of electrical activity was found in a large portion (85 %) of the head sucker detachments and APs travelling from the tail to the head appeared consistently (Fig R.4G).

Electrical patterns underlying crawling

In previous sections, it has been shown that during stationary states both $<AFR_i>$ and $<\rho_{ij}>$ declined and that the motion of the animal is associated to large values of the firing rate of individual motoneurons and of the firing rate cross-correlation between individual motoneurons. The next step in the work was to ask whether it could be inferred from the firing rate of motoneurons if the leech is elongating or contracting its body and whether it was possible to determine if it is crawling, swimming or pseudo-swimming.

The swimming and the crawling are two central pattern generators extensively studied in the leech (see the introduction of this thesis). When a leech is touched or disturbed, depending on the magnitude of the information that receives, it can swims or crawls; so these behaviours are considered an escape reaction (Kristan, 2005; Zoccolan, 2002). The swimming central pattern generator, which is an oscillator, can be started with a cascade of neurons activations that will be briefly described in the next lines (for a more detailed description see the review from Kristan, 2005): the resting potential of sensorial neurons like T, P or N can be activated by a sensorial input, or it can be also originated by the sensillar movement receptor (SMR1). The nervous impulse is transmitted to any of the so called trigger neurons, which almost automatically can produce the necessary commands to other cells to initiate or terminate the swimming: Tr1 triggers for initiating and Tr2 trigger-toggle which can initiate (or terminate) the swimming from the subesophageal ganglion. Another path exists and it can trigger via the subesophageal ganglion: the SE1 (swim excitor neuron 1) and SIN1 (swim inhibitor neuron 1), which are interneurons that elicit the same objectives. The impulse is transmitted, then, to the gate control neurons: the set of serotonin-containing neurons, cells 21/61, which can gate the swimming, and the set 204/205 which are excitatory interneurons unpaired in ganglia and are restricted to the posterior half of the nerve cord. The next step of the signal involves the group of oscillator interneurons which are present in every ganglion of the mid body, which oscillates their potential activating and deactivating cells like ventral excitors and inhibitors, dorsal excitors and inhibitors and a flattener neuron. The oscillators comprises: 208, 115, 27 and 28 (Kristan, 2005).

In the case of the central pattern generator which drives the crawling, the knowledge is less detailed but what is known is that the initiation starts with the R3b1, located in the third neuromere of the subesophageal ganglion. This neuron can initiate the crawling motor pattern in both semi-intact and isolated nerve cord preparations (Esch *et al.*, 2002). R3b1 oscillates above its resting potential during the continuation of the behaviour and even its depolarization can produce swimming, or a combination of swimming and crawling.

The burst activity from the initiator activates as a chain reaction the downstream motoneurons: cell L, which exhibits depolarization of the action potentials and elevate its firing rate to ~10 Hz in the initial phases of the crawling step (Baader, 1997). The wave of activation continues to motoneurons cell 3 and cell 5 which exhibit depolarization in the resting membrane potential, an this can be reflexed in high burst activity during half to end phase of the contraction step (Baader, 1997). Some other interneurons and inhibitors have been recorded and present preference for contraction (S, AP, and 159) and elongation steps (1, 2, CV, 4, 151 and 152; interneurons 204 and 208, 258, 213) (Briggman & Kristan, 2006). A possible candidate of decision is the interneuron 204 (Baader, 1997).

Semi-intact dissections with two ganglia exposed and limited injury to the leech allowed the animal to display its usual behaviours such as crawling and swimming. Indeed, a semi-intact leech could crawl as it is shown in the upper images of fig R.5A. During crawling, the total elongation of the leech measured with the distance between its head and tail (upper trace in fig R.5A), oscillated with a period of approximately 40 seconds, alternating episodes of elongation and contraction. In several experiments with double ganglia, it was possible to reliably discriminate between 20 and 30 APs, sorting the motoneurons from the processed recordings. During the contraction phase of the crawling, several longitudinal excitatory motoneurons, such as motoneuron or 3, L increased their *AFR* (second and third rows in fig R.5A), while other motoneurons, such as the AE, CV, 109 and 102 (4th to 8th rows in fig R.5A) decreased their *AFR*. Instead, during the elongation phase most of the identified motoneurons inverted their firing pattern (figs R.5A).

An analysis of the *AFR* density from motoneurons during complete crawling cycle of contraction and elongation showed three classes of motoneurons: pure contractors activated only during the contraction phase (black traces comprising motoneurons 3 and L), pure elongators activated during the elongation phase (red traces comprising motoneurons AE, CV, 109 and 102) and intermediate units activated both during contraction and elongation (green traces:

motoneurons 119, 110, 101, 166, 10 and other cells not identified). In agreement with previous observations (Ort *et al.*, 1976A; Kristan *et al.*, 1976; Stern-Tomlinson, *et al.*, 1986; Baader & Kristan, 1997; Baader, 1997; Pinato *et al.*, 2000; Arisi *et al.*, 2001; Zoccolan *et al.*, 2002; Kristan, 2005; Briggman & Kristan, 2005; Briggman & Kristan, 2006), pure contract motoneurons were found in the DP root and pure elongate motoneurons in the AM root (Fig R.5C).

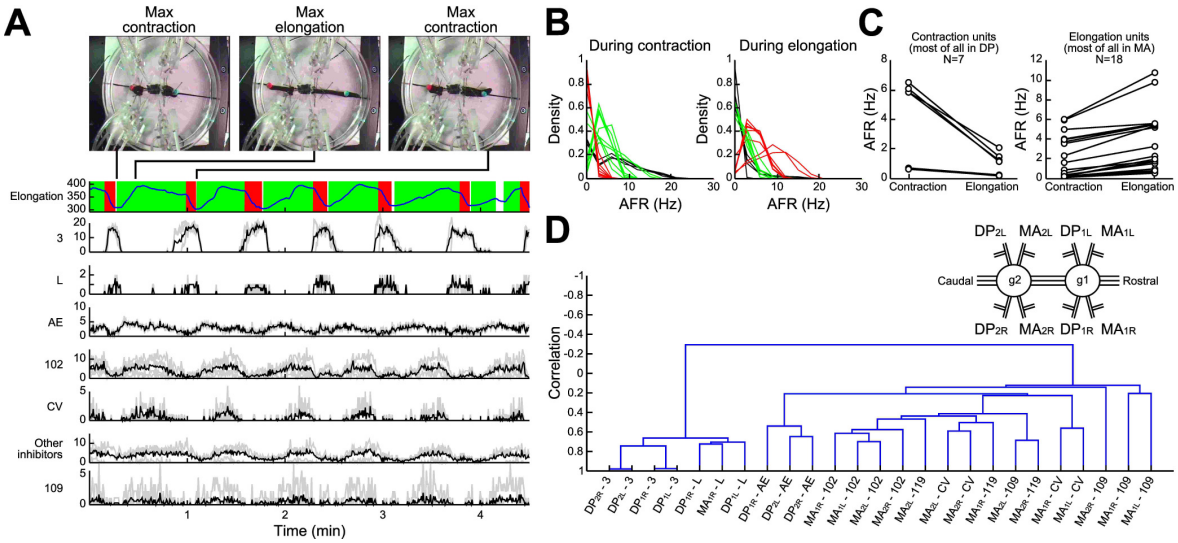

Figure R.5. ***Electrical patterns underlying crawling***. **A**. The crawling phases are shown and compared to the elongation trace (first plot, blue line). The contraction phase (red area) and the elongation phase (green area) were defined by processing the first time-derivative of the elongation trace. A custom supervised spike-sorting algorithm was launched on the 8 available electrophysiological recordings (4 DPs and 4 MAs). 25 different units were detected and subsequently classified. Considering the spike size (i.e. the peak amplitude) and the coherence between the resulting firing rates, each unit was labelled as one of the 6 plausible cells that can be recorded from DP and AM roots. **B**. Density plots of the average firing rate of each unit during contraction (left plot) and elongation phases (right plot). Three families of neurons can be distinguished: pure contractors (black traces), pure elongators (red traces) and intermediate units (green traces). **C**. Scatter plots of the average firing rate of each unit detected in the DP root (left plot) and in the MA root (right plot). During elongation, most of the units identified in the DP root decrease their *AFR*, while the contrary happens in MA units. **D**. A blind hierarchical clustering of each unity *AFR* was performed, using the single-linkage method with the correlation as a metric. The resulting dendrogram returns two families of neurons whose activities are anti-correlated: the contractor neurons are listed on the left, while the elongators are on the right. Root names are referred to the inset; i.e. DP_{2L}: Left Dorsal Posterior root of the 2nd ganglion (1 = rostral, 2 = caudal). Ganglia are numbered for simplicity: numberings are not referred to actual segments.

In order to identify and characterize patterns of electrical activity during crawling, a hierarchical clusterization of the involved motoneurons was developed using the single-linkage method with the correlation as a metric (see Methodology). This procedure returned a dendrogram describing in a compact form the degree of correlated and anti-correlated activity of motoneurons during the crawling cycle, in both contraction and elongation phases (fig R.5D). Two groups of motoneurons were correlated at some extent among them and they were mutually

anti-correlated; this result coincided with the observation that the *AFR* of one group increased during contraction and the other during elongation, as mentioned before. Observing the dendrogram in detail, it is possible to notice that motoneurons 3 and L from neighbour ganglia and contralateral were highly correlated between them (left arm, fig R.5D) forming a solid arm, while other motoneurons, such AE and 102 were similarly correlated each other but at less extent to the left and belonged to the arm opposed. In the opposite side of the dendrogram, other groups of motoneurons were formed (right arm: two CV cells and four 109) which were anti-correlated to motoneurons of the left arm of the dendrogram. Some other motoneurons were situated centrally (cells 119) and belonged to MA root recording, but could not form a group.

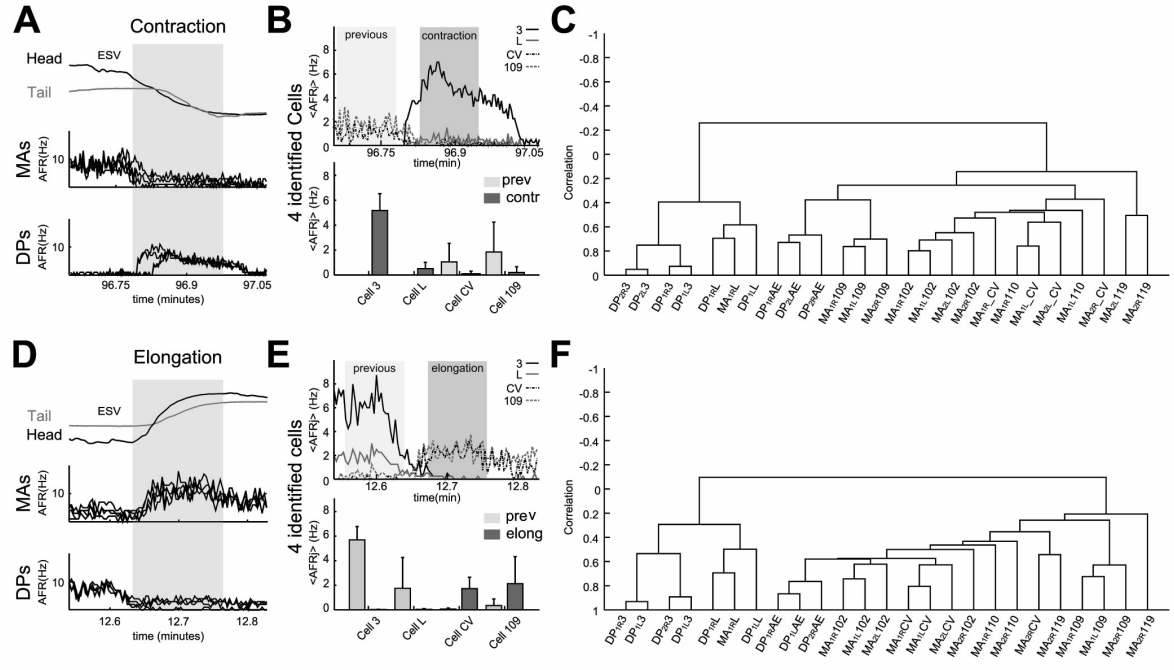

Figure R.6 ***Electrical patterns underlying contraction and elongation.*** Representative examples of time varying *AFR* from roots and identified neurons during episodes of contraction (respectively A & B) and elongation (respectively D & E) obtained from one experiment to calculate the corresponding dendrogram (C & F), without distinction of the stereotyped crawling behaviour. **A**. Response of eight roots (4 DP and 4 MA) to the whole body contraction elicited during 30 s (dark zone, scale in minutes) of an experiment. The 4 MA and 4 DP roots exhibited respectively decay and rise in their *AFR* during contraction. **B**. Top: traces show the $<AFR_j>$ from 4 cells from the same type (e.g. four cells 3). The different motoneurons identified were cell 3, cell L, cell CV and cell 109. Bottom bars: mean of the $<AFR_j>$ in 30 s episodes of previous (clear zone) and contraction (dark zone) calculated in each cell. Excitors from DP exhibited a rise in their activity (in Hz): Cell 3 rose from 0 to 5.72 ±1.3; cell L, from 0 to 0.71 ±0.35. Inhibitors exhibited a fall in their activity: cell CV, from 1.02 ±1.3 to 0.18 ±0.15; and, cell 109, from 1.88 ±1.9 to 0.20 ±0.15. **C**. Dendrogram resulted from the hierarchical analysis computed with the all the contraction episodes detected on the complete experiment. **D**. Similar plot as A presenting an episode of elongation of 30 s duration (scale in minutes) from the same experiment occurred around minute 12 (dark zone). The *AFR* was inverted (with respect to contraction) and the 4 MA and 4 DP roots exhibited respectively rise and decay. **E.** As in B, top traces show the $<AFR_j>$ from the same cells during detected elongation episodes. Excitors from DP exhibited a fall in their activity: Cell 3, from 5.89 ±0.99 to 0; cell L, from 1.61 ± 1.85. Inhibitors exhibited a fall in their activity: cell CV, from 0.01 to 1.56 ±0.6; and, cell 109, from 0.32 ±0.2 to 2.12 ±2.30. **F**. Resulted dendrogram from the hierarchical analysis for the elongation episodes from the experiment.

Electrical patterns underlying contraction and elongation

During crawling, leeches alternated contraction and elongation episodes with a characteristic pattern of motoneuron firing. As leeches shorten and elongate their body also during other behaviours, the next question to cover was whether the firing pattern of motoneurons during elongation (or contraction) was the same in other behaviours or as it happened during crawling; so, the *AFR* from motoneurons was analyzed during contractions and elongations not associated to crawling (fig R.6).

During all contraction episodes, the *AFR* recorded from the DP roots increased and the one recorded from the MA roots decreased (fig R.6A). The *AFR* of motoneurons 3 and L increased during contractions and the one of motoneurons CV and 109 decreased (fig R.6B). An almost opposite behaviour was observed during elongations (fig R.6D and E): during these events the *AFR* from the MA roots increased significantly as well as the *AFR* of motoneurons CV and 109, while the *AFR* from the DP roots and of longitudinal excitatory motoneurons, such as 3 and L decreased.

Electrical patterns of motoneurons firing during all elongations, either during crawling or during exploration, were similar and had almost the opposite pattern observed during contractions. Even though the dendrograms during contraction (fig R.6C), elongation (fig R.6F) and crawling (fig R.5D) were similar, some significant differences were observed between the groups of neurons. The three dendrograms have two major arms of anti-correlated activity, with each arm being composed by mutually correlated motoneurons. However, the degree of activity correlation varied with the specific behaviour: motoneurons 3 and L were more correlated during crawling than during pure elongation and contraction.

Electrical patterns underlying swimming and pseudo-swimming

Swimming and pseudo-swimming are related behaviours. Swimming consists of a wave of rearward moving crests and troughs of the flattened body, produced by phasic contractions of longitudinal muscles in ventral and dorsal segmental body wall (Kristan *et al*, 1974). During swimming, the head and tail oscillate with a frequency of ~1.5 Hz (Mazzoni *et al*, 2005). Leeches produce another rhythmic behaviour, usually referred as ventilation or pseudo-swimming (Magni & Pellegrino, 1978; Mazzoni *et al*, 2005). During pseudo-swimming the

rostral part of the body oscillates while the caudal part is motionless and the tail sucker is tightly attached.

Neuronal circuits underlying swimming have been extensively investigated (Kristan, *et al*, 1974; Ort *et al,* 1974; Kristan *et al*, 1974b; Friesen *et al*, 1978; Poon *et al* 1978; Stent *et al*, 1978; Weeks & Kristan, 1978; Brodfuehrer & Friesen, 1986; Brodfuehrer & Friesen, 1986b; Nusbaun & Kristan, 1986; O'gara & Friesen, 1995; Taylor *et al*, 2003). Pseudo-swimming, in contrast, has been less extensively analyzed. It is known that a strong discharge of L motoneurons blocks pseudo-swimming and allows the animal to enter in another state (Magni & Pellegrino, 1978). Pseudo-swimming frequency is also ~1.5 Hz as in swimming, but in pseudo-swimming, the tail sucker does not oscillate and remains attached (Mazzoni *et al*, 2005).

Swimming and pseudo-swimming can also be observed in semi-intact leeches. Indeed it was possible to observe the head and tail oscillating in antiphase with a frequency close to 1 Hz during the swimming (fig R.7A: ESV traces). For this stereotyped behaviour, the *AFR* from motoneurons 3 was the first clue in the searching for a motoneuron pattern. The inspection of the traces from sorted neurons shown that four motoneurons cell 3 oscillated vigorously all together with their *AFR* passing from ~10 Hz of crests to almost 0 Hz during swimming (fig R.7A). No other cell type exhibited a marked pattern, although other motoneurons entered in phase or antiphase: the cells 119 and 102, whose act as inhibitory motoneurons exhibited oscillating patterns in their *AFR* (with crest that reached approximately 2.5 Hz). AE cells elicited an *AFR* of ~ 4 Hz but with a slightly oscillatory pattern. CV cells exhibited a poor participation during the swimming, while L and 109 cell elicited oscillations that reached crests of around 1 Hz (fig R.7A).

Often the head of semi-intact leeches oscillates with frequencies varying from 0.5 to 2 Hz, while the tail remains still with its sucker firmly attached to the bottom of the recording dish (fig R.7B). These episodes were identified as pseudo-swimming (Mazzoni *et al.*, 2005; Garcia-Perez *et al.*, 2005; Bisson & Torre, personal comm.). During pseudo-swimming the *AFR* of identified motoneurons was very similar to those AFR exhibited by the identified neurons in swimming episodes (fig R.7B). Some differences are present in the firing activities from the same motoneurons analyzed on swimming episodes. The group of cells 3 exhibited still an oscillating pattern in their *AFR* but the crests in the oscillation pattern were diminished to ~3 Hz (fig R.7B). AE and 109 motoneurons analyzed exhibited firing rates similar to those exhibited in swimming episodes and CV, L and 102 elicited poor activities, nevertheless cell 102 oscillations were not constant as in swimming. Interestingly, the inhibitors 119 apparently rose their activity during the pseudo-swimming and this was noticed in the valleys of the signals (fig R.7B).

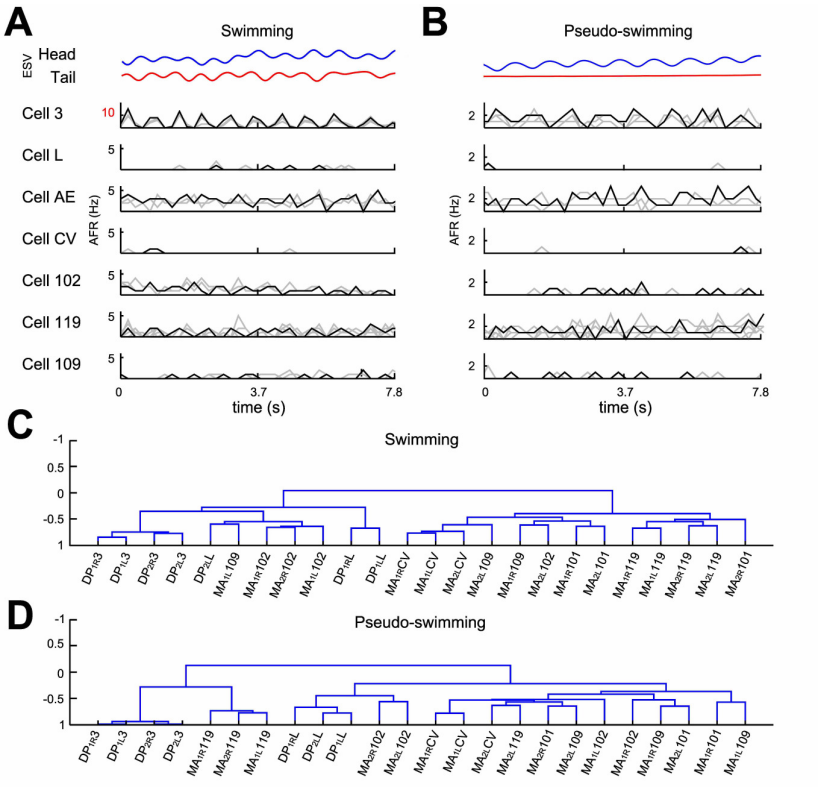

Figure R.7. ***Electrical patterns underlying swimming and pseudo-swimming***. Episodes of the stereotyped behaviours identified as swimming and pseudo-swimming. Both episodes were obtained from a semi intact preparation and elicited the same duration (7.8 seconds). **A**. Swimming episode elicited. From top to bottom are presented the next time-varying traces: the local elongation variables from head and tail (*ESV* in blue and red respectively) and the *AFR* from motoneurons obtained with the spike sorting (Hz scale vs. the time): cell 3, L, AE, CV, 119, 102 and 109. Four motoneurons from the same type were identified from double ganglion preparation (contralateral and neighbouring neurons from 4 MAs and 4 DPs extracellular recordings). Cell 3 was fit to be compared with the other cells (see the red number in *AFR* scale). **B**. plots representing the same variables in A but for the stereotyped behaviour of pseudo-swimming (see the continuity in ESV_{tail} which confirmed motionless). Notice that the cell 3 exhibited less firing activity. **C**. Dendrogram resulted from the hierarchical analysis applied during the swimming with the motoneurons shown in A. **D**. Dendrogram (as in C) resulted from the hierarchical analysis applied during pseudo-swimming episodes of the experiment. In hierarchical analysis the AE motoneuron was excluded.

A hierarchical analysis was applied with the correlations of motoneurons identified by the spike sorting (fig. R. 7C and D). The dendrograms excluded the cells AE, nevertheless, inhibitory motoneurons 101 (3 cells) were used to confront the activities from pure contractors and elongators with their corresponding inhibitors. As results, motoneurons 3 were grouped and correlated in the same way during both behaviours and can be seen situated in the left arm of the dendrograms although there was a striking difference in their level of correlation (fig. R. 7C & D). The activity of the inhibitory motoneurons 119 interestingly changed their positions in the dendrogram from the right extreme during swimming (demonstrating total anti-correlation with

cell 3) to the left position in the pseudo-swimming behaviour (fig R.7D). The cells CV and L shown correlated activity and were grouped almost all together as result of the analysis; nevertheless, each type was located centrally and in opposite branches of the dendrograms (central part fig R.7C & D). Motoneurons 102, were grouped during swimming, nevertheless in pseudo-swimming were dispersed over the dendrogram. For the case of motoneurons 109, they resulted dispersed in the right arm of the dendrogram (fig R.7D).

DISCUSSION

Neuroscience assumes that most animals and possibly all interact with the environment following common rules and similar principles: they receive stimuli from the exterior transforming physical-chemical external changes into internal electrical/nervous signals using their sensory organs, then they process this information changing their internal states and even store part of this information. The final outcome of this process is the action, resulting from their *motor system* culminating in a behaviour selected from a range of possible repertoires.

The aim of the author's Ph. D thesis was focused on understanding some aspects of the *motor control* of the leech, emphasizing its internal states in relation to elicited external activities denoted here as basic and complex spontaneous behaviours. In this thesis signals obtained from experimental registrations were interpreted with a Computational Neuroscience approach; in other words, the information was transformed into simple variables, analyzed and interpreted thanks to computational algorithms.

Semi intact preparation and technical considerations

The methodology employed to monitor behaviour and nervous system activity was the leech *semi-intact* preparation (Kristan, 1974A). Its importance lies in the access to the nervous system parallel to the measure of the animal's motion as well as in the use of leeches as resistant organisms able to survive for hours since their dissection. It is relevant to mention that mounting the preparation required mental concentration, careful manual precision and undoubtedly patience, and, this technical aim can be reached with the practice of many experiments performed and, at the same time, appropriate use of dissection's instrumental.

The semi-intact leeches demonstrated strong resistance against the damage provoked to the skin and tissue removal. Two different techniques were applied on the cleaning of the roots; the one applied in the first half of the project, informally named "pin technique", provoked difficulties which affected the time needed to obtain a complete preparation, and as a reflex, the health of the animal and of the nerve tissue. Nevertheless, this technique can be applied to small preparations, like the local bending or the single ganglia in which it is not required the health condition of a complete animal. The second technique, or "scissors technique", improved with high efficiency the time needed to obtain the complete preparation (8 roots cleaned), the healthy conditions of the roots and obviously of the animals to record. This was learned after personal

training sessions with Dr. William Kristan Jr. (University of California San Diego, USA), whom the author acknowledges. It is important to mention this point because the healthier are the roots, the better is the recording of their signals and the longer is the duration of the experiments; so, recordings could last even up to 10 hours or overnight.

Another technical consideration concerns the quality and the use of the electrodes during the experimental sessions. In particular, the tip's diameter was crucial to sucks the roots into electrodes with the risk to provoke damage to the fibre if the electrode was sharpened. So, a correct polishing of the tip tackled the problem. Defects in the tip polishing or diameter provoked poor glass-nerve contact, resulting in scarce signals or momentarily lost. This could happen because of root's retraction outside the electrode with the consecutive blocking of the tip with debris or mucus from preparation. So, the technical improvement of preparations lied also in learning the use and the fabrication of the suction pipettes.

Attaching beads to the skin of the animal concluded the same objective of previous works (Mazzoni *et al.*, 2005; García-Perez *et al.*, 2005), which consisted in transform the behaviour in variables to analyze. Semi-intact animals elicited different stereotyped behaviours, whose recognition was possible through off-line visual inspection of videos and acquisition and processing of variables. The behaviours were the following: stationary states, shortening (contraction)-elongation of local or whole body, exploring head and tail, crawling, pseudo-swimming (ventilation) and swimming. Not all the stereotyped behaviours were elicited in one experiment, so the selection of the experiments also depended on the behaviour to analyze.

Leeches are accustomed to stay in dark zones (Sawyer, 1986). During recordings the head commonly was searching for shadows projected by electrode holders situated over the preparations, occulting the beads to the camera. To avoid this, the holders were modified in material and conformation: transparent acrylic pieces were mounted on holders with micromanipulators grouped in a "spider-like-arm" built in lab. The electrodes acquired independent mobility and it was possible to change their position, searching the appropriate angle.

Intact versus semi-intact leeches

When leeches were gently dissected, they could move their head and tail and could exhibit stereotyped behaviours. Nevertheless in some preparations it was noticed that animals exhibited low motion behaviours, which made suppose that the preparation was an ineffective technique to reach these thesis' objectives. The differences in the speed of free animals video-recorded and

semi-intact preparations rose more doubts (fig M.1B). One way to test if the preparation was ineffective consisted in comparing the states of the sucker transition states in free, intact-pinned and semi-intact animals (fig R.3). Logically, the differences between free and restricted animals were marked; so then, the analysis was centred on the comparison of pinned and semi-intact. Those which were pinned down to the experimental dish elicited some of the stereotyped behaviours as well as the semi-intact. Indeed, they could rhythmically shorten and elongate their whole body with almost the same frequency observed during the crawling shown in fig R.5. Similarly, semi-intact leeches and pinned-intact could move their head and tail in the same manner as during swimming and pseudo-swimming (fig R.7). Interestingly, in several observations, both kind of preparations exhibited peristalsis behaviour (fig R.3E), which could change its definition from a variant of the stationary states (Mazzoni *et al.*, 2005; García-Perez *et al.*, 2005) into a escape behaviour in such a way that animals try to release itself. The statistics of sucker attachment and detachment of intact/pinned and semi-intact/pinned leeches was rather similar (fig R.3), suggesting that the gentle surgery necessary to obtain a semi-intact leech does not alter dramatically the leech behaviour and patterns of the underlying electrical activity.

About the signals obtained from semi-intact preparations

Two different types of signals were obtained during recording sessions: the behavioural signal from the beads glued to the body and the electrical recordings from the CNS (fig R.1A). Both types of signals were processed off-line to achieve the relation between them. Three *behavioural signals* were processed to obtain new automated variables: *ESV* or *Elongation-Shortening Vector*, *Right-Left* position, represented by the angle position *theta* θ of head and tail (fig M.3), and the *Sucker Attach-Detach* (fig M1.B). In the case of the *electrical signals*, extracellular recordings were visualized using two kinds of *descriptors*: the *Average Firing Rate* (*AFR*) over time (fig. M.1C & R.1A) and the *auto-* and/or *cross-covariance* (ρ) over windows of time calculated from the *AFR* (fig R.1A). Different bin widths were applied to inspect the *AFR* descriptor from roots or connectives, especially in the case of identified neurons, which demanded small bin widths to identify patterns along the experiments. The selection of any specific bin width was chosen according to the expected values of ρ along the traces, this information was previous analyzed in similar extracellular recordings (Mazzoni *et al.*, 2007). The *cross-covariance* (ρ) descriptor resulted in three possible cases over the time: correlation, anti-correlation and non-correlation.

The electrical recordings have been presented in numerous works showing the spikes' activity of roots, i.e. DP, during shortening periods of crawling (e.g. Baader & Kristan 1995; Baader & Bächtold, 1997; Baader, 1997) or intrinsically during swimming (e.g. Ort *et al*, 1974; Briggman & Kristan, 2006). So, a technical innovation of this thesis was the compact presentation of large quantity of data obtained from spontaneous experiments with long-time duration, visualizing up to four variables of behaviour and the most possible *AFR* (8) from roots, identifying some motoneurons.

The DP and MA roots were mainly compared in experiments of double ganglia as they performed markedly correlations and anti-correlations during cyclic contraction-elongation periods (fig R.1A and M.3). This correlations and anti-correlations were produced by the bursting activity of excitors and inhibitors from the mentioned roots. Identifying neurons belonging to any of the mentioned roots was not an easy task, but the algorithms employed allowed an arbitrary but solid identification of motoneurons, reinforced with information from literature. The codes and computational kernel were a mix of MATLAB scripts usually found open in internet from scientific sources. The organization and rewriting of the algorithms permitted to create a powerful tool for the recognition of cell activity along the spontaneous experiments. It is necessary to emphasize the importance of the programming and the organization of the information as a task that can be performed by people with knowledge in the exact sciences, in this case, Dr. Giacomo Bisson performed must of the tasks in relation with computing and analysis, and whom the author of this thesis acknowledges. Parts of the kernel for the spike's sorting algorithm was used in studies of the local bending of the leech (Pinato, 2000; Arisi *et al.*, 2001; Zoccolan *et al.*, 2002).

Electrical patterns underlying behaviours: stationary states

Semi-intact leeches spend a considerable time in *stationary states*, during which they do not move and the head and tail velocity is negligible (Mazzoni *et al.*, 2005). It is important to clear that the concept of *stationary states* is not related to the homonymic concept in quantum mechanics, but, as defined in previous works, it is related to the motionless of the acquired beads (Mazzoni *et al.*, 2005). So, beyond the simple external observation on leeches, following the idea to know patterns of electrical activity, this project pointed to the knowledge of the existence of any electrical pattern associated to this stereotyped behaviour. Indeed, as was previously shown, during stationary states, the overall electrical activity decreases and both the average firing rate $\langle AFR_i \rangle$ and the average cross-correlation $\langle \rho_{ij} \rangle$ have small values. However, as shown in fig

R.1C, a small value of $< \rho_{ij} >$ is a better classifier than a small value of $<AFR_i>$ of stationary states; instead, when the leech is not in a stationary state a change of $<AFR_i>$ is a better reporter than a change of $< \rho_{ij} >$ concerning variations of tail or head velocities (fig R.1). So as brief summary, these observations concluded two goals in the distinction of electrical patterns produced by the neurons' populations in mid-body ganglia: it is possible to identify and discriminate between motionless and motion from the internal states of the animal; and, that the cross-covariance is a better classifier of the stationary states. However, these conclutions can trigger questionable considerations about the explanation of the nature or role of the stationary states in the animal.

Stationary states: sleep and/or attention?

The first possible explanation of the presence of stationary states could be related to circadian rhythms in the animal. Sleep appears as a periodical state of quiescence, in which there is minimal processing of incoming sensory information; in other words, it is a suspension of the activities of a so called waking state. This information have been demonstrated in vertebrates and considering that, when an animal falls asleep, slow coherent oscillations emerge in the cerebral cortex in different frequency bands (delta waves 1–4 Hz and spindles 7–14 Hz) (Steriade, 1993) characterizing a first sleep state called slow-wave sleep. These oscillations are organized into complex wave sequences by a very slow oscillation, which usually ranges 0.6–1 Hz, and are concomitant with a progressive sensory disconnection (Oishi *et al.*, 2007; Contreras & Steriade, 1995; Steriade *et al.*, 1990). Nevertheless, in leeches there is no reported evidence of electrical patterns during their sleeping cycle. Though the induction of stationary states could be possibly mediated by serotonin which presumably could induce states of calm, as in parallel, it has been described in vertebrates about the low firing spikes activity during Quiet Waking behaviours (Rector *et al.*, 2009), which could be equivalent to leeches' stationary states. Possibly any of the neurons from the leech system could be related to the induction of stationary states, and those serotonin containing ones could be the targets; examples of this are the 21/61 set from the swimming mechanism behaviour (Kristan, 2005) or the giant Retzius cells in the dorsal side of the ganglion (Nicholls & Purves, 1972; Cooper *et al*, 1992).

Another and more reasonable explanation for the presence of stationary states can be found in their association to lapses of attention in the animals. This idea comes from works that reported the changes of the degree of correlated electrical activity which were associated to attention (Pesaran, 2010; Cohen & Maunsell, 2009). It is also known that a decrease of

correlations among firing of neurons in visual area V4 underlies attentional improvement (Cohen & Maunsell, 2009). These attention-dependent changes in neural correlations depend on the specific visual area under examination and on the specific frequency range: attention increases the power of local field potential (LFP) in the gamma frequency range (30–50 Hz) in V4 but not in V1 (Chalk *et al.*, 2010).Therefore, changes of the degree of correlated electrical activity during attention are not uniform in all visual areas.

Motion states and positive correlations: links to memory?

Contrary to the fact that during the stationary states there's low correlation that could be associated to attention, a higher correlated electrical activity seems to be essential for memory formation and consolidation (Jutras & Buffalo, 2010). The fact that modulations in the gamma-frequency and theta-frequency (4–8 Hz) ranges are proposed to underlie in particular spike timing-dependent plasticity, conducts to the idea that the neuronal synchronization in a network linked by the cellular process underlie learning and memory (Jutras & Buffalo, 2010). Having these considerations, in some of the recordings of the motor control in the leech, were observed episodes in which the correlation between the ganglia's members ranked high levels, either roots or neurons (fig R.1 & R.2B). One could discard this idea due to the fact that in this thesis was analyzed the activity of a motoneurons' network, nevertheless it must be considered that all these outputs observed in recordings are sensed by the hierarchical interneuronal network level, and considering that both networks are interconnected in between (as e.g. the visual areas V1 and V4) cortical zones), then it is logic to think that the correlations provoked in certain episodes of the spontaneous behaviours can act in plasticity phenomena form the global network point of view. In fact, it has been reported that in the ganglion's network interneurons and motoneurons acts together in such an associative way to effect to elicit crawling or swimming, and this have been sensed by changes in the signals of voltage sensitive dyes (Briggman & Kristan 2005; Briggman & Kristan, 2006; Briggman & Kristan, 2008); these works have been focused in the idea of the decision process to pass from one central pattern generator to the other supported by the role of some interneurons (as 208 and 204); so this contributions can support the idea that the interaction between the hierarchical networks can produce effects that could induce plasticity and therefore processes of memory.

Sucker attachment and detachment

Suckers' attachment and detachment have been analyzed in the generation of the crawling behaviour (Baader & Kristan, 1995; Baader, 1997; Baader & Bächtold, 1997). For normal and in free animals, the attachment and the release of the rear sucker are important components of the crawling cycle. A failure of the rear sucker to release would prevent the animal from pulling forward. Likewise, the animal normally releases its front sucker to begin a new step after it has firmly attached its rear sucker (Baader & Bächtold, 1997). These events, essentials of the crawling, must be synchronized with motoneurons' activity during contraction and elongation phases (figs R.5 & R.6). In this way, considering the importance of suckers in the leech motion, the searching of an electrical pattern could be related in its correct timing and synchronization with motoneuron activity; this could be achieved by command neurons sending an appropriate neural signal along the connective fibres linking the head and tail sucker.

Some possible neural candidates that trigger the crawling steps are located in the head and the tail brains (Baader, 1997; Baader & Bächtold, 1997; Esch *et al.*, 2002; Mesce & Pierce-Shimomura, 2010). Those for the tail brain (at least 6 identified) have been related to the sucker release command and send their spikes into connective fibres during the initial contraction of the crawling (Baader & Bächtold, 1997). In the other extreme, in the head brain, the R3B1 neuron is a command-like neuron that modulates its spikes' frequency during the crawling when is triggered by a sensorial stimulus (Esch *et al.*, 2002). A third important interconnected system related to crawling generation is the fast conducting system (FCS) (Moss *et al.*, 2005; Magni & Pellegrino, 1978; Shaw & Kristan, 1999), which is considered a essential and fast pathway that communicates the head and the tail. Together, the spikes of all these neurons can be detected along the connectives (fig R4 E & F); and, more important for this thesis, all together contribute to the bursting activity before or after any events of the sucker's in the attach (fig R4 A & B) or detach (fig R4 C & D).

Curiously before a detach, it was found in the connectives a small burst of activity travelling from tail to head in a range of 8 seconds (fig R4 F & G); so it is proposed that between the spikes of this burst, are present the input commands necessary for the detach. A probable mechanism proposed by the author is that: a) a combination of sensorial spikes like P cells are sent to the connectives via FCS (Pinato *et al.*, 2000; Arisi *et al.*, 2001; Zoccolan *et al.*, 2002) stimulating to R3B1 in the head (Esch *et al.*, 2002); b) the head sends back a response to the tail via FCS that activate at least the interneurons IN902, IN904 and IN401 and motoneurons N31-33 and N41 from the tail brain (Baader & Bächtold, 1997). c) The information is processed and

"computed" in both brains to finally trigger a response either one or both. Here one must consider that signals can cross from the head to the tail in around 125 ms (Baader & Bächtold, 1997), then, one possible solution to the mechanism is that the travelling information, as trains of spikes, together to other types of FCS (embedded in the connective noise) enter in the cord in a state of "toing and froing", travelling via head tail or vice versa in more than one occasion; d) this electrical information activates a decision network (Briggman & Kristan, 2005; Briggman & Kristan, 2006; Briggman & Kristan, 2008) that permit the interaction interneuron-motoneuron during interchange of information between the brains, taking a decision; e) after decision, the system computes first of all a sucker's release (preferring the head sucker) depending on the strength of the initial stimulus, finally an escape behaviour (crawling or swimming) is elicited.

Dendrograms

The leech motor system consists of 19 pairs of excitatory motoneurons that innervate longitudinal, oblique, and circular fibres (Stuart, 1970; Ort *et al.*, 1974; Mason & Kristan, 1982; Norris & Calabrese, 1987). These motoneurons have been extensively investigated using force and length transducers and electrophysiology tools (Stuart, 1970; Mason & Kristan, 1982; Kristan, 1982; Norris & Calabrese, 1987); however, there is still lack of a complete description of their activation patterns during the performance of stereotyped behaviours such as swimming and crawling. To address this issue, a hierarchical classification was used according to the firing rates of spike sorted activities recorded from 8 roots. This classification can be described as the activity of a set of objects divided into a smaller number of classes in such a way that objects in the same class are similar to one another and dissimilar to objects in other classes. The classes are not known *a priori,* but have to be discovered; in this case, the objective was to investigate how single cell activities are related to one another and if a particular hierarchy may encode a stereotyped behaviour, such as swimming or crawling. This leads to an interest in hierarchically-nested sets of partitions, commonly represented in rooted tree diagrams. Hierarchical clustering permits to investigate how classes of similar objects are related to one another. If it is possible to measure the similarity between clusters, then the dendrogram is usually drawn to scale, to show the similarity between the clusters that are grouped. An example in which a hierarchical classification is relevant occurs in taxonomy, in which an object belongs successively to a species, a genus, a family, and an order; the most natural representation of hierarchical clustering is a corresponding tree, called a dendrogram, which shows how the samples are grouped. A dendrogram is constructed from a dissimilarity matrix $[d_{ij}]$, which contains the n x n (where n is

the number of objects to be classified) pairwise dissimilarities between the *i*th and jth objects, by means of various strategies, such as agglomerative, divisive, constructive, and direct optimization. The project focused on agglomerative algorithms because they are computationally less demanding than the others. Agglomerative algorithms start with n singleton classes and at each stage, the most similar pair of classes is amalgamated. Agglomerative algorithms can be divided in single linkage (shortest distance), complete linkage (furthest distance), incremental sum of squares (Ward, 1963) and many others methods. Some of these methods (e.g. Ward's linkage) require that the objects are represented by points in some Euclidean space, and that the measure of pairwise dissimilarity is proportional to squared Euclidean distance. The metric employed (uncentred correlation) is not Euclidean, however, it is not rare to find studies that make use of Ward's linkage regardless this fact. A single linkage has been indicated as a connectivity method that tends to yield rather elongated clusters of objects, and complete linkage is a method that favours compact clusters having a minimum diameter (Johnson, 1967). The single linkage method has been used in biological sciences, where clustering specimens that are minimally different is felt to correspond to the pattern of evolutionary change (Sneath, 1969). The complete linkage method is used extensively in the social sciences where the interest is more in forming compact clusters that are as internally homogeneous as possible (Baker, 1974). Baker demonstrated that single linkage grouping method, as it relies on the shortest distance between objects, is more sensitive to noise than the complete linkage method (furthest distance). Ward's distance returned dendrograms that were very similar to those obtained with complete linkage; however, Ward's linkage may be used only on Euclidean dissimilarity matrices: this led us to choose the complete linkage method as the best candidate for our hierarchical clustering.

Once a reference dendrogram was estimated for every single behaviour under consideration, the reliability of such estimates was tested by comparing a time-dependent dendrogram, estimated over a sliding time window (see methods) with a reference dendrogram (e.g. the crawling reference dendrogram). A time-dependent dendrogram was expected to bee reasonably similar to the reference one in those time intervals during which the reference behaviour was performed. This would prove the specificity of a reference dendrogram to the considered behaviour, and not to others. A method for comparing two hierarchical clusterings is described by Fowlkes & Mallows, (1983), and is based on the derivation and use of a measure of similarity, *Bk,* derived from the matching matrix $[m_{ij}]$, formed by cutting the two hierarchical trees and counting the number of matching entries in the resulting k clusters in each tree. Wagner & Wagner (2007) give a survey of the most important similarity measures that can be employed in comparing two clusterings, and all can be adapted to the framework of hierarchical clustering,

providing that a cutting on both the trees is done. After testing the majority of these similarity measures between dendrograms, the Fowlkes-Mallows Index and the Mutual Information Index were chosen as the best candidates to assess the similarity between two dendrograms. More than 80% of the total swimming episodes were identified correctly by comparing the time-dependent dendrogram with the swimming reference dendrogram. Moreover, the comparison reported only ~5% of false positives. Regarding crawling, a better true positive rate was obtained (reaching 90% of correctly classified events) and again ~5% of false positives. The low rate of false positives produced by the comparison of the two dendrograms is a clear index of the high specificity of each reference dendrogram, and, thus, of its high reliability.

Since the dendrogram based on the correlation metric is a compressed representation of the correlation matrix (which contains the correlations between all the possible pairs of spike sorted firing rates), the performance of a behaviour classifier was compared based on the correlation matrix coefficients $<\rho_{ij}>$ and other based on the raw spike sorted firing rates.

A classifier is a mapping of instances into a certain class. The classifier result can be in a real value (continuous output) in which the classifier boundary between classes must be determined by a threshold value, for instance to determine whether a person has hypertension based on blood pressure measure, otherwise it can be in a discrete class label indicating one of the classes. If the classifier results in just two classes, it is called a binary classifier. In this thesis, binary classifiers were only considered: the first classifies stationarity states by thresholding the average covariance signal, leading to two classes, i.e. stationarity (value 1) and non-stationarity or movement (value 0). Other classifiers implemented in this thesis apply a threshold on the similarity measure between a dendrogram, estimated in a sliding time-window, and a pool of reference dendrograms, each one describing a particular behaviour (crawling or swimming). In this way, the classifier resulted in two classes: detected behaviour (being crawling or swimming), having value 1, or not detected behaviour, having value 0. Another way of decoding the behavioural state of the leech, starting from the spike sorted activities, would be to run a discriminant analysis on some time-varying features that are believed to vary accordingly to the particular behavioural state of the animal. As a set of features either the $n\,(n-1)/2$ coefficients of the covariance matrix estimated from the spike sorted activities in a sliding time-window or the raw activities alone were chosen: the n (n-1)/2 coefficients of the covariance matrix estimated from the spike sorted activities in a sliding time-window, or the raw activities alone. Discriminant analysis uses training data to estimate the parameters of discriminant functions of the predictor variables. Discriminant functions determine boundaries in predictor space between

various classes. The resulting classifier discriminates among the classes (the categorical levels of the response) based on the predictor data.

To test the performance of different classifiers (see methods) based on the correlation matrix coefficients or on the raw firing rates and the dendrogram-matching classifier, a receiver operating characteristics (*ROC*) analysis was used. A *ROC* graph allows visualizing, organizing and selecting classifiers based on their performance. *ROC* graphs have long been used in signal detection theory to depict the trade-off between hit rates and false alarm rates of classifiers (Egan, 1975). Considering this analysis, it was concluded that the performance of the dendrogram-matching classifiers was between those obtained for the classifiers, based on the correlation matrix coefficients (performing better), and those obtained for the classifiers, based on the raw firing rates (performing worse).

The most striking consequence of using correlation-based dendrograms is that the motoneurons result grouped accordingly to the known literature on the stereotyped behaviours: the dendrograms follows finely the correlation structure of the internal, interneuron-based network which switches its dynamical state according to the performed behaviour, with consequent changes on its output layer, constituted by motoneurons.

CONCLUSIONS

This thesis describes the research performed to elucidate some aspects of the motor control in the leech *Hirudo medicinalis*. The ***semi-intact*** preparation has been chosen as a methodological strategy to analyze internal and external states of the biological subject. The analysis, identification and characterization of electrical patterns underlying different behaviours in *Hirudo medicinalis* are the main results reached within this PhD thesis. The information obtained from experiments has been processed with automated methodologies, which allowed storing compact easily accessible data. Afterwards, neural and behavioural information have been identified and characterized obtaining as descriptors, the Average Firing Rate (***AFR***), the auto and cross-covariance (ρ) and the behaviours transformed into variables of elongation-contraction (***ESV***) and position (angle θ) on the preparation. Finally, it has been possible to relate the information between the automated, identified and characterized signals**.** Considering the starting hypothesis and all the gained results, it is possible to conclude that *when the neural population in charge of the motor control in mid body ganglia produces uncorrelated activity between its members, the semi-intact leech enters in a stationary state, while, when the same population originates bursting changes which provoke correlations and/or anti-correlations between its members, the animal enters in a motion state*.

These are the major conclusions of the thesis:

a) Simple behaviours from the suckers (attach/detach) situated in the head and tail of the animal have been associated to electrical patterns recorded from the connective fibres, taking a further step in the detection of specific spikes (command-like systems) immersed in the connective electrical information which travels along the neural cord;

b) The activity of the ganglion's neural population and some neurons, identified using computational strategies, have been associated to stereotyped behaviours of the head (and/or tail), such as shortening (contraction), elongation and pseudo-swimming (ventilation);

c) Dendrograms, calculated from the correlations between the neuron's population sorted by an algorithm, are a new descriptor of the patterns of electrical activity underlying motoneuron activity of different simple and complex stereotyped behaviours.

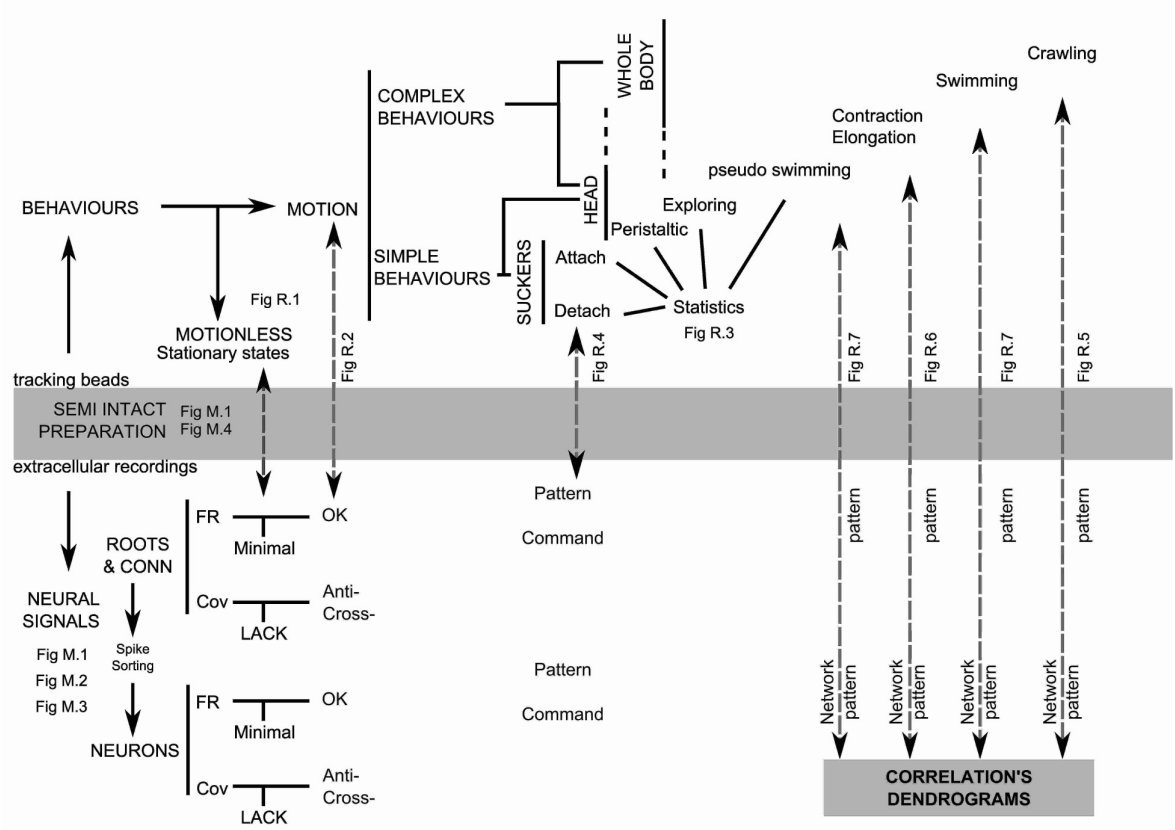

Figure C.*1 Overall view*. Summary of the strategy covered to study motor control in the leech within this Ph. D thesis.

REFRENCES

Adrian E.D., Buytendijk F.J. (1931). Potential changes in the isolated brain stem of the goldfish. J Physiol. 25;71(2):121-35

Arisi I., Zoccolan D., Torre V. (2001) Distributed motor pattern underlying whole-body shortening in the medicinal leech. J Neurophysiol 86:2475-2488.

Baader A.P. & Kristan W.B. Jr (1992). Monitoring neuronal activity during discrete behaviours: a crawling, swimming and shortening device for tethered leeches. J Neurosci Methods 43, 215-223.

Baader A.P. & Kristan W.B. Jr (1995). Parallel pathways coordinate crawling in the medicinal leech Hirudo Medicinalis. J Com Physiol [A] 176, 715-726.

Baader A.P. (1997). Interneuronal and motor patterns during crawling behavior of semi-intact leeches. J Exp Biol 200(9), 1369-1381.

Baader A.P. & Bächtold D. (1997). Temporal correlation between neuronal tail ganglion activity and locomotion in the leech, Hirudo Medicinalis. Invert Neurosci 2, 245-251.

Bagnoli P, Brunelli M, Magni F, Pellegrino M. (1975). The neuron of the fast conducting system in hirudo medicinalis: identification and synaptic connections with primary afferent neurons. Arch Ital Biol. 113(1):21-43.

Bagnoli P, Francesconi W, Magni F. (1979). Interaction of optic tract and visual wulst impulses on single units of the pigeon's optic tectum. Brain Behav Evol. 1979;16(1):19-37.

Baker F.B. (1974) Stability of two hierarchical grouping techniques case 1: sensitivity to data errors. Journal of the American Statistical Association 69:440–445

Baker, B. (1938) In: Magnus Enquist & Stefano Ghirlanda: Neural Networks and Animal Behavior. Monographs in Behavior and Ecology. Princeton University Press. Chapter 1: Understanding animal behaviour. pp: 2-18.

Blackshaw S.E. (1981a). Sensory cells and motorneurons. from: Muller K.J., Nicholls J.G. & Stent G.S. *Neurobiology of the leech*. Cold Spring Harbour Laboratory, 51-78.

Blackshaw S.E. (1981b). Morphology and distribution of touch cell terminals in the skin of the leech. J Physiol 320, 219-228.

Blackshaw S.E., Nicholls J.G. & Parnas I. (1982). Physiological responses, receptive fields and terminal arborizations of nociceptive cells in the leech. J Physiol (Lond) 326:251-60.

Blackshaw S.E. (1993). Stretch receptors and body wall muscles in leeches. Comp Biochem Physiol 105A(4), 643-652.

Blackshaw S.E. & Nicholls J.G (1995). Neurobiology and development of the leech. J Neurobiol 27(3), 267-276.

Boulis NM, Sahley CL (1988) A behavioral analysis of habituation and sensitization of shortening in the semi-intact leech. J Neurosci 8: 4621-4627.

Briggman KL, Abarbanel HDL, Kristan WB (2005) Optical imaging of neuronal populations during decision making Science 307:896-901

Briggman KL, Abarbanel HDL, Kristan WB (2006) Imaging dedicated and multifunctional neural circuits generating distinct behaviors J. Neurosci. 26:10925-10933

Briggman KL, Kristan WB.(2008) Multifunctional pattern-generating circuits. Annu Rev Neurosci.;31:271-94. Review.

Brodfuehrer P.D. & Cohen A.H. 1990. Initiation of swimming activity in the medicinal leech by glutamate, quisqualate and kainate. J Exp Biol. Nov;154:567-72.

Brodfuehrer P.D. & Cohen A.H. 1992. Glutamate-like immunoreactivity in the leech central nervous system. Histochemistry. 97(6):511-6.

Brodfuehrer PD, Thorogood MS (2001) Identified neurons and leech swimming behavior. Prog Neurobiol 63: 371-381.

Brodfuehrer P.D. & Friesen W.O. (1986). Initiation of swimming activity by trigger neurons in the leech ganglion, I. Output connections of Tr1 and Tr2. J Comp Physiol. 159, 489-502

Brodfuehrer P.D., Debski A., O'Gara B. & Friesen W.O. (1995a) Neuronal control of leech swimming. J Neurobiol 27(3), 403-418.

Brodfuehrer P.D., Parker H.J., Burns A. & Melissa B. (1995b). Regulation of the segmental swim-generationg system by a pair of identified interneurons in the leech head ganglion. J Neurophysiol 73(3), 983-992.

Brodfuehrer PD, Kogelnik AM, Friesen WO, Cohen AH. 1993. Effect of the tail ganglion on swimming activity in the leech. Behav Neural Biol. 59(2):162-6.

Buonomano DV, Maass W.(2009). State-dependent computations: spatiotemporal processing in cortical networks. Nat Rev Neurosci. 10(2):113-25. Review.

Caccaciatore T.W., Brodfuehrer P.D., Gonzalez J.E., Jiang T., Adams S.R., Tsien R.Y., Kristan W.B. Jr & Kleinfeld D. (1999). Identification of neural circuits by imaging coherent electrical activity with FRET-based dyes. Neuron 23, 449-459.

Cacciatore T.W., Rosenshteyn R. & Kristan W.B. Jr (2000). Kinematics and modelling of leech crawling: evidence for an oscillatory behaviour produced by propagating waves of excitation. J Neurosci 20(4), 1643-1655.

Calabrese R.L. (1977). The neural control of alternate heartbeat coordination states in the leech, Hirudo medicinalis. J Comp Physiol 122, 111-143.

Calabrese R.L., Nadim F. & Olsen O.H. (1995). Heartbeat control in the medicinal leech: a model system for understanding the origin, coordination and modulation of rhythmic motor patterns. J Neurobiol, 27(3), 390-402.

Canepari M, Campani M., Spadavecchia L. & Torre V. (1996). CCD imaging of the electrical activity in the leech nervous system. Eur Biophys J 24, 359-370.

Carlton V. & McVean A. (1995). The role of touch, pressure and nociceprive mechanoreceptors of the leech in unrestrained behaviour. J Comp Physiol [A] 177, 781-791

Cellucci C.J., Brodfuehrer P.D., Acera-Pozzi R., Dobrovolny H., Engler E., Los J., Thompson R., Albano A.M. (2000). Linear and nonlinear measures predict swimming in the leech. Phys Rev E Stat Phys Plasmas Fluids Relat Inter. Top. 62(4 Pt A):4826-34.

Chalk M, Herrero JL, Gieselmann MA, Delicato LS, Gotthardt S, Thiele A. (2010). Attention reduces stimulus-driven gamma frequency oscillations and spike field coherence in V1. Neuron. 66(1):114-25.

Cohen & Boothe, 2003. Sensorymotor interaction and central pattern generators. In: Magnus Enquist & Stefano Ghirlanda: Neural Networks and Animal Behavior. Monographs in Behavior and Ecology. Princeton University Press. Chapter 1: Understanding animal behaviour. pp: 2-18.

Cohen M.R., Maunsell J.H.(2009) Attention improves performance primarily by reducing interneuronal correlations. Nat Neurosci. 12(12):1594-600.

Contreras D, Steriade M. (1995). Cellular basis of EEG slow rhythms: a study of dynamic corticothalamic relationships. J Neurosci. 15(1 Pt 2): 604-22.

Crisp K.M. & Mesce K.A. (2004). A cephalic projection neuron involved in locomotion is dye coupled to the dopaminergic neural network in the medicinal leech. J Exp Biol. 207(Pt 26): 4535-42.

Crisp K.M. & Mesce K.A. (2003). To swim or not to swim: regional effects of serotonin, octopamine and amine mixtures in the medicinal leech. J Comp Physiol A Neuroethol Sens Neural Behav Physiol. 189(6):461-70.

Crisp K.M., Klukas K.A., Gilchrist L.S., Nartey A.J., Mesce K.A. (2002). Distribution and development of dopamine- and octopamine-synthesizing neurons in the medicinal leech. J Comp Neurol. 442(2):115-29.

Deitmer J.W. & Kristan W.B. Jr (1999). Glial responses during evoked behaviors in the leech. 26(2) 186-189.

Derganc M Zdravic F. (1960) Venous congestion of flaps treated by application of leeches. Br J Plast Surg. 13:187-92.

Egan JP (1975) Signal detection theory and *ROC* analysis. Academic Press New York.

Eisenhart FJ, Cacciatore TW, Kristan WB, Jr. (2000) A central pattern generator underlies crawling in the medicinal leech. J Comp Physiol [A] 186: 631-643

Enquist M. & Ghirlanda S. (2005). Neural Networks and Animal Behaviour. (Monographs in Behavior and Ecology). Princeton University Press. Chapter 1: Understanding animal behaviour. pp: 2-18.

Esch T., Mesce K.A., Kristan W.B. (2002). Evidence for sequential decision making in the medicinal leech. J Neurosci. 22(24):11045-54.

Fawcett T., (2006). An introduction to ROC analysis. Pattern recognition letters 7:861–874.

Fernández-de-Miguel F, Drapeau P. (1995).Synapse formation and function: insights from identified leech neurons in culture. J Neurobiol. 27(3):367-79.

Cooper R.L., Fernández-de-Miguel F., Adams W.B., Nicholls J.G. (1992). Anterograde and retrograde effects of synapse formation on calcium currents and neurite outgrowth in cultured leech neurons. Proc Biol Sci. 249(1325): 217-22.

Fielding, A.H. (2007). Cluster and Classification Techniques for the Biosciences. Cambridge University Press. Chapter 6: Cluster analysis. p. 46-77.

Foucher G, Braun FM, Merle M, Michon J. (1981). Transplantation of the second toe in the reconstruction of fingers. Rev Chir Orthop Reparatrice Appar Mot. 67(3):235-40.

Fowlkes E.B. & Mallows C.L. (1983). A method for comparing two hierarchical clusterings. Journal of the American Statistical Association. 78: 553–569

Fred A.L., Jain A.K. (2005). Combining multiple clusterings using evidence accumulation. IEEE Trans Pattern Anal Mach Intell. 27(6):835-50.

Frank E., Jansen J.K., Rinvik E. (1975). A multisomatic axon in the central nervous system of the leech. J Comp Neurol. 159(1):1-13.

Friesen W.O., Poon M., Stent G.S. (1978). Neuronal control of swimming in the medicinal leech. IV: Identification of a network of oscillatory interneurones.J Exp Biol.75:25-43.

Friesen W.O. (1981). Physiology of water motion detection in the medicinal leech. J Exp Biol 92, 255-275.

Friesen WO, Hocker CG. (2001). Functional analyses of the leech swim oscillator. J. Neurophysiol. 86(2):824-35.

Futuyama, (1998). In : Enquist M. & Ghirlanda S. Neural Networks and Animal Behaviour. (Monographs in Behavior and Ecology). 2005. Princeton University Press. Chapter 1: Understanding animal behaviour. pp: 2-18.

Gabbiani F. & Cox S.J. (2010). Mathematics for Neuroscientists. Academic Press. Chapters 15, 20, 24 and 27.

Garcia-Perez E., Zoccolan D., Pinato G., Torre V. (2004). Dynamics and reproducibility of a moderately complex sensory-motor response in the medicinal leech J Neurophysiol 92:1783-1795

Garcia-Perez E., Mazzoni A., Zoccolan D., Robinson H.P.C., Torre V. (2005) Statistics of decision making in the leech. J Neurosci 25:2597-2608.

Gardner C.R., Walker R.J. (1982). The roles of putative neurotransmitters and neuromodulators in annelids and related invertebrates. Prog Neurobiol 18: 81-120.

Gascoigne L. & McVean A. (1991). Neuromodulatory effects of acetylcholine and serotonin on the sensitivity of leech mechanoreceptors. Comp Biochem Physiol 99C(3), 369-374.

Gaudry Q, Kristan WB Jr. (2010a).Feeding-mediated distention inhibits swimming in the medicinal leech. J Neurosci. 30(29):9753-61.

Gaudry Q, Ruiz N, Huang T, Kristan WB 3rd, Kristan WB Jr. (2010b). Behavioral choice across leech species: chacun à son goût. J Exp Biol. 213(Pt 8):1356-65.

Gaudry Q, Kristan WB Jr. (2009). Behavioral choice by presynaptic inhibition of tactile sensory terminals. Nat Neurosci. 12(11):1450-7.

Gilchrist LS, Klukas KA, Jellies J, Rapus J, Eckert M, Mesce K.A. (1995). Distribution and developmental expression of octopamine-immunoreactive neurons in the central nervous system of the leech. J Comp Neurol. 353(3):451-63.

Goodwin L.D. & Leech N.L. (2006). Understanding Correlations: Factors That Affect the Size of ρ. The Journal of Experimental Education, 74(3), 251–266.

Grant G. (2010). Gustaf Retzius (1842-1919). J Neurol. 2010 Nov 5.

Granzow B., Friesen W.O. & Kristan W.B. Jr (1985). Physiological and morphological analysis of synaptic transmission between leech motor neurons. J Neurosci 8(5), 2035-2050.

Gray, J., Lissman, tt.W., Pumphrey, R. J. (1938). The mechanism of locomotion in the leech (*Hirudo medicinalis*). J. exp. Biol. 15, 408-430.

Gu X. (1991). Effect of conduction block at axon bifurcations on synaptic transmission to different postsynaptic neurons in the leech. J Physiol 441, 755-778.

Hashemzadeh-Gargari H. & Friesen W.O. (1989). Modulation of swimming activity in the medicinal leech by serotonin and octopamine. Comp Biochem Physiol, 94C(1), 295-302.

Hill *et al.*,(2003) In: Enquist M. & Ghirlanda S. (2005). Neural Networks and Animal Behaviour. (Monographs in Behavior and Ecology). Princeton University Press. Chapter 1: Understanding animal behaviour. pp: 2-18.

Hille B. (2001). Ion Channels of Excitable Membranes, Third Edition. Sinauer Associates. P.23-58

Hinde RA, 1970. *Animal Behaviour*. Tokyo: McGrawHill Kogakusha, 2 edition.

Hodgkin, A., and Huxley, A. (1952): A quantitative description of membrane current and its application to conduction and excitation in nerve. J. Physiol. 117:500–544

Hogan R, Curphy GJ, Hogan J. (1994). What we know about leadership. Effectiveness and personality. Am Psychol. 49(6):493-504. Review

Jansen J.K.S. & Nicholls J.G. (1972). Regeneration and changes in synaptic connections between individual nerve cells in the central nervous system of the leech. Proc Nat Acad Sci USA 69(3), 663-639.

Jellies J, Johansen J (1995) Multiple strategies for directed growth cone extension and navigation of peripheral neurons. J Neurobiol 27: 310-325.

Johnson S.C. (1967). Hierarchical clustering schemes. Psychometrika 32:241–254

Jutras M.J., Buffalo E.A. (2010). Synchronous neural activity and memory formation. Curr Opin Neurobiol. 20(2):150-5. Review.

Kandel R., Schwartz J., Jessell T. (1981). Fifth Edition on March 24, 2010): Principles of Neural Science Elsevier.

Kaplan *et al.*, (2005): In: Fielding, A.H. (2007). Cluster and Classification Techniques for the Biosciences. Cambridge University Press. Chapter 6: Cluster analysis. p. 46-77.

Kristan WB, Jr., Stent GS (1976) Pepherial feedback in the leech swimming rhythm. Cold Spring Harb Symp Quant Biol 40:663-74.: 663-674.

Kristan W.B. (1982). Sensory And Motor Neurones Responsible For The Local Bending Response in Leeches, J Exp Biol 96, 161-180.

Kristan W.B. Jr & Nusbaum M.P. (1982). The dual role of serotonin in leech swimming. J Physiol (Paris) 78(8) 743-747

Kristan WBJr, Wittenberg G, Nusbaum MP, Stern-Tomlinson W (1988) Multifunctional interneurons in behavioral circuits of the medicinal leech. Experientia 44: 383-389.

Kristan WBJr, Lockery SR, Lewis JE (1995) Using reflexive behaviors of the medicinal leech to study information processing. J Neurobiol 27: 380-389.

Kristan WB Jr, Calabrese RL, Friesen WO. (2005). Neuronal control of leech behavior. Prog Neurobiol. 76(5):279-327. Review.

Kristan WB Jr. (2008). Neuronal decision-making circuits. Curr Biol. 18(19): R928-32. Review.

Kristan Jr., W.B., Stent, G.S., Ort, C.A., 1974a. Neuronal control of swimming in the medicinal leech. I. Dynamics of the swimming rhythm. J. Comp. Physiol. 94, 97–119.

Kristan Jr., W.B., Stent, G.S., Ort, C.A., 1974b. Neuronal control of swimming in the medicinal leech. III. Impulse patterns of the motor neurons. J. Comp. Physiol. 94, 155–176.

Krzanowski WJ (1998) An introduction to statistical modelling. Arnold London.

Kuffler S.W. & Potter D.D. (1964). Glia in the leech nervous system: physiological properties and neuron-glia relationships. J Neurophysiol 27, 290-320.

Kuffler S.W. & Nicholls J.G. (1966). The physiology of neuroglial cells. Ergeb Physiol Biol Chem Exp Pharmakol 57, 1-90.

Kumar A, Rotter S, Aertsen A. (2010). Spiking activity propagation in neuronal networks: reconciling different perspectives on neural coding. Nat Rev Neurosci. 11(9):615-27. Review.

Kupfermann, I., & Weiss, K.R. (1978). The command neuron concept. Behav. Brain. Sci. 1, 3–39.

Lent C.M., Dickinson M.H. (1984). Retzius cells retain functional membrane properties following 'ablation' by the neurotoxin 5,7-DHT. Brain Res. 300(1):167-71.

Lent CM. (1985). Serotonergic modulation of the feeding behavior of the medicinal leech. Brain Res Bull. 14(6):643-55.

Lent C.M., Dickinson M.H. (1987). On the termination of ingestive behaviour by the medicinal leech. J Exp Biol. 131:1-15.

Lent CM, Fliegner KH, Freedman E, Dickinson MH.(1988). Ingestive behaviour and physiology of the medicinal leech. J Exp Biol. 137:513-27.

Lewis J.E. & Kristan W.B. Jr (1998a). Representation of touch location by a population of leech sensory neuron. J Neurophysiol 80(5) 2584-2592.

Lewis J.E. & Kristan W.B. Jr (1998b). A neuronal network for computing population vectors in the leech. Nature 391, 76-79.

Lewis J.E. & Kristan W.B. Jr (1998c). Quantitative analysis of a directed behaviour in the medicinal leech. J Neurosci 18(4), 1571-1582.

Lorenz K. (1970) Studies in animal and human behavior. Cambridge, MA: Harvard University Press. Vol. 1. In: Magnus Enquist & Stefano Ghirlanda: Neural Networks and Animal Behavior. Monographs in Behavior and Ecology. Princeton University Press. Chapter 1: Understanding animal behaviour. pp: 2-18.

Magni F. & Pellegrino M. (1978). Neural mechanisms underlying the segmental and generalized chord shortening reflexes in the leech. J Comp Physiol 124, 339-351.

Mar A. & Drapeau P. (1996). Modulation of conduction block in leech mechanosensory neurons. J Neurosci 16(14), 4335-4343.

Martindale M.Q. & Shankland M. (1990). Intrinsic segmental identity of segmental founder of the leech embryo. Nature 347, 672-674.

Mason A. & Kristan W.B. Jr (1982). Neuronal excitation, inhibition and modulation of leech longitudinal muscle. J Comp Physiol 146, 527-536.

Mazzoni A, Garcia Perez E, Zoccolan D, Graziosi S, Torre V (2005) Quantitative characterization classification of leech behavior. J.Neurophysiol 93:580-593.

Mazzoni A, Broccard FD, Garcia-Perez E, Bonifazi P, Ruaro ME, Torre V. (2007). On the Dynamics of the Spontaneous Activity in Neuronal Networks. PLoS ONE 2(5): e439. doi:10.1371/journal.pone.0000439

Mayr, E. 1961. Cause and effect in biology. Science, 134:1501-1506.

McFarland DJ, 1999. Animal Behaviour: Psychobiology, Ethology and Evolution. Harlow, England: Longman, 3 edition.

Melinek R. & Muller K.J. (1996). Acton potential initiation site depends on neuronal excitation. J .Neurosci 16(8), 2585-2591.

Mesce K.A., Pierce-Shimomura J.T. (2010). Shared Strategies for Behavioral Switching: Understanding How Locomotor Patterns are Turned on and Off. Front Behav Neurosci. 4: 49.

Mesce, K.A., Crisp, K.M., Gilchrist, L.S., 2001. Mixtures of octopamine and serotonin have nonadditive effects on the CNS of the medicinal leech. J. Neurophysiol. 85, 2039–2046.

Misell, L.M., Shaw, B.K., Kristan Jr., W.B., 1998. Behavioral hierarchy in the medicinal leech, Hirudo medicinalis; feeding as a dominant behavior. Behav. Brain Res. 90, 13–21.

Modney, B.K., Sahley, C.L., Muller, K.J., 1997. Regeneration of a central synapse restores nonassociative learning. J. Neurosci. 17, 6478–6482.

Moss BL, Fuller AD, Sahley CL, Burrell BD. (2005). Serotonin modulates axo-axonal coupling between neurons critical for learning in the leech. J Neurophysiol. 94(4):2575-89.

Muller KJ, Nicholls JG. (1974). Different properties of synapses between a single sensory neurone and two different motor cells in the leech C.N.S. J Physiol. 238(2):357-69.

Muller K.J., Nicholls J.G. & Stent, G.S. (1981b). The nervous system of the leech: a laboratory manual. from: Muller K.J., Nicholls J.G. & Stent G.S. *Neurobiology of the leech*. Cold Spring Harbour Laboratory, 249-276.

Nicholls, J.G. & Baylor, D.A. (1968). Specific modalities and receptive fields of sensory neurones in CNS of the leech. J Neurophysiol 31, 740-756.

Nicholls JG, Purves D. (1972). A comparison of chemical and electrical synaptic transmission between single sensory cells and a motoneurone in the central nervous system of the leech. J Physiol. 225(3):637-56.

Norris B.J. & Calabrese R.L. (1987). Identification of motoneurons that contain FMRFamidelike peptide and the effect of FMRFamide on longitudinal muscle in the medicinal leech, Hirudo Medicinalis. J Comp Neurol 266, 95-111.

Nusbaum, M.P., Kristan Jr., W.B., 1986. Swim initiation in the leech by serotonin-containing interneurones, cells 21 and 61. J. Exp. Biol. 122, 277–302.

Nusbaum, M.P., Friesen, W.O., Kristan Jr., W.B., Pearce, R.A., 1987. Neural mechanisms generating the leech swimming rhythm; swim-initiator neurons excite the network of swim oscillator neurons. J. Comp. Physiol.A 161, 355–366.

O'Gara B.A. & Friesen W.O. (1995). Termination of leech swimming activity by a previously identified swim trigger neuron. J Comp Physiol [A] 177, 627-636.

O'Gara B.A., Illuzzi F.A., Chung M., Portnoy A.D., Fraga K. & Frieman V.B. (1999). Serotonin induces four pharmacologically separable contractile responses in the pharinx of the leech Hirudo Medicinalis. Gen Pharmacol 32(6) 669-681.

Oishi N., Mima T., Ishii K., Bushara K.O., Hiraoka, T., Ueki T., Fukuyama H., and Hallett M. (2007). Neural correlates of regional EEG power change. NeuroImage 36: 1301–1312.

Oppenheim, AV, Willsky, AS, Nawab, H., Hamid S. (1998). Signals and Systems. Pearson Education.

Ort, C.A., Kristan, W.B. Jr & Stent G.S.(1974). Neuronal control of swimming in the medicinal leech II. Identification and connections of motor neurons. J Comp Physiol 94, 121-154.

Pastor J., SoriaB. & Belmonte C. (1996). Properties of nociceptive neurons of the leech segmental ganglion. J Neurophysiol, 75(6), 2268-2279.

Payton B. (1981b). Structure of the nervous system of the leech. from: Muller K.J., Nicholls J.G. & Stent G.S. Neurobiology of the leech. Cold Spring Harbour Laboratory, 35-50.

Pearce R.A. & Friesen W.O. (1985a). Intersegmental coordination of the leech swimming rythm: I. Roles of cycle period gradient and coupling strength. J Neurophysiol 54(6), 1444-1459.

Pearce R.A. & Friesen W.O. (1985b). Intersegmental coordination of the leech swimming rythm: II. Comparison of long and short chains of ganglia. J Neurophysiol 54(6), 1460-1472.

Pesaran B. (2010). Neural correlations, decisions, and actions. Curr Opin Neurobiol. 20(2):166-71. Review.

Peterson E.L. (1985a). Visual interneurons in the leech brain.I. Lateral visual cells in the subesophageal ganglion. J Comp Physiol [A] 156, 697-706.

Peterson E.L. (1985b). Visual interneurons in the leech brain.II. The anterior visual cells of the supraesophageal ganglion. J Comp Physiol [A] 156, 707-717.

Pinato G., Parodi P., Bisso A., Macri D., Kawana A., Jimbo Y. & Torre V. (1999). Properties of the evoked spatio-temporal electrical activity in neuronal assemblies. Rev Neurosci 10, 279-290.

Pinato G., Battiston S. & Torre V. (2000). Statistical independence and neural computation in the leech ganglia. Biol Cybern (in press).

Pinato G. & Torre V. (2000). Coding and adaptation during mechanical stimulation in the leech nervous system. J Physiol (submitted).

Poon, M., Friesen, W.O., Stent, G.S., 1978. Neural control of swimming in the medicinal leech. V. Connexions between the oscillatory interneurones and the motor neurones. J. Exp. Biol. 75, 45–63.

Puhl J.G. & Mesce K.A. (2010). Keeping it together: mechanisms of intersegmental coordination for a flexible locomotor behavior. J Neurosci. 30(6):2373-83.

Puhl J.G. & Mesce K.A. (2008). Dopamine activates the motor pattern for crawling in the medicinal leech. J Neurosci. 28(16):4192-200

Quiroga Q.R., Panzeri S. (2009). Extracting information from neuronal populations: information theory and decoding approaches. Nat Rev Neurosci. 10(3):173-85.

Rector DM, Schei JL, Van Dongen HP, Belenky G, Krueger JM.(2009) Physiological markers of local sleep.Eur J Neurosci. 29(9):1771-8. Review.

Reynolds S., French K., Baader A. & Kristan W. (1998). Development Of Spontaneous And Evoked Behaviors In The Medicinal Leech, Journal Comp. Neurology. 402(2) 168-180.

Rieke F., Warland D., Ruyter van Steveninck R.D. and Bialek W. (1997). Spikes: exploring the neural code. Massachusetts institute of technology (MIT) Press. Chapters: 1, 2 & 4.

Rolls T.E. & Treves A. (1998). Neural Networks and brain function. Oxford University Press. Chapters: 1, 2 & 10.

Sahley C.L., Modney B.K., Boulis M.B. & Muller K.J. (1994a). The S cell: an interneuron essential for sensitization and full dishabituation of leech shortening. J Neurosci 14(11), 6715-6721.

Sahley C.L., Boulis M.B. & Schurman B. (1994b). Associative learning modifies the shortening reflex in the semi-intact leech Hirudo medicinalis: effects of pairing, predictability and CS preexposure. Behav Neurosci 108(2), 340-346.

Sawada M., Wilkinson J.M., MacAdoo D.J., Coggeshall R.E. (1976). The identification of two inhibitory cells in each segmental ganglion of the leech and studies on the ionic mechanism of the inhibitory junctional potentials produced by these cells. J Neurobiol 7(5), 435-45.

Sawyer R.T. (1981). Leech biology and behaviour. from: Muller K.J., Nicholls J.G. & Stent G.S. *Neurobiology of the leech.* Cold Spring Harbour Laboratory, 7-26.

Schlüter, E. (1933). Die Bedeutung des Centralnervensystems von *Hirudo medicinalis* fiir Locomotion und Raumorientierung. Z Wiss Zool 143:538-593

Schmidt J, Deitmer JW. (1996). Photoinactivation of the giant neuropil glial cells in the leech Hirudo medicinalis: effects on neuronal activity and synaptic transmission. J Neurophysiol. 76(5):2861-71.

Shain D.H., Ramirez-Weber Joyce-Hsu F.A. & Weisblat D.A. (1998). Gangliogenesis in leech: morphogenetic processes leading to segmentation in the central nervous system. Dev Genes Evol 208, 28-36.

Shaw B. K. & Kristan W.B. Jr (1995). The whole-body shortening reflex of the medicinal leech: motor pattern, sensory basis, and interneuronal pathways. J Comp Physiol [A] 177(6) 667-681.

Shaw B. K. & W.B. Kristan Jr (1997). The neuronal basis of the behavioral choice between swimming and shortening in the leech: control is not selectively exercised at higher circuit levels. J Neurosci 17(2) 786-95.

Shaw B. K. & Kristan W.B. Jr (1999). Relative roles of the S cell network and parallel interneuronal pathways in the whole-body shortening reflex of the Medicinal leech. J Neurophysiol 82, 1114-1123.

Siddall M.E., Trontelj P., Utevsky S,Y., Nkamany M. & Macdonald III, K.S. (2007). Diverse molecular data demonstrate that commercially available medicinal leeches are not *Hirudo medicinalis*. Proc. R. Soc. B. 274, 1481–1487

Sigworth F.J. (1994). Voltage gating of ion channels. Q. Rev. Biophys. 27:1-40.

Sneath, P. (1969). Evaluation of Cluster Methods" in A.J. Cole, ed., Numerical Taxonomy, London: Academic Press, Inc., 1969

Stein, J.Y. (2000). Digital signal processing: A computer science perspective. Ed. John Wiley & Sons. Chapter 2. p. 15-64.

Stent G.S., Kristan W.B. Jr, Friesen W.O., Ort C.A., Poon M. & Calabrese R.L. (1978). Neuronal generation of the leech swimming movement. Science 200, 1348-1357.

Steriade, M., Gloor, P., Llinas, R.R., Lopes de Silva, F.H., Mesulam, M.M.,(1990). Basic mechanisms of cerebral rhythmic activities. Report of IFCN Committee on Basic Mechanisms. Electroencephalogr. Clin. Neurophysiol. 76, 481–508.

Steriade, M., 1993. Cellular substrates of brain rhythms, In: Niedermeyer, E., Lopes da Silva, F.H. (Eds.), Electroencephalography: Basic Principles, Clinical Applications and Related Fields, 3rd ed. Williams

and Wilkins, Baltimore, pp. 27–62 Stern-Tomlinson W, Nusbaum MP, Perez LE, Kristan WB Jr. A kinematic study of crawling behavior in the leech, Hirudo medicinalis. J Comp Physiol A. 158(4):593-603.

Stuart A.E. (1970). Physiological and morphological properties of motoneurones in the central nervous system of the leech. J Physiol (Lond) 209(3) 627-646.

Szczupak L. & Kristan W.B. Jr (1995). Widespread mechanosensory activation of the serotonergic system of the medicinal leech. J Neurophysiol, 74(6), 2614-2624.

Taylor AL, Cottrell GW, Kleinfeld D, Kristan WB Jr.(2003). Imaging reveals synaptic targets of a swim-terminating neuron in the leech CNS. J Neurosci. 23(36):11402-10.

Thorogood M.S.E. & Brodfuehrer P.D. (1995). The role of glutamate in swim initiation in the medicinal leech. Invert Neurosci 1, 223-233.

Tinbergen, N. (1951). The Study of Instinct, Oxford University Press,Oxford.

T. Trappenberg, (2002). Fundamentals of Computational Neuroscience. New. York, NY: Oxford Press.

Uexküll, Jakob von.1905a. *Leitfaden in das Studium der experimentellen Biologie der Wassertiere. Wiesbaden: J.F.Bergmann.* From: Torsten Rüting (2004). History and significance of Jakob von Uexküll and of his institute in Hamburg. *Sign Systems Studies* 32. 1-2. pp: 35-72.

Wagner S. & Wagner D., (2007). Comparing Clusterings- An Overview. Available at: http://citeseerx.ist.psu.edu/viewdoc/summary?doi=10.1.1.164.6189

Ward J.H. Jr. (1963). Hierarchical grouping to optimize an objective function. Journal of the American statistical association 58:236–244

Weeks J.C. (1982). Segmental specialization of a leech swim-initiating interneuron, cell 2051. J Neurosci. 2(7): 972-85.

Weeks JC. (1982b) Neuronal basis of leech swimming: separation of swim initiation, pattern generation, and intersegmental coordination by selective lesions. J Neurophysiol. 45(4):698-723

Weeks JC, Kristan Jr WB (1978) Initiation, maintenance and modulation of swimming in the medicinal leech by the activity of a single neuron. J Exp Biol 77:71– 88.

Willard A.L. (1981). Effects of serotonin on the generation of the motor program for swimming by the medicinal leech. J Neurosci 1(9), 936-944.

Wilson M.A. & McNaughton B.L. (1994). Dynamics of the hippocampal ensemble code for space. Science 261, 1055-1058.

Wilson R.J., Breckenridge L., Blackshaw S.E., Connolly P., Dow J.A., Curtis A.S. & Wilkinson C.D. (1994). Simultaneous multisite recordings and stimulation of single isolated leech neurons using planar extracellular electrode arrays. J Neurosci Methods 53(1), 101-110

Wittenberg, G. & Kristan W.B. Jr (1992a). Analysis and modelling of the Multisegmental Coordination of Shortening Behaviour in the Medical Leech. I. Motor Output Pattern. J Neurophysiol 68(5), 1683-1692.

Wittenberg, G. & Kristan W.B. Jr (1992b). Analysis and modelling of the Multisegmental Coordination of Shortening Behaviour in the Medical Leech. II. Role of identified interneurons. J Neurophysiol 68(5), 1693-1707.

Yau, K.W. (1976a) Physiological properties and receptive fields of mechanosensory neurones in the head ganglion of the leech. Journal of Physiology 263(3), 489-512.

Yau K.W. (1976b). Receptive fields, geometry and conduction block of sensory neurones in the central nervous system of the leech. Journal of Physiology 263(3), 513-538.

Yu X., Nguyen B & Friesen W.O. (1999). Sensory feedback can coordinate the swimming activity of the leech. J Neurosci 19(11), 4634-4643.

Zoccolan D, Pinato G, Torre V (2002) Highly variable spike trains underlie reproducible sensorimotor responses in the medicinal leech. J Neurosci 22:10790-10800

APPENDIX: PUBLICATION IN PROGRESS (FEB. 2011)

Patterns of electrical activities underlying different behaviours in the leech *Hirudo medicinalis*

León Jacobo Juárez Hernández [1], Giacomo Bisson [1**] & Vincent Torre [1,2**]*

[1]Neurobiology Sector, International School for Advanced Studies (SISSA), via Bonomea, 265, 34136, Trieste, Italy
[2]IIT, Italian Institute of Technology, SISSA-Unit, Trieste, Italy
** Experiments, analysis & writing. ** Analysis & writing*

Abstract

In the present manuscript we relate the firing of action potentials (APs) recorded from neurons of the leech nervous system to its behaviour. In semi-intact leeches in a stationary state, the electrical activity of neurons and motoneurons was poorly correlated. When the leech moved its head and/or tail, in contrast, APs firing in distinct neurons became highly correlated. When the head or tail suckers detached from the bottom of the observation tank specific patterns of electrical activity were detected on the roots and the connective fibres. During elongation and contraction the electrical activity of motoneurons in the Medial Anterior and Dorsal Posterior roots increased respectively and several motoneurons were activated both during elongation and contraction. During crawling, swimming and pseudo-swimming the electrical activity of most motoneurons changed but with a specific pattern, here described by the dendrogram of cross-correlations between firing of motoneuron pairs, describing in a compact way the distinct relationships among motoneurons during different behaviours.

Introduction

The understanding of the nervous system, from the perspective of Systems Neuroscience, requires the identification of patterns of electrical activity associated to sensory perceptions and to specific behaviours (Saberi, *et al.*, 2010, Keller & Takahashi (1996), Putrino et al (2010), Ghosh., et al (2009), Moreno-Bote R. & Parga 2010). Patterns of electrical activity can be recorded with multi units electrodes (Yoshida K. *et al.*, 2009, Gullo, F. *et al.*, 2009, Kim S. *et al.*, 2009) and imaging of the global activation of brain areas (Vanni & Rosenstrom, 2010, Aspell *et al.*, 2010, Casali A. et al, 2010). In vertebrates, motor behaviours, are thought to result from the flexible combination of a small number of behavioural units (for a review see Tresch *et al.*, 2002). These behavioural units correspond to the control of groups of functionally related muscles, often referred to as muscle synergies (d'Avella and Bizzi, 1998; Tresch *et al.*, 1999; Bizzi *et al.*, 2000). In this view, grouping together synergistic muscles allows the nervous system of vertebrates to cope with the many degrees of freedom related to the control of limbs, muscles, motor units, spinal motor circuits, etc (Tresch *et al.*, 2002). Addressing such an issue in vertebrates is very challenging, however the way in which different classes of muscles and motoneurons are combined in order to produce specific motor behaviours, can be more directly assessed in the neuromuscular systems of invertebrates, due to a lower number of available degrees of freedom.

An exhaustive and complete analysis is difficult in higher vertebrates, but is possible and certainly easier in invertebrates (Byrne *et al.*, 1974; Castellucci and Kandel, 1974; Frost and Kandell, 1995; Kristan, 1982; Nicholls and Baylor, 1968; Stuart, 1970; Stent *et al.*, 1978; Tsau *et al.*, 1994; Wittenberg and Kristan, 1992a, b). In the CNS of the leech, at ganglion mechanical inputs are transduced by 7 pairs of mechanosensory neurons; 3 specific for light pressure (touch or T cells), 2 for strong pressure (pressure or P cells), and 2 for noxious mechanical stimuli (N cells), (Nicholls and Baylor, 1968; Kristan *et al.*, 1982; Lewis and Kristan, 1998a; Pinato & Torre 2000). The leech motor system consists of 19 pairs of excitatory motoneurons in each ganglion that innervate longitudinal, oblique and circular fibres (Stuart, 1970; Ort *et al.*, 1974; Mason and Kristan, 1982; Norris and Calabrese, 1987). These motoneurons have been extensively investigated using force and length transducers and electrophysiology tools (Stuart, 1970; Mason and Kristan, 1982; Kristan, 1982; Norris and Calabrese, 1987).

In the present manuscript we use a semi-intact leech preparation (Kristan & Calabrese 1976), where one or two ganglia were exposed so to allow electrical recordings, while the leech was still able to move in the observation dish. If leeches were gently dissected, they exhibited their stereotype behaviours and could crawl, elongate and even swim. Under these experimental conditions, by using suction pipettes it is possible to record patterns of electrical activity from motoneurons: indeed by using 8 suction electrodes we were able to monitor the occurrence of action potentials (APs) from several tens of motoneurons and from interneurons. A red and a green bead were glued on its head and tail, so that their motion was tracked for 1 or 2 hours by using CCD cameras and its behaviour could be quantified. Therefore it was possible to compare behaviours and identify patterns of electrical activity specific to each behaviour.

When the leech was at rest in a stationary state, the average firing rate (AFR) of neurons and motoneurons decreased becoming uncorrelated: indeed a low degree of cross-correlation is a good signature of a stationary state, during which the leech does not move either the head or the tail. In contrast, when the leech moves the electrical activity of motoneurons increases and becomes highly correlated. During elongation and contraction of the leech body the electrical activity of motoneurons in the Medial Anterior (MA) and Dorsal Posterior (DP) roots increases respectively and we identified motoneurons which are activated both during elongation and

contraction. We propose to characterize patterns of electrical activity, specific for leech behaviours with a dendrogram, describing in a compact way the hierarchy of correlations between motoneurons.

Methods

The set-up used to in the experiments described in the present manuscript is illustrated in Fig.1A. Animals were positioned on a Petri dish with a diameter of 15cm (Fig.1A left). Eight suction electrodes were used to record extracellular APs from roots and connective fibbers. Two coloured beads were glued over its skin next to head and tail suckers. By using a coloured CCD camera the position of the two coloured beads was followed in real time, and acquired data were transferred to a PC computer (Fig.1A central). The leech behaviour was monitored by acquiring the *x,y* positions of head $(x,y)_{head}$ and tail $(x,y)_{tail}$ (Fig.1A right). In this way it was possible to correlate the leech behaviour (Fig. 1B) to the recorded patterns of electrical activity (Fig. 1C).

Animals and Semi-intact preparation

Adult leeches *Hirudo medicinalis* or *Hirudo verbana* obtained from Ricarimpex (Eysines, France) were kept at 5°C in tap water dechlorinated by previous aeration for 24 h. Before every experiment, animals were anesthetized with an 8% ethanol (ethanol: water) solution at room-temperature for 15-20 minutes. Leeches were extended and the skin was dried carefully. Colour beads of 5 mm diameter were glued on the dorsal side of the leech with Nexaband S/C tissue adhesive (Abott Labs, Chicago, USA) near their head and tail. Once beads were correctly glued, leeches were moved to the Petri dish covered with sylgard elastomere (Corning corp., U.S.A.). The leech was immersed in 150-200 ml chilled normal ringer solution (in mM: 115 NaCl, 1.8 $CaCl_2$, 4 KCl, enriched with 10 glucose and buffered with 10 Tris-maleate pH 7.4 with NaOH). Leeches still under anaesthesia were pinned with fine needles in their mid-body. Animals were dissected so to expose two central ganglia (Fig. 1A, right image).During the dissection, the temperature was maintained at 6-8°C using a cold chamber. Roots and connectives were cleaned carefully as suggested us by Prof. William Kristan (personal communication). In some experiments, a complete segment (skin from mid dorsal to mid ventral) was left innerved by roots form one side, recording electrical signals controlaterally and the changes of the skin area was analyzed. At the end of the dissection, animals were left to recover from anaesthesia and left to adapt to room temperature for 30 minutes. Experiments were performed at room's temperature (19-22° Celsius) and the semi-intact leech was illuminated using a white light lamp without abrupt spatial and/or temporal gradients (Olympus Highlight 3100, Europe).

Imaging

A colour CCD camera (640×480 pixels; model WAT-231S; Watec, Tsuruoka, Japan) was used to acquire images of semi-intact leeches (Fig.1A left image). Acquired images were sent by a frame grabber (PCI-1394; Texas Instruments) to a personal computer, able to process images in real time. Colour beads were tracked at 25 Hz using an appropriate software program. Images were directly acquired in the hue/saturation/lightness colour space. The detection of sucker attachment and detachments was obtained by visual inspection of acquired images using a standard analysis software (VirtualDub v. 1.6.14; General Public License, 2006).

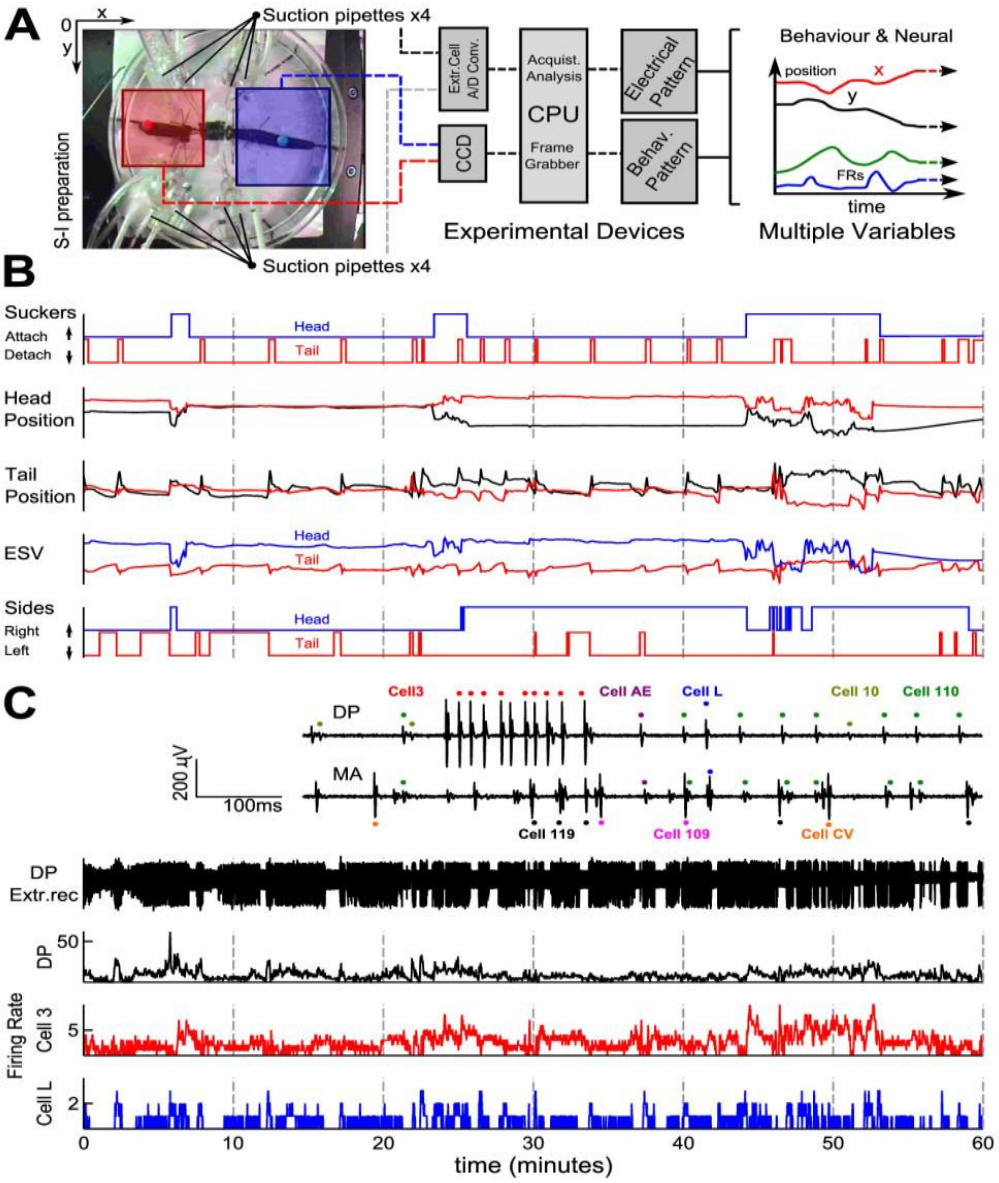

Figure 1. *Recording set-up and signals processing of behavioural and electrical data*. **A**. *The experimental Set up*. Left Image shows a semi intact preparation viewed from the CCD camera. Blue area represents the region where the head is usually located (set manually by a Lab-view program-interface) necessary to filter and track the colour bead during the experiment. Red area refers to the tail. Suction pipettes were positioned at left and right sides of the leech in such ay not to occlude the beads. Centre diagram represent a side view of the CCD camera situated at about 17 cm above the preparation. Right diagram represents the x,y (red and black respectively) coordinates of a bead detected during a representative experiment. **B**. *Behaviour characterization* based on detected behaviour variables obtained by visual inspection (sucker attachment and detachment) and automatic processing (the other behaviour variables). *Suckers*: the head (tail) sucker corresponds to blue (red) trace. Up indicates that sucker was free (detached) while down indicates attached sucker. *Head and tail positions*: represent the x and y coordinates (red and black respectively) of head and tail in pixels. *ESV*: Elongation-Contraction Vector obtained by computing head and tail position with an automated process, blue represents the head's performance while Red represents the tail. *Right-Left*: represents the head and tail on animal's side (in blue and red respectively). Up indicates motion on the right side while down indicates motion on the left side. C. *Electrical recordings signals. DP root*: analogical trace from an extracellular recording from a dorsal posterior. *Firing Rate*: firing rate (FR) from the DP root recorded over 500 ms windows. *3 cell & L cell FR*: firing rates of motoneuron 3 and L, identified as described in the Methods (see also the inset). *Inset DP & MA*: zoom of the extracellular recordings from a DP and a MA root. Spikes from L cell (blue dots) are present on MA and DP roots as Annulus Erector cell (AE, green dots) but the amplitude of the spikes in every root recorded helps to determine the nature of the cells following an identification table (Arisi, 2002).

Behaviour quantification

In order to quantify the leech behaviour, the following quantities (Fig.1B) were determined using the MatLab Software off-line (MathWorks, USA):

1 - Sucker attachment/detachment. Using visual inspection from video recordings the times of sucker attach and detach were determined over the time. An example of the results from one experiment is visualized as two step traces corresponding to the head (in blue) and tail (in red) sucker (fig.1B *suckers*).

2 - Head & Tail position and velocity

Head and tail coordinates were recorded and represented as $(x\ ,y)_{head}$ and $(x,y)_{tail}$ (Fig 1B: *Head & Tail position*). The head and tail velocity $(v_x,v_y)_{head}$ and $(v_x,v_y)_{tail}$ were calculated by convolution with the derivative with a Gaussian function as previously described (Mazzoni *et al.,* 2005).

3 – Head and Tail Elongation (ESV)

We fixed a reference point corresponding to the centre of one of the two dissected ganglia $M(x,y)$. The head (tail) elongation was computed as the distance between $(x,y)_{head}$ ($(x,y)_{tail}$) and $M(x,y)$. The total elongation of the leech was equal to the sum of the head and tail elongation.

Semi-intact leech behaviour

Six different behaviours were previously detected in the intact leech (Mazzoni *et al.*, 2005, García-Perez *et al.*, 2005). These stereotyped behaviours were: Swimming, Exploring Head, Pseudo-swimming, Crawling, Peristalsis and Stationary States. Similar behaviour could be detected also in semi-intact preparations and were characterized by the following properties:

Swimming. Leeches detached both the head and tail suckers from the bottom of the Petri dish and the head and tail beads oscillated with a frequency of ~1.5 Hz.

Exploring Head. Leeches detached their head sucker keeping the tail sucker attached to the bottom of the Petri disc and the head bead had variable and irregular elongations and contractions without any periodicity.

Ventilation or pseudo-swimming. Leeches kept their tail sucker attached and the head sucker detached and the head bead oscillated as during swimming episodes but with a lower frequency (Head movement frequency in intact animals: 2 Hz; in semi-intact animals: 1.5 Hz).

Crawling. Leeches alternated sucker attachment and detachment in a coordinated way while leeches elongated and shortened, as during crawling in intact leeches. The frequency of these cycles was lower in semi-intact leeches. (Crawling frequency in intact animals: 0.1-0.2 Hz; in semi-intact animals: 0.04-0.08 Hz).

Peristalsis. Leeches has both suckers attached but the leech elongation had periodic cycles with a frequency of about 0.03 Hz.

Stationary states. Leeches head both suckers attached and did not move.

Glass Suction Electrodes.

Suction pipettes were obtained from borosilicate glass capillaries (World precision instruments, Germany) pulled by a conventional puller (P-97, Sutter Instruments Co., USA). The electrode tip was cut using a diamond sharpen tip mounted on an appropriate manipulator under

a stereoscopic microscope (Olympus SZ40, Europe). Electrodes with final diameters between 150 and 200 μm, were polished using an incandescent filament under a 20x objective mounted on a upright microscope (Zeiss, Germany).

Electrical recordings

Suction electrodes filled with normal ringer leech solution were connected to an extracellular recording amplifier (Pinato & Torre 2000, Pinato *et al.*, 2000) . Extracellular signals were digitized at 10 kHz by a A/D converter (model digidata-1322, 16 bit converter; Axon, molecular Devices, U.S.) and data were transferred and stored on a PC computer. Signals were recorded and visualized using respectively Clampex v.8.1 and Clampfit v.9.2 software (Molecular Devices, USA). Electrical recordings were obtained from cleaned roots or connectives (in *en passant* configuration) from one or two ganglia. Recordings from a single ganglion were obtained with 8 electrodes sucking the left and right of Anterior anterior root (AA), Medial anterior(MA), Dorsal posterior (DP) and Posterior posterior roots (PP) (Pinato et al, Arisi *et al.*, 2001). Recordings from two ganglia were obtained with 8 electrodes sucking the left and right AA and DP roots of both ganglia. Ganglia were dissected from the mid body between the 9th and the 13th segments.

Spike detection

Spike sorting was carried out by an appropriate software using MatLab v.2007 (MathWorks, Natick,USA). After spike sorting, defined shapes of APs were attributed to identified motoneurons (Stuart, 1970). In several experiments, we identified a signature of recorded extracellular APs of specific motoneurons (Stuart, 1970; Muller & Nicholls, 1974; Kristan *et al.*, 1974B; Magni & Pellegrino, 1978; Stent *et al.*, 1978; Muller *et al.*, 1981; Bagnoli *et al.*, 1975; Baader & Kristan, 1995; Baader, 1997; Shaw & Kristan, 1999; Pinato *et al.*, 2000; Arisi *et al.*, 2001; Zoccolan *et al.*, 2002; Kristan, 2005), as shown in the inset of Fig. 1C. Spikes elicited by motoneurons 3 and 107 produce the largest extracellular signals observed on the DP and AA root respectively. Extracellular spikes of motoneurons annulus erector (AE) and longitudinal (L) were identified because they were visible in both MA and DP roots.

Average firing rate and Cross- covariance coefficient

The duration of the recording was divided into bins of constant width. Different widths (varying between 100 and 500 ms) were used to compare properties at different time scales. The choice of the binwidth relies on the time-scale of interest. For each single neuron the number of spikes occurring in each bin was counted and the resulting discrete time series represented the neuron average firing rate (AFR). The same procedure was applied to roots providing the root AFR. For pairs of neuron AFR - or pairs of root AFR - the time-varying unbiased cross-covariance of the neuron (root) firing rates was computed in a bin-width of 50 s as

$$\rho_{12}(m) = \begin{cases} \dfrac{1}{N-|m|} \displaystyle\sum_{n=0}^{N-|m|-1} \left[f_1(n+m) - \frac{1}{N}\sum_{i=0}^{N-1} f_1(i) \right] \left[f_2(n) - \frac{1}{N}\sum_{i=0}^{N-1} f_2(i) \right], & m \geq 0 \\ \rho_{21}(-m), & m < 0 \end{cases}$$

where f_1 and f_2 represent the pair of firing rates in a window of 500 ms. The usual value for N was 100 samples. The window width of 100 samples was chosen in order to ensure a reliable

estimate of the covariance coefficients at low lags. The obtained value $\rho_{12}(0)$ was assumed to located in the point corresponding to the centre of the time window. A single, scalar value, was then obtained by averaging $\rho_{12}(m)$ for m in the range [-5,5]. This procedure was used to reduce noise and to sample also values of m around 0, where the cross-covariance is usually large.

Dendrograms

The firing rates of up to 30 spike sorted motoneurons were classified into clusters, with similar properties. One of the most intuitive measures of similarity between two firing rates is the Pearson's correlation coefficient, providing a NxN matrix when the firing of N neurons is available. In our case, we want to investigate how single neuron activities are related each other and if the NxN matrix of cross-covariance can be clustered in a suitable hierarchy providing a compact coding of electrical patterns underlying a stereotyped behaviour, such as swimming or crawling: this leads to hierarchically-nested sets of partitions, commonly represented in rooted tree diagram, or dendrogram. In our study we used the uncentred correlation coefficient (i.e. one minus the sample Pearson's correlation between single cell activities) as a metric and a dissimilarity matrix was constructed using the functions *pdist* and *squareform* implemented in Matlab. The dissimilarity matrix $[d_{ij}]$ contains the N x N pairwise dissimilarity values. Once the dissimilarity matrix was obtained, the hierarchical cluster tree was obtained by means of the *linkage* function (using the complete linkage method) and visually represented with the *dendrogram* function, both implemented in Matlab. We used the complete linkage method because it is less sensitive to noise (Baker, 1972) and may be used with non-Euclidean dissimilarity matrices, such as the uncentred correlation. The hierarchical clustering procedure explained above was run on time intervals during which the leech was either swimming, pseudo-swimming, crawling, elongating or shortening. Separated episodes were clumped together.

Comparison among dendrograms

By considering time intervals during which the animal was crawling, swimming, or pseudo-swimming, as well as shortening or elongating, we estimated a dendrogram for each of these behaviours, by running the aforementioned hierarchical clustering algorithm on the spike sorted activities of up to 30 motoneurons. Once these dendrograms were estimated, we used them as templates to be compared with a generic dendrogram calculated on a sliding time-window of 100 s width and 2 s sliding step. To compare two dendrograms, one needs a measure of similarity between them. Usually, similarity indexes are normalized and range between zero and one, where zero represents complete dissimilarity, while one complete equality. We obtained the best comparisons both with Fowlkes-Mallows Index (B_k) and Normalized Mutual Information by Fred & Jain (2003). The former index can be interpreted as the geometric mean of precision (ratio of the number of retrieved relevant documents to the total number of retrieved documents) and recall (ratio of the number of retrieved relevant documents to the total number of relevant documents), while the latter has its origin in information theory and is based on the notion of entropy. Near to zero values are usually observed when comparing a dendrogram resulting from time intervals during which the animal is stationary (see Fig.2) and the correlations are known to be low, resulting in flat dendrograms. Near to one values may be observed when comparing a dendrogram estimated over an episode of the behaviour under consideration (e.g. crawling) and the reference dendrogram estimated apart.

Discriminant analysis

Another approach to decode the behavioural state of the leech from the spike sorted activities, is to run a discriminant analysis on some time-varying features that are believed to vary accordingly to the particular behavioural state of the animal. As a set of features we chose the n(n-1)/2 coefficients of the covariance matrix estimated (using the *xcov* function in unbiased mode) from the spike sorted activities in a sliding time-window (100 s wide, 2 s step), or the raw activities alone. This was achieved by using the function *classify* implemented in Matlab, and passing, as input argument, the matrix of all the time-varying covariance coefficients (or the matrix of the raw activities), and a short training episode, half containing 0-class events (i.e. not during the behaviour under consideration) and half containing 1-class events (i.e. during the behaviour under consideration). We tested different types of classifier options: *linear*, which fits a multivariate normal density to each group, with a pooled estimate of covariance, *diaglinear,* i.e. naive Bayes classifier with a pooled estimate of covariance, *quadratic*, which fits multivariate normal densities with covariance estimates stratified by group and *diagquadratic*, i.e. naive Bayes classifier with covariance estimates stratified by group; see Krzanowski, W. J. 1998 for a thorough review. The function output assumes unity values when the behaviour under consideration is supposed to be performed and zero value vice versa. When testing these classifiers on all the 276 covariance matrix coefficients, we were forced to reduce the dimensionality, and thus the number of available coefficients, in order to obtain a training set covariance matrix that is positive definite. This was achieved with a principal component analysis on the original covariance matrix (*pcacov* function, Matlab), and selecting the first 100 principal components, thus reducing the feature space dimensionality.

ROC analysis

To assess the performance of a classifier, being it the simple threshold classifier, or the discriminant analysis or the dendrogram matcher, we used Receiver operating characteristics (ROC) graphs. Given a classifier and an instance, there are four possible outcomes. If the instance is positive and it is classified as positive, it is counted as a true positive; if it is classified as negative, it is counted as a false negative. If the instance is negative and it is classified as negative, it is counted as a true negative; if it is classified as positive, it is counted as a false positive. Given a classifier and a set of instances (the test set), a two-by-two confusion matrix (also called a contingency table) can be constructed representing the dispositions of the set of instances. This matrix forms the basis for many common metrics. The true positive rate (TPR) of a classifier is estimated as the ratio of the true positives count to the sum of the true positives and false negatives counts; the false positive rate (FPR) of a classifier is estimated as the ratio of the false positives count to the sum of the false positives and true negatives counts. ROC graphs are two-dimensional graphs in which TPR is plotted on the Y axis and FPR is plotted on the X axis. The perfect classifier is represented by the point (0,1). By varying the classifier type (as in the discriminant analysis case) or the threshold parameter (Fig.2B) it is possible to get different performances. Informally, one classifier in the ROC space is better than another if it is to the northwest (TPR is higher, FPR is lower, or both) of the first. We investigated the ROC space and determined which classifier was performing better by looking at the closest point to the upper-left corner.

Results

Leeches gently dissected can move their head and tail, surviving for several hours in the recording dish. In semi-intact preparations, leeches are pinned to the bottom of the recording, so to allow electrical recording but they can still exhibit their stereotype behaviours: indeed they can crawl (Fig.6) and rhythmically shorten and elongate their whole body as during swimming and pseudo-swimming (Figs. 7 and 8). Semi-intact leeches can be studied for several hours while recording their electrical activity and monitoring their behaviour (Fig.1) allowing the identification and characterization of patterns of electrical activity underlying specific behaviours.

In a typical experiment we measured the elongation of the leech, i.e. the distance between the bead glued on its head and the bead glued on its tail (first row of Fig.1A; see also Methods). A sudden decrease of the elongation signals a contraction of the leech and an increase of it occurs when leeches stretch their whole body and elongate. Periodic patterns of the elongation are seen when leeches crawl (Fig.6).

Electrical patterns underlying stationary states

Intact leeches as well as semi-intact leeches spend a considerable time in a stationary state, during which they do not move and the head and tail velocity is negligible. During these stationary states the leech elongation does not change and both or at least one sucker is attached to the bottom of the observation tank. A leech was assumed to be in a stationary state when its head v_{head} and tail velocity v_{tail} were less than 3σ for longer than 10 sec, where σ is the standard deviation of the position measured with our CCD camera of a coloured bead glued on the bottom of the observation tank. σ was 2.5 pixels/sec.

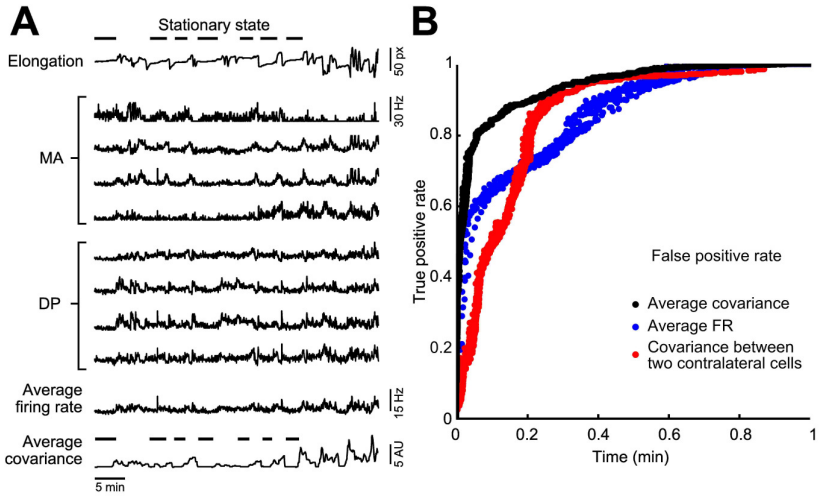

Figure 2. *Stationary states classification*. **A**. A representative experiment in which the total leech elongation was measured (upper trace) and compared to the AFR recorded from 4 DP and 4 AM roots in the 11th and 12th segmental ganglia. The average of these extracellular signals is also reported along with the average of the 8 time-varying auto-covariances and the cross-covariances between all the possible 28 pairs of AFR. **B**. To compare the performance of different classifiers a ROC analysis was performed considering as a reference (i.e. perfect classifier) the velocity classifier. Varying the binarization parameters (i.e. the threshold level, the minimum time interval

between two subsequent events and the minimum duration) results in a ROC curve. The perfect classifier is represented by the point (0,1). Three classifiers were compared: the binarized average cross-covariance (black dots), the binarized average firing rate (blue dots) and the binarized cross-covariance between two contralateral 3 cells identified with a custom spike sorting algorithm (red dots). The former of the three represents the best choice, as it is closer to the perfect classifier in the upper-left corner.

From the analysis of the leech elongation we identified the stationary states indicated by the horizontal bars over the upper trace in Fig.2A. In semi-intact leeches it is possible to measure with suction electrodes extracellular voltage signals originating from neurons and motoneurons innervating the Medial Anterior (MA) roots and Dorsal Posterior (DP) roots (Fig.2A). From these recordings, it is possible to precisely measure the firing patterns of identified motoneurons, as shown in Fig.6 and 8 (see also Methods). From these electrical signals we measured the total firing rate $<AFR_i>$ averaged over all the electrical signals recorded from the 4 MA and 4 DP roots. We measured also the covariance ρ_{ij} between the firing of APs recorded from all pairs of roots (the 4 MA and 4 DP roots). In order to have a measure of the correlation of the overall electrical activity we averaged ρ_{ij} over all pairs of roots, so to obtain the average covariance $< \rho_{ij} >$. As shown at the bottom of Fig.2A, during stationary states both $<AFR_i>$ and $< \rho_{ij} >$ have low values. Therefore we asked which features of the electrical activity characterize stationary states and whether stationary states are better identified by a low value of $<AFR_i>$ or of $< \rho_{ij} >$.

In order to understand which features of the electrical activity best identified stationary states we set a variable threshold T and for each value of T we identified all times $t_{<AFRi>}$ for which $<AFR_i>$ was less than T and all times $t_{<\rho ij>}$ for which $< \rho_{ij} >$ was less than T . For each value of T we computed the rate of true positive identifications, i.e. all the times properly identified as a stationary state and the rate of false positive identifications, i.e. all the times erroneously identified as a stationary state. These true and false positive identifications were computed for both $t_{<AFRi>}$ and $t_{<\rho ij>}$ as a function of T providing a pair of numbers corresponding to the true and false positive rates. The value of T for $<AFR_i>$ varied from 1 to 20 Hz and for $< \rho_{ij}>$ varied from 0.01 to 1 Hz^2. These pairs are plotted in Fig.2B, for the classifier based on $<AFR_i>$ (blue dots) and $< \rho_{ij}>$ (black dots) respectively. When the value of T decreases the rate of both true and false positive decrease. As shown in Fig.2B, the identification of stationary state based on the average cross-covariance $< \rho_{ij}>$ approaches the ideal classifier better than the identification based on average firing rates $<AFR_i>$. The best accuracy for the firing rate-based classificator is reached for a threshold that ranges between 2.5 and 4 Hz and, for the correlation-based classificatory, is reached for a threshold that ranges between 0.1 and 0.3 Hz^2. Identification of stationary states based on the cross-covariance ρ_{ij} of a single pair of identified controlateral motoneurons (red dots) is less efficient than the identification based on properties averaged over a population of neurons.

These results show that during stationary states both $<AFR_i>$ and $< \rho_{ij} >$ have small values and that the absence of correlation among the electrical activity of neurons firing is a good marker of them.

Electrical patterns underlying the sucker attachment and detachment

Head and tail suckers are formed by layers of circular, radial and longitudinal muscles (Miller *et al.*, 1981; Baader & Kristan, 1995; Reynolds *et al.*, 1998; Kristan *et al*, 2005) and have a complex network of neurons and sensory units connected to their respective brains. The head sucker is essential during feeding and its sensory units are used also during exploration (Payton, 1981). The tail sucker is formed by the fusion of 7 modified segments in the posterior region and

is usually attached to substrate when the leech is at rest (Kristan et al, 2005). A controlled attachment and detachment of the head and tail suckers is essential during crawling (Schlüter, 1933; Gray et al 1938; Baader & Kristan, 1995) and it is not known whether sucker attachment/detachment is controlled by command neurons such the pair of neurons R3b-1, controlling swimming and/or crawling (Esch *et al.*, 2002) and the trigger neurons Tr1 and Tr2 initiating and terminating swimming (Brodfuehrer and Friesen, 1986). We investigated, therefore, properties of sucker attachment and detachment with the aim to identify the associated patterns of electrical activity.

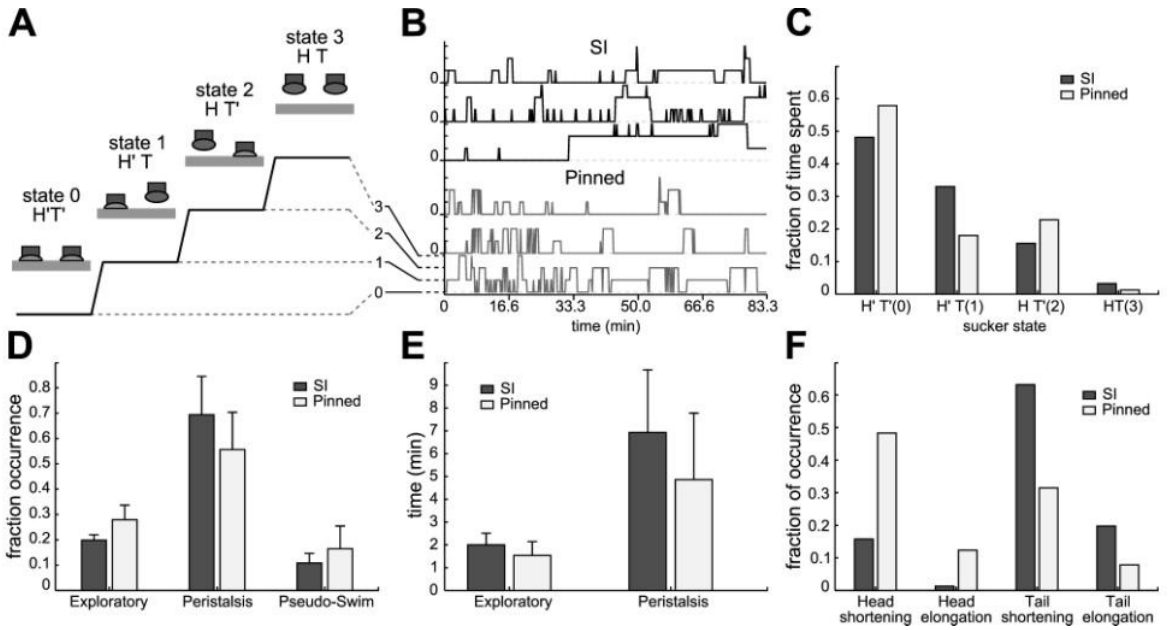

Figure 3. *Behaviours from head and tail sucker*. **A**. Diagram representing the four behavioural states of the suckers: State 0, both suckers are attached (H'T'). State 1, head's sucker is attached while tail's sucker is detached (H'T), State 2: Head sucker is detached while tail's sucker is attached (HT') . Finally state 3: head and tail's suckers are detached (HT). **B.** Sucker states evolution from three semi-intact experiments (top traces in black) and three Pinned experiments (bottom traces in gray). **C**. Frequency distribution of sucker states. **D**. Fraction of occurrence of exploratory, peristalsis and ventilation when the tail sucker was attached but not the head sucker (state T'H). Comparison between pinned but intact (dark bars) and semi intact (grey bars) leeches. **E**. Mean duration of exploratory and peristalsis episodes. Comparison between pinned but intact (dark bars) and semi intact (grey bars) leeches. **F**. Fraction of occurrence of body contraction and elongation following head and tail detachment of pinned but intact (dark bars) and semi intact (grey bars) leeches.

We first analysed and compared the statistics of sucker attachment and detachment in intact but pinned leeches and in semi-intact leeches (Fig.3). By visual analysis of videos recorded during the experiments we determined whether the head sucker was attached (H') or detached (H) and similarly whether the tail sucker was attached (T') or detached (T). Therefore the leech could be in four different states, i.e. H'T', H'T, HT' and HT (Fig.3A) according whether its head and tail suckers are attached and/or detached. We compared semi-intact leeches and intact - but pinned in the observation tank - and we asked whether the removal of part of the animal body had major effects on the suckers attachment and detachment. As shown in Fig.3B, both semi-intact and intact-pinned leeches attached and detached their head and tail suckers. We analysed 4 semi-intact and 4 intact-pinned leeches for several hours and we quantified the occurrence and statistics of the four possible different states H'T', H'T, HT' and HT. As shown in Fig.3C, for

semi-intact leeches the fraction of time spent in states H'T', H'T, HT' and HT was 0.48±0.06, 0.32±0.06, 0.15 ±0.06 and 0.05±0.06 respectively. For intact-pinned leeches the fraction of time spent in states H'T', H'T, HT' and HT was 0.58±0.06, 0.17±0.06, 0.22 ±0.06 and 0.03±0.06 respectively.

When leeches were in state T'H, their tail sucker was attached and their head could move and different behaviours were observed: indeed leeches could explore, stretch their head (Peristalsis) or be involved in a pseudo-swimming behaviour (Fig.3D). Also for this situation we could not see any statistical significant difference between semi-intact and intact-pinned leeches. The duration of continuous episodes of exploratory and peristalsis behaviour was very similar in semi-intact and intact-pinned leeches (Fig.3E). Following detachment of the head sucker an intact but pinned leech shortened its whole body, more often than a semi-intact leech (fig.3F). A different behaviour was observed following detachment of the tail sucker: in this case the semi-intact leech shortened its body more often than an intact but pinned leech (Fig.3F).The results shown in Fig.3 suggest that semi-intact leeches are able to attach and detach their head and tail suckers very similar to what observed in intact-pinned leeches. We next asked whether we could identify patterns of electrical activity underlying sucker attachment and detachment.

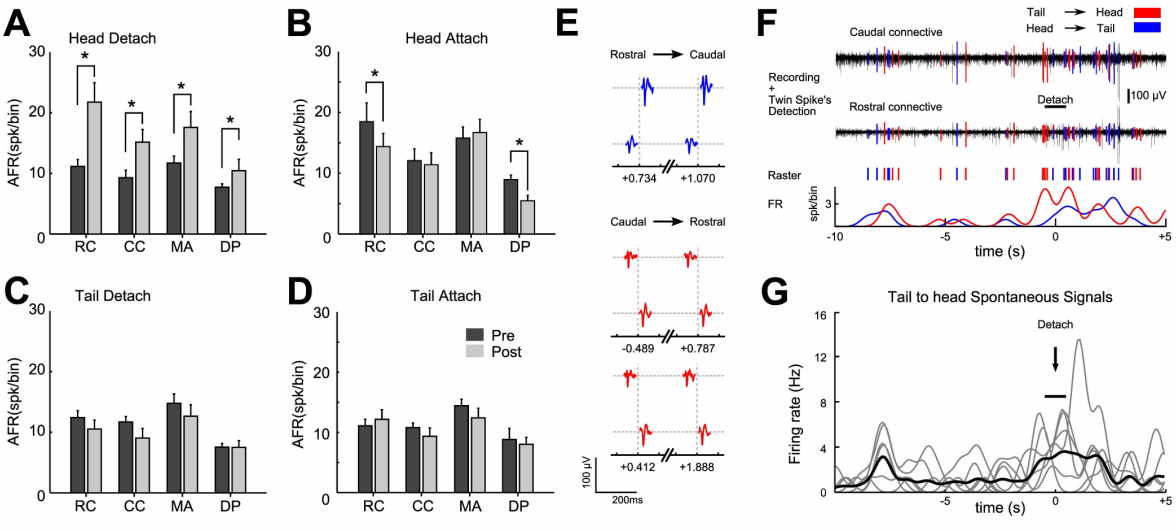

Figure 4. *Identification of electrical patterns underlying head sucker Detach*. **A**: Electrical activity recorded from two connectives (black traces). A cell with fixed latency of ~6 ms between the caudal and the rostral connectives has been identified and highlighted in red: upper red trace shows its raster plot and the inset shows the shape of its spikes recorded on the two connectives. The traces are aligned to a spontaneous head sucker detach event (occurring at the middle of the traces, set as time 0; time range is the same for panels A, B, C and D). **B**: Zoom from recording during the detach event shown in A. Three different twin-spikes identified due the same latency but different waveform pointed by green, blue and red dots. Delay time = 9 ms **C**: Firing rate of 7 units (gray traces) identified as described in panel A, and mean firing rate (black trace). A common activation pattern can be observed for the identified cell: a burst of 3-4 Hz precedes (by about 8 seconds) the head detach, during which another burst of the same average frequency, occurs.

Having identified transitions between different states we aligned the electrical activity recorded during these transitions and we investigated events in a time window of 30 sec before and after sucker attachment and detachment. In these experiments we used suction electrodes in an *en passant* configuration to record the electrical activity also from the connectives. In order to identify APs from possible command neurons associated to sucker attachment and

detachment, we used one electrode to record from the rostral connective (RC) and an other electrode to record from the caudal connective (CC) relative to the dissected and exposed ganglion. Other suction electrodes were used to record APs from the DP and AM roots.

When the head sucker detached and very often the leech shortened its whole body, we observed a significant increase of the AFR in the RC, CC and in DP and AM roots (Fig.4A). When the head sucker attached, we observed a small decrease of AFR in the RC and in the DP roots, but not in the CC and in the AM roots (Fig.4B). We could not detect any significant change of the AFR from the RC, CC and from DP and AM roots either when the tail sucker detached (Fig.4C) or attached (Fig.4D).

As we were able to detect a significant increase of the AFR of signals measured from the connective fibres during the head sucker detachment, we analysed in more details APs travelling along the connectives with the aim to identify possible command neurons for head attachment. In electrical recordings obtained from the RC and CC we identified several APs (see Fig.4E) travelling from the head to the tail (indicated in blue) and from the tail to the head (indicated in red). These APs appeared always as twin APs with a stereotypes shape and amplitude in the CC and RC separated by a delay of 4-6 msec. We found that APs travelling from the head to the tail and vice versa appeared approximately 8 seconds before the detachment of the head sucker (Fig.4F). This burst of 3-8 APs was followed by a larger burst of APs during sucker detachment. APs preceding the detachment of the head sucker could be part of the electrical commands underlying this behaviour. This pattern of electrical activity was found in a large portion (85 %) of head sucker detachments and APs travelling from the tail to the head appeared consistently (Fig.4G).

Electrical patterns underlying crawling

In previous sections, we have seen that during stationary states both $<AFR_i>$ and $< \rho_{ij} >$ declined and that the motion of the animal is associated to large values of the firing rate of individual motoneurons and of the cross-correlation of the firing rate between individual motoneurons. Therefore we asked whether we could infer from the firing rate of leech motoneurons whether the animal is elongating or contraction its body and whether it is possible from the firing rate of these motoneurons to determine whether the leech is swimming, pseudo-swimming or crawling.

Swimming and pseudo-swimming are related behaviours. Swimming consists of a wave of rearward moving crests and troughs of the flattened body, produced by phasic contractions of longitudinal muscles in ventral and dorsal segmental body wall (Kristan *et al*, 1974). During swimming, the head and tail oscillate with a frequency of ~ 1.5Hz (Mazzoni *et al*, 2005). Each leech ganglion contains at least 7 interneurons which can independently sustain swim oscillations and are considered part of a swim segmental oscillator. These oscillator interneurons receive tonic excitatory drive (from segmental swimming interneurons) and fire with a triphasic rhythm. These three phases of activity centre around 0, 120, and 240 degrees and provide both excitatory and inhibitory drive to motoneurons. Although the segmental oscillatory interneurons fire in a triphasic rhythm, these neurons produce a four-phase rhythm in segmental body wall motoneurons. Each of these four classes of motoneurons fire for ~25% of the cycle. These classes consist of dorsal and ventral excitatory as well as inhibitory motoneurons. Leeches produce another rhythmic behaviour, usually referred as ventilation or pseudo-swimming (Magni & Pellegrino, 1978; Mazzoni *et al*, 2005; Bisson & Torre, 2010). During pseudo-swimming the rostral part of the body oscillates while the caudal part is motionless and the tail sucker is tightly attached.

Neuronal circuits underlying swimming have been extensively investigated (Kristan, *et al*, 1974; Ort *et al,* 1974; Kristan *et al*, 1974b; Friesen *et al*, 1978; Poon *et al* 1978; Stent *et al*, 1978; Weeks & Kristan, 1978; Brodfuehrer & Friesen, 1986; Brodfuehrer & Friesen, 1986b; Nusbaun & Kristan, 1986; O'gara & Friesen, 1995; Taylor *et al*, 2003). Pseudo-swimming, in contrast, has been less extensively analyzed. It is known that a strong discharge of L motoneurons blocks pseudo-swimming and allows the animal to enter in another state (Magni & Pellegrino, 1978). Pseudo-swimming frequency is also ~1.5Hz as in swimming, but in pseudo-swimming, the tail sucker does not oscillate and remains attached (Mazzoni *et al*, 2005).

During crawling, the coordinated activities of nine excitatory and inhibitory motoneurons of the longitudinal and circular muscles were recorded (Bader 1995). Thus, during crawling, the leech uses motor output components known to contribute to other types of behaviour, such as swimming or the shortening/local bending reflex. Interneurons with identified functions in these other types of behaviour exhibit membrane potential oscillations that are in phase with the behaviour pattern. Therefore, the recruitment of neuronal network elements during several types of behaviour occurs not only at the motor neuron level but also involves interneurons.

If the dissection of the semi-intact leech is obtained with a limited injury to the animal, the leech, although pinned and not intact, can display its usual behaviours such as crawling and swimming. Indeed a semi-intact leech can crawl as shown in the upper images of Fig.5A. During crawling, the elongation of the leech, measuring the distance between its head and tail (upper trace in Fig.5A) oscillate with a period of approximately 40 seconds, alternating episodes of elongation and contraction. During the contraction phase of crawling several longitudinal excitatory motoneurons, such as motoneuron 3 and L increased their AFR (second and third rows in Fig.5A) while other motoneurons, such as the AE, CV, 102,109 (Fig.5A) decreased their AFR. During the elongation phase most identified motoneurons reverted their firing pattern.

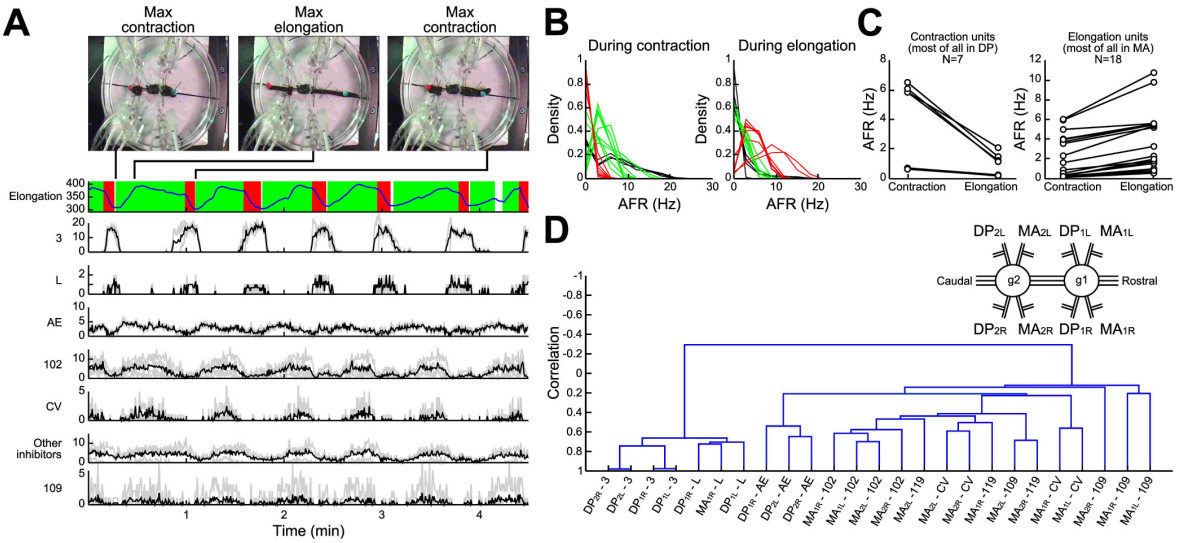

Figure 5. *Electrical patterns underlying crawling.* **A**. The crawling phases are shown and compared to the elongation trace (first plot, blue line). The contraction phase (red area) and the elongation phase (green area) were defined by processing the first time-derivative of the elongation trace. A custom supervised spike-sorting algorithm was launched on the 8 available electrophysiological recordings (4 DPs and 4 MAs). 25 different units were detected and subsequently classified. Considering the spike size (i.e. the peak amplitude) and the coherence between the resulting firing rates, each unit was labelled as one of the 6 plausible cells that can be recorded from DP and AM

roots. **B**. Density plots of the average firing rate of each unit during contraction (left plot) and elongation phases (right plot). Three families of neurons can be distinguished: pure contractors (black traces), pure elongators (red traces) and intermediate units (green traces). **C**. Scatter plots of the average firing rate of each unit detected in the DP root (left plot) and in the MA root (right plot). During elongation, most of all the units identified in the DP root decrease their AFR, while the contrary happens in MA units. **D**. A blind hierarchical clustering of each unity AFR was performed, using the single-linkage method with the correlation as a metric. The resulting dendrogram returns two families of neurons whose activity is anti-correlated: the contractor neurons are listed on the left, while the elongators are on the right. Root names are referred to the inset; DP_{2L} means Left Dorsal Posterior root of the 2^{nd} ganglion (H=head, T=Tail). Ganglia are numbered for simplicity: numberings are not referred to actual segments.

In several experiments we were able to identify reliably from the electrophysiological recordings between 20 and 30 APs from different motoneurons. Their AFR during contraction (left panel of Fig.5B) and elongation (right panel of fig.5B). From this analysis we identified three classes of motoneurons: pure contractors activated only during the contraction phase (black traces, comprising motoneuron 3, …), pure elongators activated primarily during the contraction phase (red traces comprising motoneuron 102, CV…) and intermediate units activated both during contraction and elongation (green traces). In agreement with previous observations (REF a Kristan), pure contractor motoneurons were found in the DP root and pure elongator motoneurons in the AM root (Fig.5C).

In order to identify and characterize patterns of electrical activity during crawling we developed a hierarchical clusterization of involved motoneurons using the single-linkage method with the correlation as a metric (see Methods). This procedure returns a dendrogram describing in a compact form the degree of correlated and anti-correlated activity of motoneurons during crawling (Fig.5D). This analysis identifies two groups of motoneurons correlated at some extent among them both during the contraction and elongation phase. These two groups of motoneurons are mutually anti correlated: the AFR of one group of motoneurons increases during contraction and the other during elongation. The dendrogram describes the pattern of correlated and anti correlated activity during the entire crawling, both during the contraction and elongation phase.

Motoneurons 3 and L from different ganglia and both on the right and left right are highly correlated (see the left arm of the dendrogram of Fig.5C) while other motoneurons, are similarly correlated each other but at a lesser extent (see right arm) and are anti correlated to motoneurons of the left arm of the dendrogram.

Electrical patterns underlying contraction and elongation

During crawling leeches alternate contraction and elongation episodes with a characteristic pattern of motoneuron firing. As leeches shorten and elongate their body also during other behaviours we asked whether the firing pattern of motoneurons during elongation (or contraction) is the same during other behaviours or elongation (or contraction) during crawling is specific. Therefore we analyzed motoneuron firing during contractions and elongations not associated to crawling (Fig.6).

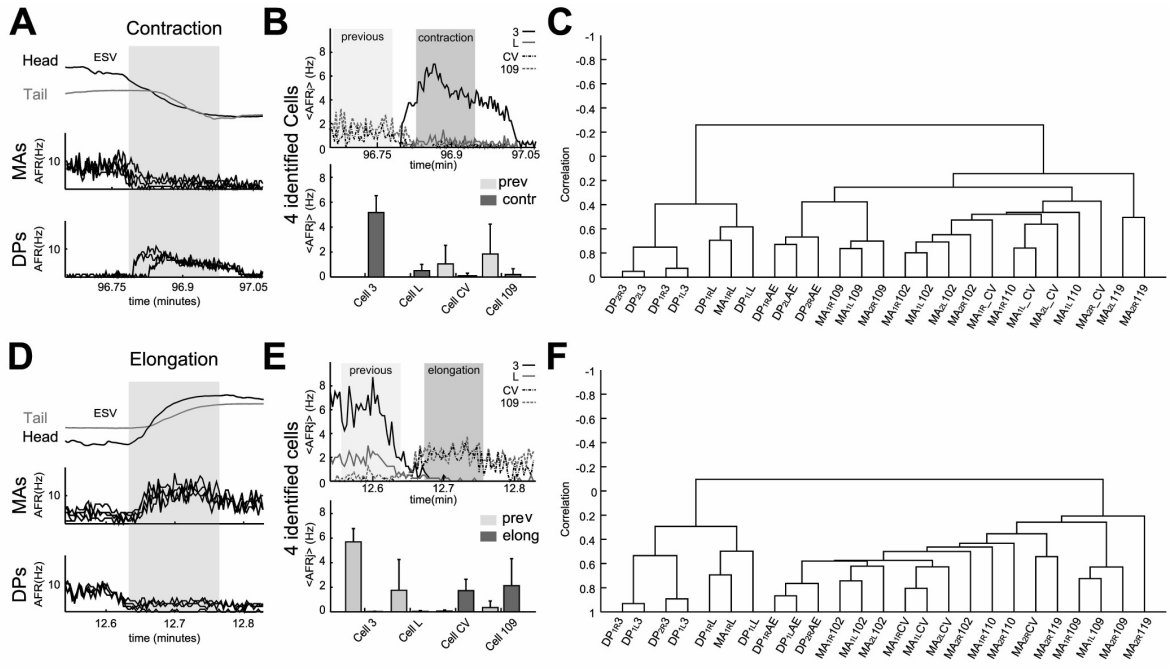

Figure 6. *Electrical patterns underlying contraction and elongation.* Dendrograms of the cell activities recorded during whole body contraction (A) and elongation (B).

During all contraction episodes, the AFR recorded from the DP roots increased and that recorded from the Ma roots decreased (Fig6A se also). The AFR of motoneurons 3 and 109 increased during contractions and that of motoneurons CV and 109 decreased (Fig.6B). An almost opposite behaviour was observed during elongations (Fig.6D and E): during these events the AFR from the AM roots increased significantly as well as the AFR of motoneurons CV and 109 and the AFR from the DP roots and of longitudinal excitatory motoneurons, such as 3 and 5 decreased.

Electrical patterns of motoneurons firing during all elongations, either during crawling or during exploration, were similar and had almost the opposite pattern observed during contractions. However, the dendrograms during contraction (Fig.6C), elongation (Fig.6F) and during crawling were similar but some significant differences were observed. The three dendrograms have two major arms of anti correlated activity, with each arm being composed by mutually correlated motoneurons. However, the degree of correlated activity varied with the specific behaviour: motoneurons 3 and L are more correlated during crawling than during pure elongation and contraction.

Electrical patterns underlying swimming and pseudoswimming

Swimming and pseudo-swimming can also be observed in semi-intact leeches. Indeed it is possible to observe the head and tail oscillate in anti-phase with a frequency close to 1 Hz (Fig.8A). These episodes were identified as swimming.

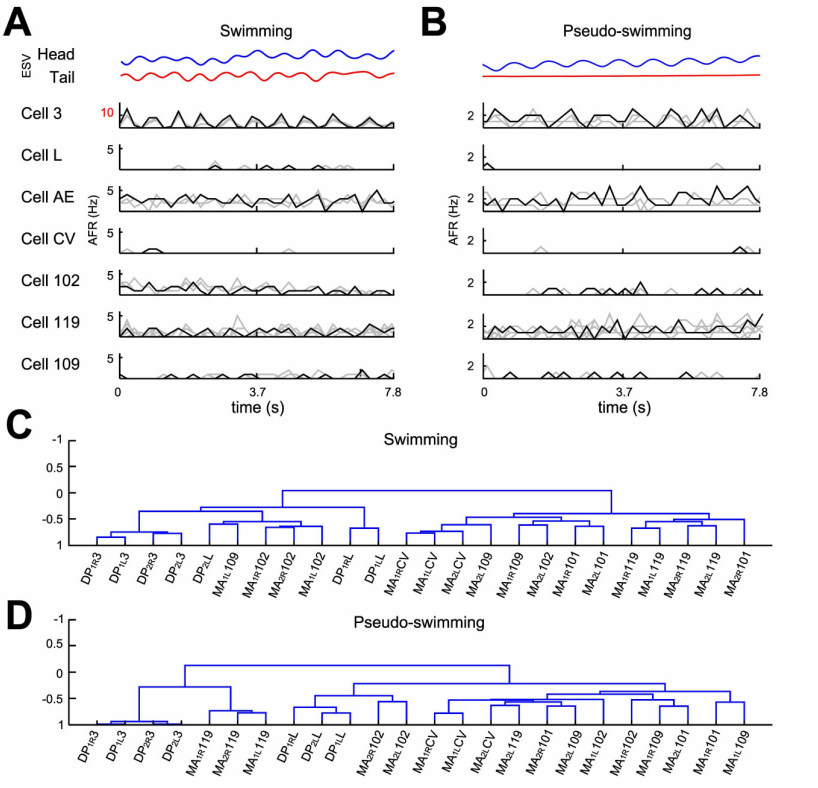

Figure 7. *Electrical patterns underlying swimming and pseudo-swimming.* **A**. Analogical signals recorded from Dorsal Posterior and Medial Anterior roots from ganglia 11 and 12 (reported in subscripts), showing episodes of swimming and pseudo-swimming. On top, elongation-contraction vectors representing the movements for head (blue trace) and tail (red trace) with evident rhythmic oscillations. The two behaviours result in very different patterns of activity. **B**. Resulting dendrograms corresponding to the two behaviours, quantifying the qualitative considerations reported for panel A. **A**. Analogical signals recorded from dorsal posterior and medial anterior roots from Ganglia 11 and 12 during selected episodes of Swimming and Ventilation (pseudo-swimming). On top, Frames obtained from recording corresponding to 1 second of motion's behaviour. Superior image represent the first frame (1) from the recording, while below, are represented 25 frames (1 second) superimposed to illustrate the presence or lack of motion in both behaviours getting or not a blurring bead image. Notice that in ventilation, on the superimposed image the Tail's bead has a lack of blurring, concluding a static motion. Middle. ESV represent the behaviour form beads on Head (blue trace) and Tail (red trace) with evident rhythmical oscillations elicited by head or tail on swimming and confirming the lack of oscillations elicited by tail's bead on ventilation behaviour. Bottom. Analogical traces from 8 roots recorded in two ganglia's preparation, it is shown the characteristic motoneuron's patterns elicited by cell 3 in the swimming but a completely different pattern during ventilation and the lack of some spikes from MA roots. Window 5s traces. **B**. Top, waveforms selected form one DP and one MA roots to illustrate the different signals and the quantity of signals sorted during the episodes selected. Bottom, firing rate (bin width 500 ms) from different motoneurons that were represented as the waveforms on top, blue waveforms on DP are represented by cell 3, and it's shown its Firing rate. Both episodes shown here corresponded to the 25s analogical signals exposed in A. The FR window correspond to the same 5 seconds from A analogical traces**.** **C**. Dendrogams from the identified neurons by spike sorting algorithm obtained from all episodes of swimming and ventilation found on one experiment.

Often the head of semi-intact leeches oscillates with frequencies varying from 0.5 to 2 Hz, while the tail remains still with its sucker firmly attached to the bottom of the recording dish (Fig.7). These episodes were identified as pseudo-swimming.

Discussion

In the present manuscript we have analyse the simultaneous electrical activity of several motoneurons and neurons during different behaviours, with the aim to identify which patterns of the electrical activity characterize and identify specific behaviours. During crawling, swimming and pseudo-swimming specific patterns of correlation and anti-correlation among motoneurons emerge, which we propose to be described by a dendrogram (see Methods). Dendrograms and the average firing rate of motoneurons identify specific behaviours.

Let us now discuss in details issues raised in the present manuscript.

Intact versus semi-intact leeches

In order to compare electrical activity and behaviour we have used a semi-intact leech preparation (Kristan WB & Calabrese R, 1976), where one or two ganglia were exposed so to allow electrical recordings. Under these experimental conditions, by using 8 suction pipettes it is possible to record patterns of electrical activity from several tens of motoneurons. When leeches were gently dissected, they could move easily their head and tail and could exhibit - although pinned down to the experimental dish – some of their stereotype behaviours: indeed they could rhythmically shorten and elongate their whole body with almost the same frequency – see Methods - observed during unrestrained crawling (see Fig.5). Similarly, semi-intact leeches could move their head and tail in the same manner as during swimming and pseudo-swimming (Fig.7).

The statistics of sucker attachment and detachment of intact/pinned and semi-intact/pinned leeches (Fig.4) was rather similar, suggesting that the gentle surgery necessary to obtain a semi-intact leech does not alter dramatically the leech behaviour and patterns of the underlying electrical activity.

Stationary states and correlated activity

Leeches in wilderness and in the tanks where are kept for several months spend a significant fraction of their time, immobile, i.e. in a stationary state. Therefore we addressed the issue to identify which patterns of electrical activity are associated to these stationary states. During stationary states, the overall electrical activity decreases and indeed both the average firing rate $<AFR_i>$ and the average cross-correlation $< \rho_{ij} >$ have small values. However, as shown in Fig.2C, a small value of $< \rho_{ij} >$ is a better classifier than a small value of $<AFR_i>$ of stationary states. When the leech is not in a stationary state a change of $<AFR_i>$ is a better reporter than of $< \rho_{ij} >$ of changes of the tail or head velocity.

Changes of the degree of correlated electrical activity have been associated to attention: a decrease of correlations among firing of neurons in visual area V4 (Cohen & Maunsell 2009) underlies attentional improvement. These attention-dependent changes in neural correlations depend on the specific visual area under examination and on the specific frequency range: attention increases the power of local field potential in the gamma frequency range (30–50 Hz) in V4 but not in V1(Chalk et al 2010).Therefore, changes of the degree of correlated electrical activity during attention are not uniform in all visual areas.

A higher correlated electrical activity seems to be essential for memory formation and consolidation. Modulations in the gamma-frequency and theta-frequency (4–8 Hz) ranges have

been proposed to underlie memory performance and in particular to spike timing-dependent plasticity (Jutras 2010). As a consequence electrical synchronization is essential to memory formation underlying the cellular mechanisms of memory storage.

Sucker attachment and detachment

Suckers attachment and detachment have been analyzed in the generation of the crawling behaviour (Baader & Kristan, 1995; Baader, 1997). These events are essential for a correct crawling and must therefore be synchronized with motoneuron contraction and elongation (Fig.6-7). A correct timing and synchronization with motoneuron activity could be achieved by command neurons sending an appropriate neural signal along the connective fibres linking the head and tail sucker. Evidence for the existence of command neurons, possibly underlying head sucker detachment are shown in Fig 4. We have not been able to identify possible command neurons for tail sucker detachment and sucker attachment.

Patterns of electrical activity and dendrograms

The leech motor system consists of 19 pairs of excitatory motoneurons in each ganglion that innervate longitudinal, oblique, and circular fibres (Stuart, 1970; Ort *et al.*, 1974; Mason and Kristan, 1982; Norris and Calabrese, 1987). These motoneurons have been extensively investigated using force and length transducers and electrophysiology tools (Stuart, 1970; Kristan, 1982; Mason and Kristan, 1982; Norris and Calabrese, 1987), however, we still lack a complete description of their activation patterns during the performance of stereotyped behaviours such as swimming and crawling. To address this issue we used a hierarchical classification on the firing rates of spike sorted activities recorded from 8 roots.

Dendrograms provide a compact a hierarchically-nested sets of partitions of the electrical activity of motoneurons during different behaviours. Once a reference dendrogram was estimated for every single behaviour under consideration, we tested the reliability of such estimates by comparing a time-dependent dendrogram, estimated over a sliding time window (see methods) with a reference dendrogram (e.g. the crawling reference dendrogram). We expected to obtain a time-dependent dendrogram reasonably similar to the reference one in those time intervals during which the reference behaviour was performed. This would prove the specificity of a reference dendrogram to the considered behaviour, and not to others. A method for comparing two hierarchical clusterings is described by Fowlkes and Mallows (1983), and is based on the derivation and use of a measure of similarity, Bk, derived from the matching matrix $[m_{ij}]$, formed by cutting the two hierarchical trees and counting the number of matching entries in the resulting k clusters in each tree. Wagner (2007) gives a survey of the most important similarity measures that can be employed in comparing two clusterings, and all can be adapted to the framework of hierarchical clustering, provided that a cutting on both the trees is done. After testing the majority of these similarity measures between dendrograms, we chose the Fowlkes-Mallows Index and the Mutual Information Index as the best candidates to assess the similarity between two dendrograms. More than 80% of the total swimming episodes were identified correctly by comparing the time-dependent dendrogram with the swimming reference dendrogram. Moreover, the comparison reported only ~5% of false positives. Regarding crawling we get a better true positive rate (reaching 90% of correctly classified events) and again ~5% of false positives. The low rate of false positives produced by the comparison of the two dendrograms is a clear index of the high specificity of each reference dendrogram, and thus its high reliability.

Since the dendrogram based on the correlation metric is a compressed representation of the correlation matrix (which contains the correlations between all the possible pairs of spike sorted firing rates) we compared the performance of a behaviour classifier based on the correlation matrix coefficients $<\rho_{ij}>$ and one based on the raw spike sorted firing rates.

A classifier is a mapping of instances into a certain class. The classifier result can be in a real value (continuous output) in which the classifier boundary between classes must be determined by a threshold value, for instance to determine whether a person has hypertension based on blood pressure measure, or it can be in a discrete class label indicating one of the classes. If the classifier results in just two classes, it is called a binary classifier. In our work we only consider binary classifiers: the first classifies stationary states by thresholding the average covariance signal, leading to two classes, i.e. stationary (value 1) and non-stationarity or movement (value 0). Other classifiers implemented in this work apply a threshold on the similarity measure between a dendrogram estimated in a sliding time-window and a pool of reference dendrograms, each one describing a particular behaviour (crawling or swimming). In this way the classifier resulted in two classes: detected behaviour (being crawling or swimming), having value 1 or not detected behaviour, having value 0. Another way of decoding the behavioural state of the leech, starting from the spike sorted activities, would be to run a discriminant analysis on some time-varying features that are believed to vary accordingly to the particular behavioural state of the animal. As a set of features we chose the n(n-1)/2 coefficients of the covariance matrix estimated from the spike sorted activities in a sliding time-window, or the raw activities alone. Discriminant analysis uses training data to estimate the parameters of discriminant functions of the predictor variables. Discriminant functions determine boundaries in predictor space between various classes. The resulting classifier discriminates among the classes (the categorical levels of the response) based on the predictor data.

To test the performance of different classifiers (see methods) based on the correlation matrix coefficients or the raw firing rates and the dendrogram-matching classifier, a receiver operating characteristics (ROC) analysis was used. A ROC graph is a technique for visualizing, organizing and selecting classifiers based on their performance. ROC graphs have long been used in signal detection theory to depict the trade-off between hit rates and false alarm rates of classifiers (Egan, 1975; Swets *et al.*, 2000). Based on this analysis, we concluded that the performance of the dendrogram-matching classifiers was between those obtained for the classifiers based on the correlation matrix coefficients (performing better) and those obtained for the classifiers based on the raw firing rates (performing worse).

The most striking consequence of using correlation-based dendrograms is that the motoneurons are clustered in agreement to the known literature on the stereotyped behaviours: the dendrograms follows finely the correlation structure of the internal, interneuron-based network that switches its dynamical state accordingly to the performed behaviour, with consequent changes on its output layer (constituted by motoneurons).

References

Abarbanel HDI (1993), The analysis of observed chaotic data in physical systems. Rew Modern Physics 65:1331-1390.

Alonso JM, Usrey WM, Reid RC (1996) Precisely correlated firing in cells of the lateral geniculate nucleus. Nature 383: 815-819.

Arisi I, Zoccolan D, Torre V (2001) Distributed motor pattern underlying whole-body contraction in the medicinal leech. J Neurophysiol 86: 2475-2488.

Baader AP (1997) Interneuronal and motor patterns during crawling behaviour of semi-intact leeches. J Exp Biol 200:1369-81.

Bair W, Zohary E, Newsome WT (2001) Correlated firing in macaque visual area MT: time scales and relationship to behaviour. J Neurosci 21: 1676-1697.

Bergman H, Feingold A, Nini A, Raz A, Slovin H, Abeles M, Vaadia E (1998) Physiological aspects of information processing in the basal ganglia of normal and parkinsonian primates. Trends Neurosci 21: 32-38.

Bialek W, Rieke F (1992) Reliability and information transmission in spiking neurons. Trends Neurosci 15: 428-434.

Bizzi E, Tresch MC, Saltiel P, d'Avella A (2000) New perspectives on spinal motor systems. Nat Rev Neurosci 1:101-108.

Brodfuehrer, P.D., Friesen, W.O., 1986. Initiation of swimming activity by trigger neurons in the leech subesophageal ganglion. III. Sensory inputs to Tr1 and Tr2. J. Comp. Physiol. A 159, 511-519.

Castellucci VF, Kandel ER (1974) A quantal analysis of the synaptic depression underlying habituation of the gill-withdrawal reflex in Aplysia. Proc Natl Acad Sci U S A 71: 5004-5008.

d'Avella A, Bizzi E (1998) Low dimensionality of supraspinally induced force fields. Proc Natl Acad Sci U S A 95:7711-7714.

de Ruyter van Steveninck RR, Lewen GD, Strong SP, Koberle R, Bialek W (1997) Reproducibility and variability in neural spike trains. Science 275: 1805-1808.

Frost WN, Kandel ER (1995) Structure of the network mediating siphon-elicited siphon withdrawal in Aplysia. J Neurophysiol 73: 2413-2427.

Furukawa S, Middlebrooks JC (2002) Cortical representation of auditory space: information-bearing features of spike patterns. J Neurophysiol 87: 1749-1762.

Georgopoulos AP (2000) Neural aspects of cognitive motor control. Curr Opin Neurobiol 10: 238-241.

Georgopoulos AP, Schwartz AB, Kettner RE (1986) Neuronal population coding of movement direction. Science 233: 1416-1419.

Gerstner W, Kreiter AK, Markram H, Herz AV (1997) Neural codes: firing rates and beyond. Proc Natl Acad Sci U S A 94: 12740-12741.

Goldberg JA, Boraud T, Maraton S, Haber SN, Vaadia E, Bergman H (2002) Enhanced synchrony among primary motor cortex neurons in the 1-methyl-4-phenyl-1,2,3,6-tetrahydropyridine primate model of Parkinson's disease. J Neurosci 22: 4639-4653.

Gullo

Ghosh, S, Putrino D, Burro B, Ring1 A (2009) Patterns of spatio-temporal correlations in the neural activity of the cat motor cortex during trained forelimb movements. Somatosens Mot Res. 26(2):31-49.

Heil P (1997) Auditory cortical onset responses revisited. I. First-spike timing. J Neurophysiol 77: 2616-2641.

Heil P, Irvine DR (1997) First-spike timing of auditory-nerve fibres and comparison with auditory cortex. J Neurophysiol 78: 2438-2454.

Hoover NJ, Weaver AL, Harness PI, Hooper SL (2002) Combinatorial and cross-fiber averaging transform muscle electrical responses with a large stochastic component into deterministic contractions. J Neurosci 22: 1895-1904.

Kantz H, Schreiber T (1997) Nonlinear time series analysis. Cambridge, UK: Cambridge University Press.

Kara P, Reinagel P, Reid RC (2000) Low response variability in simultaneously recorded retinal, thalamic, and cortical neurons. Neuron 27: 635-646.

Keller CH, Takahashi TT (1996) Binaural cross-correlation predicts the responses of neurons in the owl's auditory space map under conditions simulating summing localization. J Neurosci. 16 (13):4300-9.

Kristan WB, Jr. (1982) Sensory and motor neurones responsible for the local bending response in leeches. J Exp Biol 96: 161-180.

Kristan WBJr, Lockery SR, Lewis JE (1995) Using reflexive behaviours of the medicinal leech to study information processing. J Neurobiol 27:380-389.

Lestienne R (2001) Spike timing, synchronization and information processing on the sensory side of the central nervous system. Prog Neurobiol 65: 545-591.

Lewis JE, Kristan WBJr (1998a) A neuronal network for computing population vectors in the leech. Nature 391:76-79.

Lewis JE, Kristan WBJr (1998b) Representation of touch location by a population of leech sensory neurons. J Neurophysiol 80:2584-2592.

Lockery SR, Kristan WBJr (1990a) Distributed processing of sensory information in the leech. I. Input-output relations of the local bending reflex. J Neurosci 10:1811-1815.

Lockery SR, Kristan WBJr (1990b) Distributed processing of sensory information in the leech. II. Identification of interneurons contributing to the local bending reflex. J Neurosci 10:1816-1829.

Mainen ZF, Sejnowski TJ (1995) Reliability of spike timing in neocortical neurons. Science 268: 1503-1506.

Mason A, Kristan WB (1982) Neuronal excitation, inhibition and modulation of leech longitudinal muscle. J Comp Physiol 146:527–536

Middlebrooks JC, Xu L, Eddins AC, Green DM (1998) Codes for sound-source location in nontonotopic auditory cortex. J Neurophysiol 80: 863-881.

Morris LG, Hooper SL (1997) Muscle response to changing neuronal input in the lobster (Panulirus interruptus) stomatogastric system: spike number- versus spike frequency-dependent domains. J Neurosci 17: 5956-5971.

Morris LG, Hooper SL (1998) Muscle response to changing neuronal input in the lobster (Panulirus interruptus) stomatogastric system: slow muscle properties can transform rhythmic input into tonic output. J Neurosci 18: 3433-3442.

Morris LG, Hooper SL (1997) Muscle response to changing neuronal input in the lobster (Panulirus interruptus) stomatogastric system: spike number- versus spike frequency-dependent domains. J Neurosci 17:5956-5971.

Morris LG, Hooper SL (1998) Muscle response to changing neuronal input in the lobster (Panulirus interruptus) stomatogastric system: slow muscle properties can transform rhythmic input into tonic output. J Neurosci 18:3433-3442.

Moreno-Bote, R & Parga N. (2010) Response of integrated-and-fire neurons to noisy imputs filtered by synapses with arbitrary timescales: firing rate and correlations. Neural Computation 22:1528-1572.

Muller KJ, Nicholls JG, Stent GS (1981) Neurobiology of the leech. Cold Spring Harbord Lab., Cold Spring Harbord, New York.

Norris BJ, Calabrese RL (1987) Identification of motor neurons that contain a FMRFamide like peptide and the effects of FMRFamide on longitudinal muscle in the medicinal leech, Hirudo medicinalis. J Comp Neurol 266:95-111.

Nicholls JG, Baylor DA (1968) Specific modalities and receptive fields of sensory neurons in CNS of the leech. J Neurophysiol 31: 740-756.

Oppenheim AV, Schafer RW (1989). *Discrete-Time Signal Processing*, Englewood Cliffs, NJ: Prentice-Hall.

Ort CA, Kristan WBJr, Stent GS (1974) Neuronal Control of Swimming in the Medicinal Leech. II. Identification and Connections of Motor Neurons. J Comp Physiol 94:121-154.

Pinato G, Battiston S, Torre V (2000) Statistical independence and neural computation in the leech ganglion. Biol Cybern 83: 119-130.

Pinato G, Torre V (2000) Coding and adaptation during mechanical stimulation in the leech nervous system. J Physiol 529: 747-762.

Putrino D, Mastaglia FL, Ghosh S (2010). Neural integration of reaching and posture: interhemispheric spike correlations in cat motor cortex.Exp Brain Res. 202(4):765-77.

Raz A, Feingold A, Zelanskaya V, Vaadia E, Bergman H (1996) Neuronal synchronization of tonically active neurons in the striatum of normal and parkinsonian primates. J Neurophysiol 76: 2083-2088.

Saberi K, Takahashi Y, Konishi M, Albeck Y, Arthur BJ, Farahbod H.Effects of interaural decorrelation on neural and behavioural detection of spatial cues. Neuron. 1998 Oct;21(4):789-98.

Shadlen MN, Newsome WT (1994) Noise, neural codes and cortical organization. Curr Opin Neurobiol 4: 569-579.

Shadlen MN, Newsome WT (1998) The variable discharge of cortical neurons: implications for connectivity, computation, and information coding. J Neurosci 18: 3870-3896.

Stent GS, Kristan WB, Jr., Friesen WO, Ort CA, Poon M, Calabrese RL (1978) Neuronal generation of the leech swimming movement. Science 200: 1348-1357.

Stevens CF, Zador AM (1998) Input synchrony and the irregular firing of cortical neurons. Nat Neurosci 1: 210-217.

Stuart AE (1970) Physiological and morphological properties of motoneurones in the central nervous system of the leech. J Physiol 209: 627-646.

Tresch MC, Saltiel P, d'Avella A, Bizzi E (2002) Coordination and localization in spinal motor systems. Brain Res Brain Res Rev 40:66-79.

Tsau Y, Wu JY, Hopp HP, Cohen LB, Schiminovich D, Falk CX (1994) Distributed aspects of the response to siphon touch in Aplysia: spread of stimulus information and cross-correlation analysis. J Neurosci 14: 4167-4184.

Warzecha AK, Egelhaaf M (1999) Variability in spike trains during constant and dynamic stimulation. Science 283: 1927-1930.

Warzecha AK, Kretzberg J, Egelhaaf M (2000) Reliability of a fly motion-sensitive neuron depends on stimulus parameters. J Neurosci 20: 8886-8896.

Wittenberg G, Kristan WB, Jr. (1992a) Analysis and modeling of the multisegmental coordination of contraction behaviour in the medicinal leech. I. Motor output pattern. J Neurophysiol 68: 1683-1692.

Wittenberg G, Kristan WB, Jr. (1992b) Analysis and modeling of the multisegmental coordination of contraction behaviour in the medicinal leech. II. Role of identified interneurons. J Neurophysiol 68: 1693-1707.

Wu JY, Cohen LB, Falk CX (1994) Neuronal activity during different behaviours in Aplysia: a distributed organization? Science 263: 820-823.

Zoccolan D, Pinato G, Torre V (2002) Highly variable spike trains underlie reproducible sensorimotor responses in the medicinal leech. J Neurosci 22:10790-10800.

Zohary E, Shadlen MN, Newsome WT (1994) Correlated neuronal discharge rate and its implications for psychophysical performance. Nature 370: 140-143.